EXPERIMENTAL STUDIES AND SIMULATION ON ALTERNATIVE FUEL OPERATED MICRO-TRIGENERATION SYSTEM FOR RESIDENTIAL APPLICATIONS

Ph. D. THESIS

by

DEEPESH SONAR

(2011RME1001)

Mechanical Engineering Department

MALAVIYA NATIONAL INSTITUTE OF TECHNOLOGY JAIPUR

JAIPUR, INDIA

April 2016

EXPERIMENTAL STUDIES AND SIMULATION ON ALTERNATIVE FUEL OPERATED MICRO-TRIGENERATION SYSTEM FOR RESIDENTIAL APPLICATIONS

by

DEEPESH SONAR

(2011RME1001)

Mechanical Engineering Department

Submitted in partial fulfilment of the requirements for the degree of

DOCTOR OF PHILOSOPHY

to the

MALAVIYA NATIONAL INSTITUTE OF TECHNOLOGY JAIPUR

JAIPUR, INDIA

April 2016

Dedicated to

the most revered

GURUJI

whose divine blessings

have made this work possible

MALAVIYA NATIONAL INSTITUTE OF TECHNOLOGY JAIPUR

DEPARTMENT OF MECHANICAL ENGINEERING

DECLARATION

This is to certify that the thesis entitled "**Experimental studies and Simulation on Alternative fuel operated Micro-Trigeneration system for residential applications**" submitted to the Malaviya National Institute of Technology, Jaipur for the award of the degree of **Doctor of Philosophy** has not been submitted in part or full, to any other University or Institute for the award of any degree or diploma. I have fulfilled the requirement for the submission of this thesis.

(DEEPESH SONAR)
ID: 2011RME1001
Date: 25/04/2016

MALAVIYA NATIONAL INSTITUTE OF TECHNOLOGY JAIPUR

DEPARTMENT OF MECHANICAL ENGINEERING

CERTIFICATE

This is to certify that the thesis entitled, "**Experimental studies and Simulation on Alternative fuel operated Micro-Trigeneration system for residential applications**" submitted by Deepesh Sonar (ID: 2011RME1001) to Malaviya National Institute of Technology, Jaipur for the award of the degree of Doctor of Philosophy in Mechanical Engineering is a bonafide record of original research work carried out by him under our supervision.

It is further certified that:

1. The results contained in this thesis have not been submitted in part or in full, to any other University of Institute for the award of any degree or diploma.
2. Mr. Deepesh Sonar has fulfilled the requirement for the submission of this thesis.

Prof. S. L. Soni
Department of Mechanical Engineering,
Malaviya National Institute of Technology
Jaipur

Prof. Dilip Sharma
Department of Mechanical Engineering,
Malaviya National Institute of Technology
Jaipur

Date: 25/04/2016

MALAVIYA NATIONAL INSTITUTE OF TECHNOLOGY JAIPUR

DEPARTMENT OF MECHANICAL ENGINEERING

CERTIFICATE

This is to certify that the thesis entitled "**Experimental studies and Simulation on Alternative fuel operated Micro-Trigeneration system for residential applications**" submitted to the Malaviya National Institute of Technology, Jaipur for the award of the degree of **Doctor of Philosophy** has not been submitted in part or full, to any other University or Institute for the award of any degree or diploma. I have fulfilled the requirement for the submission of this thesis.

DEEPESH SONAR
ID: 2011RME1001
Date: 25/04/2016

This is to certify that Deepesh Sonar (ID. 2011RME1001) has worked under our supervision for the award of the degree of ***Doctor of Philosophy*** in Mechanical Engineering on the topic titled "**Experimental studies and Simulation on Alternative fuel operated Micro-Trigeneration system for residential applications**". He has successfully defended his thesis work in viva-voce examination in front of the Oral Defense Committee and satisfactory incorporated the changes suggested by examiners in this revised version of thesis.
The thesis was examined and has been recommended for the award of degree of ***Doctor of philosophy in Mechanical Engineering.***

Prof. S. L. Soni	**Prof. Dilip Sharma**
(Supervisor and Internal Examiner)	(Supervisor and Internal Examiner)

Deepesh Sonar (ID. 2011RME1001) has successfully defended his thesis work in viva-voce examination in front of the Oral Defense Committee and satisfactorily incorporated the changes suggested by examiners in this revised version of the thesis. The thesis was examined and has been recommended for the award of degree of ***Doctor of Philosophy in Mechanical Engineering.***

Prof. L. M. Das
(External Examiner)
Date: 25-04-2016

ACKNOWLEDGEMENT

First and foremost, I would like to express my utmost gratitude to **Prof. S. L. Soni** and **Prof. Dilip Sharma**, Mechanical Engineering Department, MNIT Jaipur, for providing me an opportunity to work under their supervision, and for their constant encouragement and support throughout my doctoral study which has made this work possible.

I am very thankful to the members of the Doctoral Guidance Committee, **Prof. Jyotirmay Mathur**, **Dr. G. D. Agrawal** and **Dr. Nirupam Rohatgi** for their technical input and valuable comments and suggestions.

Acknowledgements are due to **Mr. Babulal Saini** and **Mr. Bahadur Ram Naik** for their help during the fabrication and erection of the experimental set up. I express special thanks to **Mr. Ramesh Chand Meena** who constantly assisted during the experimental phase of my work in the lab.

I would also like to thank my fellow research scholars for their support and friendship during the period of this study.

Special thanks are due to my parents, sister and relatives for their blessings and good wishes to complete this work.

I am really grateful to my wife, **Archana Sonar** for her constant motivation and moral support during the entire period of the doctoral study. I acknowledge her patience in caring for the family all through these years.

My sincere thanks are due to my sons **Kaustubh** and **Manthan**, who on and off helped relieve pressure during the last phases of my work.

Last, but not the least, I would like to thank all my friends and colleagues, who directly or indirectly helped me in successful completion of this work.

Place: Jaipur

Date: 25-04-2016 **(DEEPESH SONAR)**

ABSTRACT

Trigeneration systems use waste heat from prime movers to simultaneously produce heating and cooling along with electrical power. These are more efficient, less polluting & more economic than conventional systems. Small scale trigeneration power plants, typically, below 15 kW_e, are called micro-trigeneration plants. In such small-scale systems, over 80% of fuel energy can be converted to useable energy for residential and small commercial applications. A household sized micro-trigeneration system is a good flexible energy solution for small social communities.

Currently, more than 85 % of our energy is supplied from fossil resources, which has led to increase in pollutants and CO_2 levels in atmosphere. Fossil fuels are limited and cannot be recycled. This has stimulated active research interest in alternative fuels, particularly for transportation, power generation, and agricultural sectors.

Fuels of bio-origin are renewable, and include alcohol, vegetable oils, biomass, and biogas.

Fuels for effective replacement of the conventional diesel either partially or completely are being experimented worldwide. Vegetable oil based fuels have been proved as promising alternative fuel for the fossil diesel in CI engines.

Various alternate fuels & micro-trigeneration technologies can be combined, with sharp decrease in almost all the emissions, and can meet emission reduction targets, such as the Kyoto Protocol and Agenda 21.

In the present work, a real size demonstration unit for alternative fuel based micro-trigeneration system for residential applications, with the options of space heating, space cooling, fuel preheating, along with power generation was developed. A real size cabin for space heating/cooling was erected. A set up for preheating of alternative fuels was also fabricated and installed. Four units of Electrolux vapour absorption refrigerators were selected, combined, modified and used for space cooling. An EGR set up was also fabricated, installed and used.

The prime mover selected was a small (3.7 kW) agricultural engine, widely used in rural sectors of India. Three non-edible oils (Mahua, Ricebran and Neem) were selected as base fuels. Mahua biodiesel was also prepared and used as fuel.

Experimental investigations were carried out first to find the best blend of vegetable

oils with diesel, as regards engine efficiency and emissions. Then, the injection pressure and injection timing of the engine were varied using optimally blended Mahua oil for obtaining maximum efficiency and minimum emissions, to get optimized engine settings with alternative fuel used.

Engine performance and emission characteristics were determined using optimally blended fuels in single generation, cogeneration and trigeneration modes, at both engine rated and optimized settings.

A simplified simulation model was developed for micro-trigeneration system working on vegetable oil blends, using the software Diesel-RK. The model was validated by experimental data obtained from the engine working on pure mahua oil.

Economic analysis was performed and guidelines were generated for the developed alternative fuel based micro-trigeneration system.

The test results from the experiments showed that the useful output and total thermal efficiency in case of trigeneration and cogeneration are much higher than single generation, while working on alternative fuels. CO_2 emissions and brake specific fuel consumption were also much lower in case of cogeneration and trigeneration, in comparison to single generation.

The developed micro trigeneration system with a small agricultural engine using alternative fuels for power, fuel preheating, space heating and space cooling proved to be feasible and effective.

Micro-trigeneration test facility supplies better test-rig platform for cooling, heating and power generation. Micro-trigeneration can be projected as strategic means to achieve energy security, efficiency and economy, with minimum environmental threats, thus leading to sustainable development.

CONTENTS

LIST OF FIGURES

LIST OF TABLES

NOMENCLATURE

BSFC	Brake specific fuel consumption
BTE	Brake thermal efficiency
CHP	Combined heat and power
CCHP	Combined cooling heating and power
CI	Compression ignition
CO	Carbon monoxide
COP	Coefficient of performance
EGR	Exhaust gas recirculation
FFA	Free fatty acids
HC	Hydrocarbons
IOP	Injection opening pressure
IT	Injection timing
kWe	Kilo watt-electric
kWth	Kilo watt-thermal
LiBr	Lithium bromide
M20	20% blend of Mahua oil with diesel
MB20	20% blend of Mahua biodiesel with diesel
m-CCHP	Micro-combined cooling heating and power
NOx	Oxides of nitrogen
NTU	Number of transfer units
N20	20% blend of Neem oil with diesel
R20	20% blend of Rice bran oil with diesel
SFC	Specific fuel consumption
SVO	Straight vegetable oil
SG	Single generation
VAR	Vapour absorption refrigerator

Symbols

ρ	Density
μ	Viscosity
k	Thermal conductivity
f	friction factor

c_p	Specific heat at constant pressure
Q	Heat transfer rate
W	Watt
m	mass
h	Enthalpy
bhp	Brake horse power
kWh	Kilo-watt-hour
LCV	Lower calorific value
LHV	Lower heating value
η	Efficiency
ϵ	Effectiveness

Subscripts

evap	Evaporator
gen	Generator
cond	Condenser
abs	Absorber
i	Inlet
o	Outlet
a	Air
w	Water
el	Electric
th	Thermal
h	Hot
c	Cold

CHAPTER 1

INTRODUCTION

Energy is the fundamental driver of sustainable development. Sustainable access to energy with modern fuels is strongly related to the millennium development goals of UNO. Sustainable development integrates economic, social and environmental aspects. The path towards energy sustainability is the incremental adoption of available technologies, practices and policies that help to decrease environmental impact of energy sector, with adequate standards of energy services.

Cogeneration or Combined Heating and Power (CHP) is simultaneous production of power and heat. Tri-generation or Combined Cooling Heating and Power (CCHP) is simultaneous production of power, heating and cooling. These systems use only one source of primary energy, represented by fossil fuels or by some appropriate renewable energy sources (biomass, biogas, solar energy, etc). The recovered waste thermal energy from the prime mover is used to produce heating and/or cooling along with power. Cogeneration and trigeneration systems represent strategic technologies to improve the efficiency of energy usage, reliability in energy supply at a reasonable price with reduced thermal and environmental pollution.

Small scale trigeneration power plants, typically, below 15 kWe, are called micro-trigeneration plants. In such systems, over 80% of fuel energy is converted to useable energy. Micro-trigeneration systems are especially interesting due to their technical and performance features. Such systems are emerging in various applications like residential buildings, hotels, hospitals, university campuses, automobiles, etc. A household sized micro-trigeneration system is a good flexible energy solution for small social communities. Also, in the Energy Performance of Buildings Directive of the European Union, CCHP is seen as a technology to fulfil the energy requirements of buildings. The penetration of CCHP systems can be increased after introduction of European Union Emissions Trading Scheme (EUETS), and by increasing the carbon tax. Recently, many countries have begun to run the carbon tax act.

Fossil fuels are limited in reserves and cannot be recycled. Also, over-exploitation of fossil resources has led to increase in hazardous pollutants. The fossil oil instabilities and uncertainties have adversely impacted the developing countries, like India which depend heavily on oil import.

Diesel engines play a major role in transportation, power generation and in agricultural sector, owing to their high efficiency, reliability, durability and longer service life. Furthermore, the stationary diesel engines (genset engines) are gaining popularity in developing countries due to power crisis.

New and renewable fuels for effective replacement of the conventional diesel fuel either partially or completely are being experimented worldwide. Fuels of bio-origin include alcohol, vegetable oils, biomass, and biogas. Vegetable oil based fuels have been proved as promising alternate fuel for use in diesel engines. Such fuels can be produced and used on small-scale e. g, in rural areas to run tractor, pump and small engine for power generation. These are technically feasible, economically competitive, environmentally acceptable, readily available, and can be easily blended with diesel.

India is agriculture based economy, with oil and electricity as two major energy sources. At present, India is producing only 30% of the total petroleum fuels required. India produces a host of non-edible oils such as Linseed, Mahua (Madhuca indica), Rice bran (Oryza sativum), Karanj (Pongamia pinnata), Neem (Azadirachta indica), Jatropha (Jatropha curcas), etc. Over 80 different oil bearing potential trees have been identified. The existing potential for tree borne oilseeds in India is 3.0–3.5 million tonnes, but the collection of only 0.5–0.6 million tonnes is being realized.

Advantages of using vegetable oils/biodiesels in developing country like India include reducing petroleum imports, rural development and agri-economy, besides fuel related benefits like biodegradability, non-toxic and renewable nature, safety in storage and transportation, low emissions etc. Vegetable oils can provide a solution to problems of environmental degradation, energy security as well as rural employment and agricultural economy.

Alternative fuels promote energy conservation, efficiency, environmental preservation and sustainable development. Various alternate fuels & micro-trigeneration technologies can be combined, leading to sharp decrease in almost all the emissions to meet emission reduction targets, such as the Kyoto Protocol and Agenda 21.

Micro-trigeneration systems are more efficient, less polluting & more economic than conventional systems, and can provide assured comfort for home-owners. Micro-trigeneration can prove to be strategic means to achieve energy security and efficiency, with

positive impact on economy, simultaneously reducing environmental threats, leading to sustainable development.

In this study, a real sized micro-Trigeneration system for power, space heating/cooling and fuel preheating was realized. The engine performance was experimentally optimised with varying injection pressure, injection timing and EGR using alternate fuel. The developed micro-trigeneration was operated with different alternate fuels to evaluate the performance and emissions of engine while working in single, cogeneration, and trigeneration modes. Economic analysis was done. Modelling and simulation was conducted for predicting the performance of the micro-trigeneration working on alternate fuel.

1.1 Research Gaps and Motivation

Research in the field of cogeneration and trigeneration has been underway for last many years. Trigeneration technology is mainly restricted to large scale, high-capacity applications, and very little experience exists in small capacity (micro-trigeneration) range. Also, most of these researches are theoretical/computational simulation. Widespread application of this technology in micro-level residential sector has not taken place. Very little experimental work has been reported in the field of studies on Micro-Trigeneration systems, in particular while working with diesel engines of rated capacity below 5 kW.

On the other hand, much research has been done worldwide in the field of use of vegetable oils/biodiesel in IC engines, but its application in the field of cogeneration or trigeneration is very limited.

So, in order to fill the gap, in the proposed work, it was planned to develop and optimize a demonstration unit for alternative fuel based micro-trigeneration system with fuel preheating, space cooling/heating and power generation for residential applications. It was also proposed to generate guidelines for developing alternate fuel based micro-trigeneration system.

1.2 Definition of the Problem

The suitability of alternate fuels for use in diesel engine for micro-trigeneration application was assessed. It was proposed to determine experimentally the effect of alternative fuel substitution on the performance and the exhaust emission characteristics of

diesel engine used for micro-trigeneration. The engine chosen for the proposed work is of 5 HP (3.7 kW_e) capacity, as it is the engine set most commonly used in rural India. This work may help in directing further research regarding techno-economic feasibility of micro-trigeneration on such small capacity engines.

1.3 Aims and Objectives

The major objectives of this work are:

- To experimentally optimize the performance of micro-trigeneration system operated on alternate C.I. Engine fuel for power, space heating and space cooling.
- To experimentally compare the emission characteristics and economic aspects of optimized alternate fuel operated micro-trigeneration system with the conventional single generation system.
- To develop a simulation model of the real size micro-trigeneration system and validate its performance with experimental results.
- To generate guidelines for developing alternate fuel based micro-trigeneration system.

1.4 Research Approach and Methodology

In a typical IC engine based micro-trigeneration system, waste heat can be recovered from engine cooling system or from exhaust gases. The waste heat may be utilized to produce domestic hot water, refrigeration, space heating / cooling or other similar applications. Heat exchangers play a vital role to recover the thermal energy in the gas stream. Hot water can be used for space heating. Exhaust gas/air heat exchangers may also be used directly depending on the quantity of waste heat available.

A diesel engine operated Micro-Trigeneration system was developed in lab to conduct various tests in single generation, cogeneration and trigeneration modes for power, fuel preheating and space heating/cooling applications. It was planned to utilize the waste heat from coolant and exhaust gas for producing cooling and heating effects and fuel preheating, apart from power generation.

Various alternate fuels were used in the investigation: Mahua oil-diesel blend (M20), Ricebran oil-diesel blend (R20), Neem oil-diesel blend (N20), Mahua oil methyl ester-diesel blend (MB20), Pure Mahua oil (M100)

Experimental optimization of engine parameters with M20 as fuel, was also proposed to obtain the optimum injection timing and injection pressure. Observations with EGR (to reduce increased NOx emissions) were also recorded. Experimental evaluation of engine performance and emission characteristics was proposed at both rated and optimised engine settings using these fuels in single generation, co-generation and trigeneration modes. Results obtained with alternate fuel were compared with those of base-case diesel fuel. Economic comparisons were also made for micro-level trigeneration and separate systems for power generation, heating and cooling.

1.5 Scope and Outline of the Thesis

The thesis is arranged in six chapters. First chapter is related to the introduction of the present research work. The second chapter is about the review of the current literature in the field of cogeneration/ trigeneration technologies, tools and trends, and also regarding use of vegetable oil based fuels in diesel engines. Third chapter is about the materials and methods used in conducting this research. It includes fuel selection, biodiesel preparation, design and fabrication of fuel preheating set up, modified Electrolux refrigeration units, and all other components used in fabrication of the entire micro-trigeneration unit.

Fourth chapter describes the main trigeneration set-up, the space cooling set up, the space heating set up and fuel preheating set up, various other components and measuring instruments. The detailed experimental plan is also described. Fifth chapter is related to the experiments and discussion. The sixth and last chapter reports the conclusions drawn from the study and future scope of work. In the end, appendices, references, list of publications and profile of the author are presented.

CHAPTER 2

LITERATURE REVIEW

This chapter is about the review of the current literature in the field of cogeneration/ trigeneration technologies, tools and trends. Space heating/cooling options, trigeneration market trends, status of trigeneration, and the benefits and barriers in the field of trigeneration is also discussed. A detailed literature review regarding use of vegetable oil based fuels in diesel engines is also conducted.

2.1 Theoretical concepts

2.1.1 Cogeneration and Trigeneration

Cogeneration or Combined Heating and Power (CHP) is simultaneous heating and power generation. Tri-generation or Combined Cooling Heating and Power (CCHP) is simultaneous cooling, heating and power generation. Trigeneration may be treated as an extended form of cogeneration.

These systems use only one source of primary energy, represented by fossil fuels or by some appropriate renewable energy sources (biomass, biogas, solar energy, etc). Power generation unit (PGU), which is a combination of prime mover and electricity generator, provides electricity. In single generation, i. e., only power generation, the prime mover has an electric efficiency as low as 30-35%. In trigeneration, waste heat, as a by-product, is collected to meet cooling and heating demands too, along with electricity, thus increasing the energy conversion efficiency up to 90% [1-6].

Cogeneration dates back to 1880s in U.S.A. By 1900, more than half the U.S. electricity was produced by industrial cogeneration. Trigeneration is a recent development and came to use only in mid-1990s. So, the number of trigeneration systems operating worldwide is very small [1, 6, 7, 8].

Trigeneration has clear advantages over single electricity generation and also cogeneration- higher overall efficiency, low GHG and other emissions, efficient use of energy resources, higher economical benefits, and reliability of energy supply. The benefits accrue from cascade utilization of different energy carriers from high to low temperature.

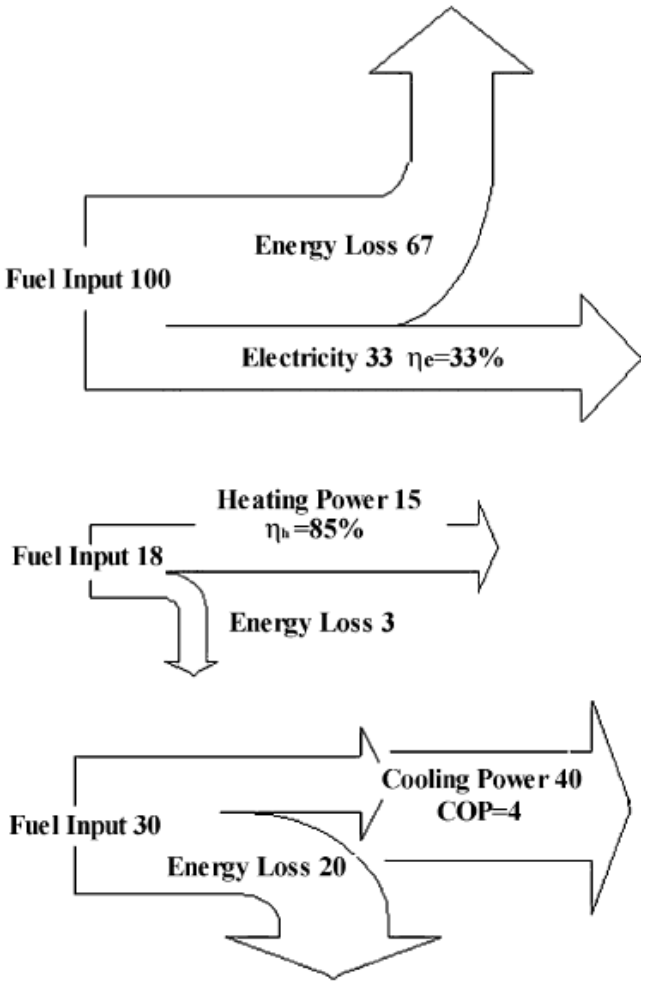

Fig. 2.1 Energy flow in traditional mode [2]

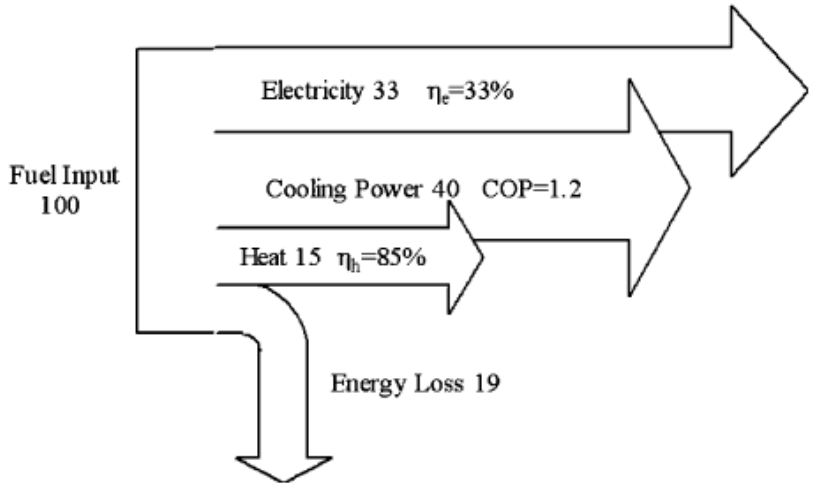

Fig. 2.2 Energy flow in typical CCHP mode [2]

Trigeneration systems can increase the overall efficiency of energy utilization to 90% and more. In case of excessive produced energy (electricity) in some months, it could be sold to the utility (grid-connected case) whereas when the production is not enough, electricity could be purchased from the utility and heat/cold could be produced.

Also, onsite electricity generation reduces generation and distribution losses. Emissions are reduced because for heating and cooling, no additional electricity supplied by fossil fired power plants is purchased from the grid [2, 3, 7, 9, 10, 11].

Quadgeneration

Quad generation extends energy conversion into four forms and generally includes heat production for use in additional heating needs, like thermoelectric energy generation, fuel preheating, process heating etc. This additional energy conversion can be accomplished by integrating new specific set up in the trigeneration plant.

Energy flows in traditional supply mode and a typical CCHP system are shown in Fig. 2.1 and Fig. 2.2. As can be seen, only 100 units of prime energy are needed for 33 units of electrical power, 40 units of cooling power and 15 units of heating power in a summer day. Compared with traditional energy supply mode, CCHP system can save 48 units of primary energy to meet the same demand of cooling, heating and power [2].

CCHP systems can cover a wide range of capacity from 1 kW to 500MW, and can be categorised as below.

- Micro-scale CCHP systems (< 15 kW) are for residential and small sector.
- Small-scale CCHP systems (15 kW- 1 MW) have been widely used in the supermarkets, retail stores, office buildings etc.
- Medium-scale CCHP systems (1-10 MW) have applications in large factories, hospitals, schools, etc.
- Large-scale CCHP systems (>10 MW) are typically used in universities and residential districts, with higher population [2, 3, 12, 13, 14].

2.1.2 Micro-trigeneration systems

Small scale poly-generation power plants, typically below 15 kWe, are called micro-

CHP (micro-cogeneration) or micro-CCHP (micro-trigeneration) plants. Micro-trigeneration plants are especially interesting due to their technical and performance features like, high overall energy conversion efficiency and low emissions.

Micro-trigeneration supplies better test-rig platform for cooling, heating and power generation, and can address all of the following requirements at once: conservation of scarce energy resources, moderation of pollutant release into environment and assured comfort for home-owners. Keystone of full energy utilization of micro-CCHP system lies in efficient recovery of waste heat from the prime movers.

Micro-trigeneration systems with high energy utilization factor (EUF) have a payback period of only about 3 years. These are emerging in various applications, like residential buildings, hotels, hospitals, university campuses, automobiles, etc [1, 2, 3, 15].

Deployment of micro-trigeneration has been considered by the European Community as one of the most effective measure to save primary energy and to reduce greenhouse gas emissions. But, the micro-trigeneration should meet all relevant codes and standards, including applicable emission standard. For residential applications, it should preferably be able to start and operate automatically. Novel technologies such as fuel cells, micro-turbines, Stirling engines, adsorption chillers, dehumidifiers etc are emerging with characteristics, like low emission, high efficiency along with waste heat recovery option [15, 16].

2.1.3 Energy Balance

Energy balance or heat balance is basically an analysis of first law of thermodynamics. In IC engines, it allocates the fuel energy to various engine components, and compares real engine processes with ideal processes.

There may be four sources of usable waste heat from an IC engine based trigeneration system: exhaust gas, engine jacket cooling water, lube oil cooling water and turbocharger cooling.

Main energy balance terms are brake power, coolant heat and exhaust heat. Friction between piston and rings, and cylinder walls is transferred as heat to the cooling medium. The remaining low temperature heat is within the exhaust gases. Unaccounted heat, mainly as convection and radiation losses is unrecoverable, and is lost to the surroundings.

Cooling water heat accounts for up to 30%, while that from the engine exhaust represents 30–50% of the fuel energy input, totalling to approximately 70–80% of recoverable energy. This waste heat is appropriate for low temperature process needs i.e., water heating, space heating, and to drive absorption chillers for refrigeration or space cooling. The efficiency of a trigeneration system is the fraction of the input fuel that can usefully be recovered as power and heat. It depends on the type and size of the prime mover, the quality of the recovered heat, working temperatures, and on the condition and operating regime of the trigeneration unit. [1, 2, 17, 18]

The energy balance for a representative reciprocating IC engine is given in **Fig. 2.3**.

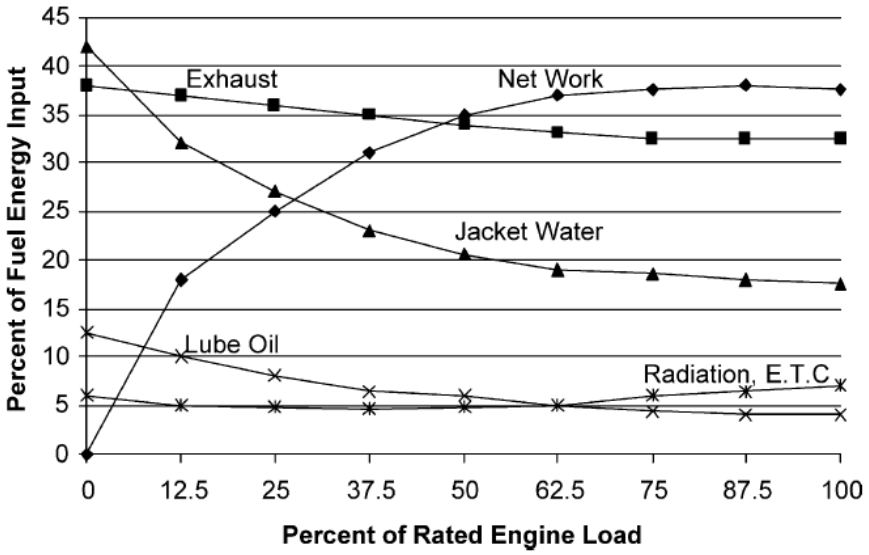

Fig. 2.3 Energy balance in a typical reciprocating I. C. Engine [1]

2.2 Methods and available technologies in trigeneration

Trigeneration system is related to energy conversion, recovery and management. A typical micro-trigeneration system comprises of five basic elements: the prime mover; electricity generator; heat recovery system; thermally activated equipment and the management and control system [2, 3].

2.2.1 Prime movers

A prime mover in a micro-trigeneration system generates the electricity and the waste

heat is recovered downstream. The selection of the prime mover depends on availability, system size, budget limitation and emission criteria.

Main prime movers include reciprocating engines, micro steam and gas turbines, stirling engines and fuel cell systems. Micro turbines, Stirling engines and fuel cells are relatively new technologies developed in last decade. Several other technologies are emerging like photovoltaic (PV) solar cell, solar thermal technology, thermoelectric technology etc [2, 3, 15].

The various energy sources and prime mover technologies are displayed in **Fig. 2.4.**

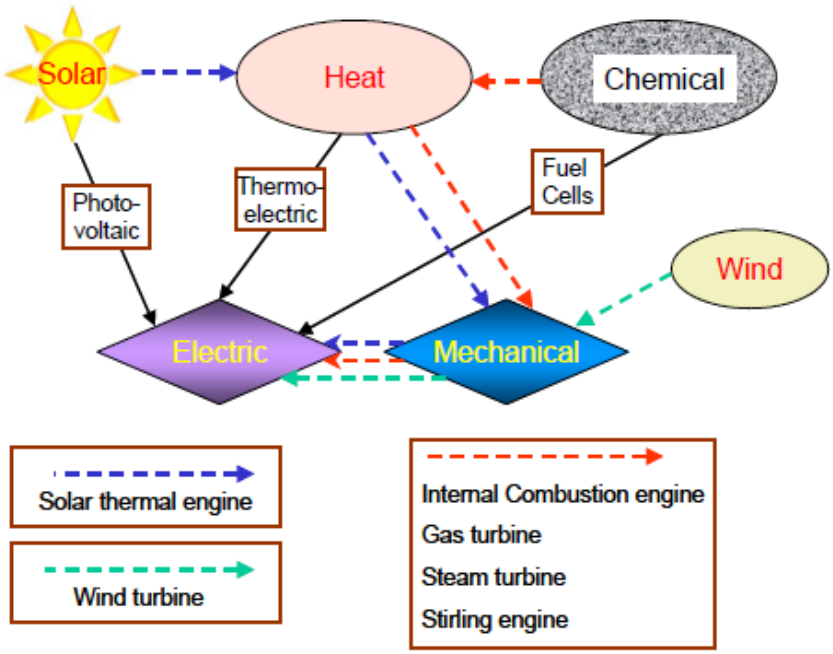

Fig. 2.4 Energy sources and prime mover technologies [15]

2.2.1.1 Reciprocating Engines

Reciprocating engines, particularly diesel engines as CCHP-prime mover have many advantages over other prime movers: proven and mature technology, availability in a range of sizes, lowest first capital costs of all trigeneration systems, fast start-up capability, high

operating reliability, fuel flexibility, moderate to high efficiency (25-45%), good load following, relatively high part load efficiency, high electricity/heat ratio, efficiency levels increases with engine size, low capital and operating cost, long operation life (15-20 years), easier adaptability to fluctuating demands, etc [1-5, 15, 17, 19].

But, there are some limitations of reciprocating engines: frequent maintenance, vibration, noise, and emissions issues. Also, full utilization of the various heat sources with diverse temperature levels in trigeneration applications is difficult [2, 3, 15].

These have been widely used in many industrial, commercial and institutional facilities for power generation, and also in trigeneration, but mostly in low and medium units.

Reciprocating engines are the obvious future option for the micro-trigeneration prime mover due to the advantages described above [2, 3, 15, 17].

2.2.1.2 Gas Turbines

Gas turbines range from 500 kW to 250 MW, making it suitable only for large-scale trigeneration systems. Part load efficiency of gas turbine being low, sizes smaller than 1 MW proves to be uneconomical [2, 3].

Gas turbines are easier to install than steam turbines, are less area intensive and have lower capital and maintenance costs.

The major limitations of gas turbines are: lower electrical efficiency, lower part load efficiency, requirement of premium fuels (especially natural gas), high temperatures involved requiring better materials, higher production costs, etc [2].

2.2.1.3 Micro turbines

Micro-turbine, or micro gas turbine is extension of combustion turbine technology to smaller scales (< 500 kW), and are based on regenerative or recuperative cycle [2, 3, 19].

Micro turbines offer many advantages: simple, compact, easy to install, long life, ease of maintenance, longer maintenance intervals, reliability, fuel flexibility, faster response, small size, less bulky, less noise and vibrations, etc. Also, the small-scale individual micro-turbine units can be combined readily into large systems with multiple units [2, 3, 15, 19].

Main limitations of micro turbines are: short track record, higher first costs, relatively low electrical efficiency, etc. Micro turbine power output decreases with higher elevation and higher temperature. Though the efficiency is low (~10%), it can work for residential micro-trigeneration because of high thermal/electric ratio [2, 15].

Recently, micro turbines have been developed using the regenerative Brayton cycle and high-speed centrifugal turbo machines, with the size ranging from 30 to 400 kW to serve small-scale applications.

However, their application in the residential sector is still very limited due to low electrical efficiency and inflexibility to load profile changes [20].

2.2.1.4 Steam Turbines

Steam turbines operate on clausius rankine cycle, a closed cycle.

Steam turbines have an extremely long life, and are very reliable. However, due to several limitations like low electrical efficiency, slow start-up time, and poor part load performance, their penetration in CHP/CCHP and distributed energy applications is very limited. These are more popular in large power plants or industrial cogenerations, where their range is from 50 kW to several hundred MW [2, 3, 15, 19].

Steam turbine technology is still in development phase for the small capacity market.

2.2.1.5 ORC engines

Organic rankine cycle (ORC) engine uses organic working fluids such as hydro-

carbons, refrigerants, silicone fluids, etc in contrast to steam rankine cycle engine which has water as working fluid.

Main advantages of ORC engine for micro-CCHP use are: robust technology, good controllability, less sensitivity to steam quality, low operating and maintenance cost, long life (>20 years), durability, cost effectiveness, lower operational temperature and pressure, high levels of safety, simplicity, possibility of utilizing heat from biomass combustion, use of waste heat and solar energy, good part load behaviour, no destructive erosion or fouling by wet vapour, etc [19, 20].

The major disadvantages in small and micro CCHP are: high specific investment costs, and low electrical efficiency (6-20%). However, in micro-CCHP, low efficiency can be countered by thermal/electric load matching for a typical application [15, 19].

ORC driven micro-CCHP are currently still in testing stage, and only a few small-scale prototypes have been studied [15, 19, 20].

2.2.1.6 Stirling Engines

Stirling engine, an external combustion device, uses a simple ambient pressure combustor, to provide a constant source of heat to move a piston, thereby doing work and produce electricity.

Two main types of Stirling engines show potential for residential trigeneration: kinematic Stirling and free-piston Stirling. Stirling engines generally are small in size, ranging from 1-25 kW, and can utilize low grade waste heat in micro-trigeneration systems [3, 19].

There are many advantages of Stirling engines: continuous and controllable combustion process, fuel flexibility, simple operation due to absence of valves, longer life, good part load performance, safe operation, low level of noise and vibration due to fewer moving parts, and low emissions. Solar driven Stirling engine is also promising.

The major limitations of Stirling engines for use in trigeneration include: high capital

cost, low specific power output and electrical efficiency (10-15%), slower response, longer start-up time and lesser durability of parts, etc [2, 3, 15, 20].

Stirling-based technology in trigeneration is still in the research phase.

2.2.1.7 Fuel Cells

Fuel cell directly converts chemical energy stored in the fuel (hydrogen) to electricity using oxygen or other oxidising agents through an electrochemical process (catalytic reaction), and produces water and heat as by-product [2, 3, 15, 19].

Most of the fuel cell micro-CCHP systems are either based on PEMFC technology, or on SOFC technology. [2, 3, 15, 19, 20].

In general, fuel cell systems have several benefits: reliable and quiet operation, clean and compact; high electrical efficiencies (up to 55%) even under varying load; modularity; very few moving parts; high reliability; produce very low emissions.

They normally run on hydrogen, but can also be run on natural gas, methanol or other fuels by external or internal reforming.

The major drawback for all fuel cells is high capital cost, short life of membrane, higher maintenance, slow in-transient behaviour, etc [2, 3, 15, 20].

Fuel cells are relatively immature technology, with unproven durability and reliability, and are still in the R & D stage. There are very few fuel-cell based micro-CCHP systems commercially available at this moment.

Schematic representation of micro-gas turbine CCHP, rankine cycle CCHP and SOFC based micro-CHP are shown in Fig. 2.5, 2.6 and 2.7 respectively.

Table 2.1 shows the comparison among different prime movers.

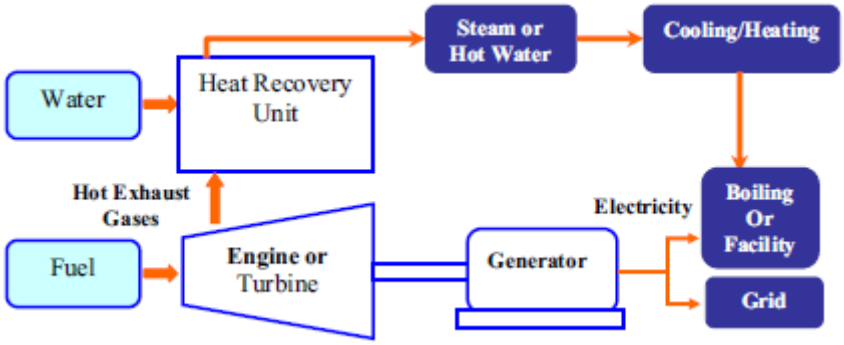

Fig. 2.5 Schematic representation of micro-gas turbine CCHP [14]

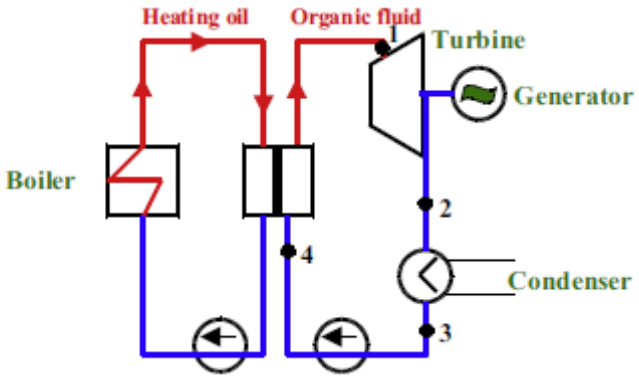

Fig. 2.6 Schematic representation of Rankine cycle CCHP [14]

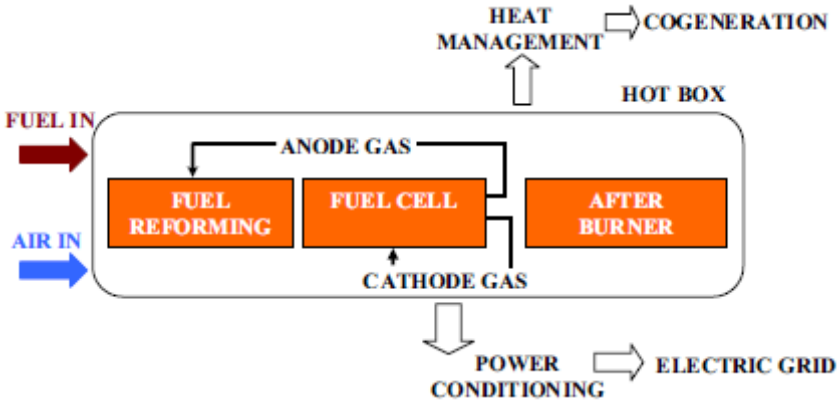

Fig. 2.7 Schematic of system interactions in SOFC based micro-CHP [14]

Table 2.1 Comparison among different prime movers [3]

Prime Mover	*Size (kW)*	*Pros.*	*Cons.*	*Emissions*	*Preferences and Applications*
IC engine	10-5000	• Low capital cost • Quick start • Good load following • High partial efficiency • High reliability	• Regular maintenance required	• High NOx using diesel • Natural gas preferred	• Working with absorption chiller • Small to medium scale
Combustion Turbine	5000-250000	• High quality exhaust heat	• Unacceptable low partial efficiency	• NOx 25 ppm • CO 10-50 ppm	• Application with huge amount of thermal need • Large scale
Steam Turbine	50-500000	• Flexible fuel	• Low electric efficiency • Long start up	• Depends on fuel	• Electricity as by product, thermal need preferred • Large scale
Micro-turbine	1-1000	• Flexible fuel • High rotation speed • Compact size • Less moving parts • Lower noise	• High capital cost • Low electric efficiency • Efficiency sensitive to ambient conditions	• NOx < 10 ppm	• Distributed energy system • Micro to small scale
Stirling Engine	Up to 100	• Safe and silent • Flexible fuel • Long service time • Can be solar driven	• High capital cost • Power output hard to tune	• Less than IC Engine	• Solar driven • Small scale
Fuel Cell	5-1200	• Operate quietly • Higher reliability than IC and combustion engine • High efficiency	• Energy consumption and GHG emissions due to H_2 production	• Extremely low	• Micro to medium scale

2.2.2 Thermally activated cooling technologies

Thermally activated technologies (TAT) typically refers to thermally activated cooling/dehumidification. Cascade utilization of waste heat using thermally activated technologies results in high efficiency and low emissions. Popular thermally activated technologies are: Sorption technology (absorption and adsorption) and desiccant dehumidification. In particular, absorption cooling is the dominant technology in micro-trigeneration, and in line with Montreal Protocol, 1987 and 1990 [2, 3, 15, 20, 21].

Vapour compression technology although reliable, compact and mature, is power intensive, and refrigerant leakages contribute to global warming and ozone layer depletion. The moving parts require frequent maintenance. Thermally activated technologies are free from these demerits [22, 23].

2.2.2.1 Absorption Cooling

While a vapour compression (VC) machine uses a rotating device (electric motor, engine, or turbine) to raise the refrigerant pressure, an absorption machine uses heat to compress the refrigerant vapours to a high pressure. The absorber and generator of vapour absorption (VA) system replace the compressor of a conventional VC system [2, 3, 19, 21].

An absorption chiller operates on absorption cooling cycle. A simple absorption cycle consists of four main components, an absorber, generator, condenser and evaporator. An absorbent and a refrigerant form a pair of working fluids. The most commonly used pairs are water/NH_3 and Li-Br/water. Usually, LiBr/water chillers are used in air cooling applications, while water/NH_3 chillers are used in small-scale air conditioning, even for refrigeration purposes in residential and industrial applications, and as heat pump in winter.

Advantages of vapour absorption chiller over conventional electric chiller are: 1) negligible electricity consumption; 2) waste heat recovery applications; 3) few moving parts (so, less noise and vibration); 4) no harmful emissions. They may be powered by steam, hot water, and oil, or can be directly fired with waste heat. But they are expensive and have slow transient response [2, 3, 15, 20, 21].

VA machines are available in 10-90 kW capacity range with COP typically between 0.5 and 0.6. Depending on number of times the heat is utilized within the chiller, absorption chillers are classified into single-effect, double-effect and triple effect VA machines. Double effect chillers can have COP up to 1.3, and triple effect chiller up to 2. But, higher stages

require higher driving temperatures, higher initial investment and more sophisticated control systems [2, 15, 19].

Ammonia-water systems

Small-scale ammonia chillers work in the range of 5-18 bar, and can operate at subzero temperatures (NH_3 freezing temperature is -77.7 °C), allowing a wide range of operation, with possibility of producing deep refrigeration.

Ammonia as refrigerant has many advantages: natural substance, low priced, no crystallisation problems, chemically stable, renders a compact construction, and is environmentally compatible. Ammonia has no ozone depletion potential (ODP = 0) and no direct global warming potential (GWP = 0).

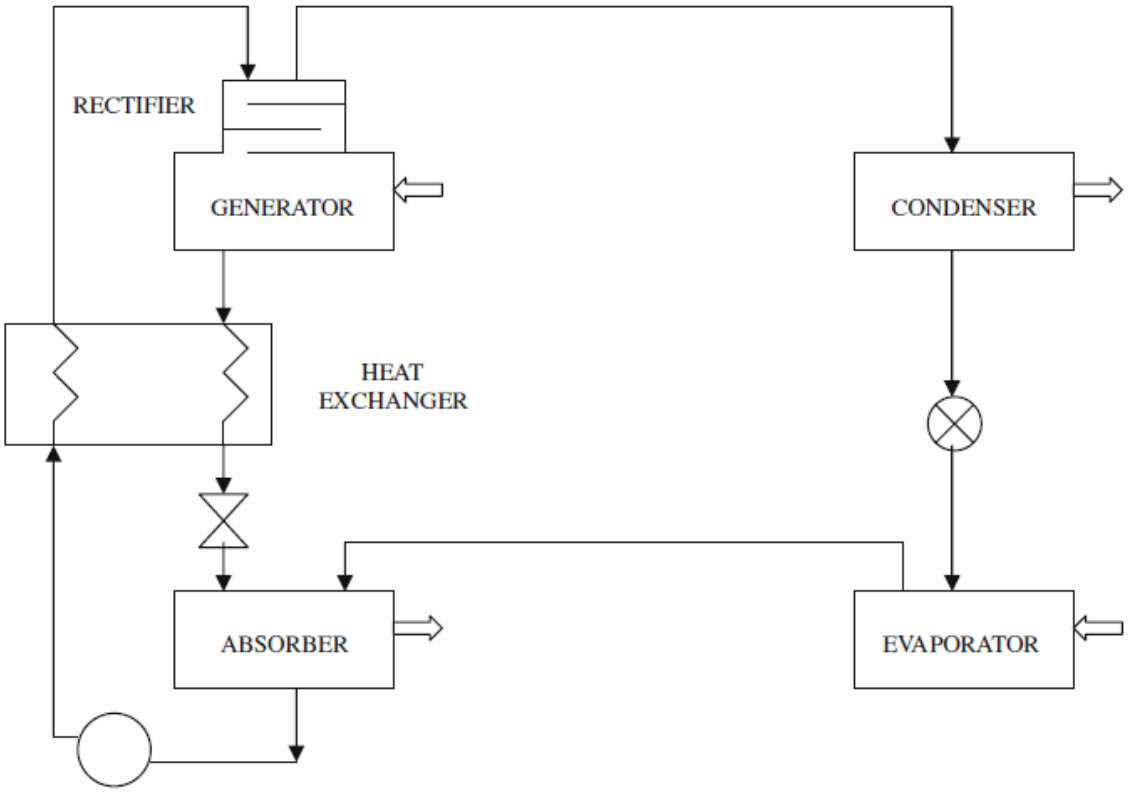

Fig. 2.8 Schematic of ammonia water refrigeration system [21]

Ammonia has a high enthalpy of vaporization and its freezing point is -77 ^{o}C, so, can be used at low temperatures. But, due to relatively low COPs, single effect absorption chillers

require a high fraction of waste heat (> 60-70%) [19]. Ammonia-water refrigeration system is shown in Fig.2.8.

Lithium Bromide-water systems

Systems operating on lithium bromide–water were commercialized in the 1940's and 1950's as water chillers for large building air conditioning. Li-Br –Water absorption system is also a well established cooling technology.

Its many advantages are similar to ammonia systems- few moving parts, less noise and vibration, no emissions, etc.

Main limitations of the water–lithium bromide are operation only at above 0^{o} C, crystallization, corrosive nature and high cost. Recently, small capacity single-effect systems (~10-30 kWth) are being developed and are available on the market [19, 21].

2.2.2.2 Adsorption Cooling

Adsorption refrigeration circuit consists of one or more solid adsorbent bed, condenser, expansion valve and evaporator. Solid adsorbent bed adsorbs and desorbs the refrigerant intermittently and provides cooling. [2, 3, 19, 20].

Advantages of adsorption technology are: robust technology, few moving parts, low electricity consumption, simple, requires no lubrication, little maintenance, quiet operation, short start-up time, no risk of crystallization, environment friendly, longer chiller life, modularity, readily scalable by additional beds for increased capacity, use of renewable energy resources, can be driven by lower temperature heat source etc.

The main limitations are: high vacuum-tight requirement, lower COP, intermittent operation, high cost, less mature technology [2, 15, 19].

2.2.2.3 Desiccant Dehumidifiers

Desiccant dehumidifiers can work alone or in combination with the sorption chillers

to meet dehumidification loads. Sensible and latent heat loads can be processed separately.

Low grade heat is required to regenerate the desiccants which can be supplied by the micro-trigeneration system [2, 20].

Desiccants are solids/liquids capable of absorbing/ adsorbing water vapour, acting on difference of water vapour pressure.

Desiccant materials include lithium chloride, calcium chloride, silica gel, zeolite or molecular sieve, aluminium oxide, etc. Solid desiccant cooling is chloro-fluoro-carbon (CFC) free, compact and saves energy, but is costly and less efficient [15, 20].

Advantages of desiccant systems are reduced power consumption, reduced growth of molds, compact equipment, etc.

Limitations include high cost of the desiccant equipment, limited application potential, clogging from foreign particles in the air stream, toxicity, and desiccant degradation if not controlled [15].

2.2.2.4 Other cooling options

New technologies for cooling options with waste heat recovery are also being developed, like engine-driven chillers, chemical heat pump, thermo-chemical accumulator, jet stream cooling machine, ejector cooling system, etc [2, 19, 20].

Other cooling options in research phase are: Metal hydrides, zeolites, thermo-acoustics systems, active magnetic regenerators, thermoelectric devices, air cooled Li-Br chillers, etc [22].

Table 2.2 shows comparison among various thermally activated technologies [3].

Table 2.2 Dominant thermally activated technologies [3]

Thermally activated technology	*Size (chilling power)*	*Pros.*	*Cons.*	*COP*	*Preference*
Absorption chiller	10 kW-1 MW	• Driven by steam • Low noise • Can be driven by low quality heat source • Low GHG emission	• Less efficient than compressor driven chiller	Up to 1.2	• Evaporation temperature LiBr/water: 5-10 ^{o}C NH_3/water: < 0 ^{o}C • Small to large scale • Double effect preferred
Adsorption chiller	5.5-500kW	• Driven by steam • Small size • Noise free • No corrosion and crystallization • No lubrication • Low GHG emission	• Can only be driven by high quality heat • High capital cost	0.6	• Small scale
Desiccant dehumidifier	N/A	• Control of humidity independent of temperature is allowed • Reduce the mechanical cooling load	• High capital cost • Regular maintenance required	N/A	• Solid:HVAC systems • Liquid: industrial and residential applications

2.2.3 Space heating methods

Space heating amounts to a quarter to third of total energy use in industrialized countries. Efficient options for space heating are concentrated in heat demand reduction, energy conversion efficiency and district heating. Traditionally, two types of heating systems are prevalent: forced air and hydronic heating. Hydronic heating systems provide even and comfortable heating, but are more expensive than a forced air heating system. The forced air heating system can also provide even heating if designed and installed properly [15].

Radiators, or radiant panels, or emitters are energy efficient sensible heating systems. In radiators, most of the heat output is by natural convection. Convection fins are used to improve their heat output, and hot water is passed through the hollow radiator.

They operate at moderate temperatures and can be directly coupled to renewable or waste energy resources, like waste heat. Central heating emitters are popular in domestic, business and industrial environments. Ducted air systems and skirting board radiators can be used to reduce the wall space occupied by radiant panels. Performance and output of heat emitters (radiators) is affected by the ventilation system, the forced convection, wall spacing and insulation. By decreasing their height from ground and increasing their spacing from wall, the output can be increased [24, 28].

Modern systems use fluid flowing in pipes (hydronic systems) to heat the floor. In underfloor heating, heat transfer takes place by conduction, radiation and convection, and is mostly based on combined radiant and convective heat transfer. Hydronic systems require skilled designers, with considerable installation and commissioning time and costs.

2.2.4 Thermal Energy Storage technologies

Thermal energy storage in a trigeneration system has many functions: reducing mismatch between heat demand and heat supply; storing the heat received from unsteady heat sources; storing excess heat when not required; overcoming the start up phase; avoiding frequent starts/stops; reducing the heat capacity of trigeneration

There are three main hot storage technologies.

• Sensible heat storages (SHS): sensible heat capacity of the storage material is utilised.

• Latent heat storages (LHS): latent heat of the storage material is used during isothermal solid/liquid phase change.

• Thermo-chemical storages: heat is stored in a reversible chemical reaction.

In addition, Metal hydride storage technology is also emerging [19].

2.2.5 Simulation and Optimization tools in trigeneration

Optimization of energy systems should be based on a systems approach, leading to better understanding about the suitability of technologies. There are possible objective functions such as minimizing carbon emissions, minimizing total costs, and maximizing

energy output. The point is to integrate them into one volume considering the pertinent regional priorities in the process of integrated analysis.

Simulation and optimization tools have played a major role in better understanding and control of polygeneration and distributed generation systems. The tools are categorised as: (1) Economic tools (RETSCREEN, HOMER, etc); (2) Simulation tools (TRNSYS, EnergyPlus, etc); (3) Optimization tools (EnergyPlan, etc); (4) Data-bases (CO2DB); and (5) Externalities and environment impact calculation tools (Extern E, ECOSENSE, etc).

Urban districts and communities represent an optimal scale for combining energy conservation programmes like distributed generation, local generation, microgeneration, polygeneration etc.

For large complex systems like a city, an advanced multidisciplinary approach is needed. Some visions of future energy systems reported are: (1) Microgrids (local distributed systems) (2) Virtual power plant (based on IT) (3) Integrated Energy System (distributed power generation) (4) Intelligent power grids (active grids) (5) Energy Hubs [26, 27].

2.2.6 Operating strategies in trigeneration

The operation strategy is important in maximising the overall performance of a trigeneration system. Good operation strategy reduces the primary energy consumption, as well as the costs and emissions [20].

Following the thermal load (FTL) and following the electric load (FEL) are the two most investigated and classical operating strategies for trigeneration. They are also referred to as thermal demand management (TDM) and electric demand management (EDM).

When the FTL strategy is implemented, the trigeneration system will first meet the thermal demand (cooling and heating), then and if electricity produced by trigeneration is not sufficient to meet the electric load, additional electricity will be purchased from the local grid to cover the gap.

When the FEL strategy is implemented, the trigeneration system will first meet the electric load, then and if heat produced by trigeneration is not sufficient to meet the thermal

demand (cooling and heating), additional fuel will be purchased to feed the auxiliary boiler to generate additional heat [3, 20].

However, both FEL and FTL strategies can inherently waste some energy. For e. g., in FEL strategy, if sufficient electricity is produced to meet electric load, yet if the thermal demand is less than that which is produced, then the excess thermal energy will be wasted. Similarly, in FTL strategy, some excess electric energy will be wasted or remain unutilised. Factors governing the choice between FEL and FTL strategy are: fuel costs, availability of thermal or electric energy storage (for storing excess energy), and option to sell electricity to grid [3, 20]

2.3 Trigeneration status and market potential

The CCHP has grown rapidly in the last decade. Various countries have developed energy policies and support mechanisms to promote the CCHP systems. A brief account of development of CHP/CCHP systems in representative countries is as follows.

2.3.1 Worldwide Status of Trigeneration

United States

After the U.S. government proposed the Public Utility Regulatory Policy Act (PURPA) in 1978 with the option of selling back the excess electricity, the installed capacity of CHP/CCHP systems grew from 12 GW in 1980 to 45 GW in 1995.

In 2005, the Energy Policy Act came in force, and by 2009, the installed capacity had achieved 91 GW.
The U.S. DOE aims for 11% increase of CHP share of the U.S. electric power by 2030 [2, 3].

European Union

In European Union (EU), there are important legislative initiatives for CCHP development, like the European Directive 2004/8/EC, the Cogeneration Directive, the

Emissions Trading Directive, the New Electricity and Gas Directives, and the Energy Performance of Buildings and Taxation of Energy Products Directives.
In 2010, the total installed capacity of CCHP in EU had exceeded 105 GW, with Germany leading with 22%, followed by Poland and Denmark with 9% [2, 3, 20].

China

China has issued a series of policies since 1980s, like the Energy Saving Law, the Renewable Energy Law, the Air Pollution Prevention Law and the Environment Protection Law, to support the development of CHP/CCHP plants.

In 2006, 'China Energy Conservation Technology Policy Outline' recommended CHP development in large and medium-sized cities.
The 2007, 'Implementation Scheme of the National 10 Key Energy Conservation Projects' further specified supporting policies for CHP.
In 1990, the total installed CHP capacity in China was only 10 GW. A goal of 30 GW in 2000, 70 GW by 2005, and 80 GW by2006 could be achieved [3].

Other countries

In Japan, the 'Energy Policies of IEA Countries: Japan 1999 Review', the target of cogeneration was expected to increase from 3.85GW in 1996 to 10GW in 2010. Russia is a leader in CCHP development in the world, with 30% of electricity generation from cogeneration. In Africa, CCHP development remains in a primary stage [2].

2.3.2 Status of trigeneration in India

In India, CCHP started with 87 new local power projects, producing 710MW from sugar cane waste. In 2001, total potential for 15GW of cogeneration capacity was estimated.

The CCHP systems capacity in India is 4.1 GW, about only 3.6 % of total electricity capacity.

Main barriers for CCHP development are highly unreliable electricity supply, lack of government grants and loans, lack of adequate policy framework, lack of technical knowledge and support services, shortage of investment finance, etc. CCHP development in India is mainly in the form of Bagasse-based cogenerations in sugar mills [2].

India still is far away from a rise in CCHP applications. User demands, technology selection and revenue consideration are the keystones to a successful CCHP application. Government policies, liberation of the electricity market and electricity/fuel prices are critical in the development of CCHP.

Fig. 2.9 shows the CHP share of total national power production of various countries.

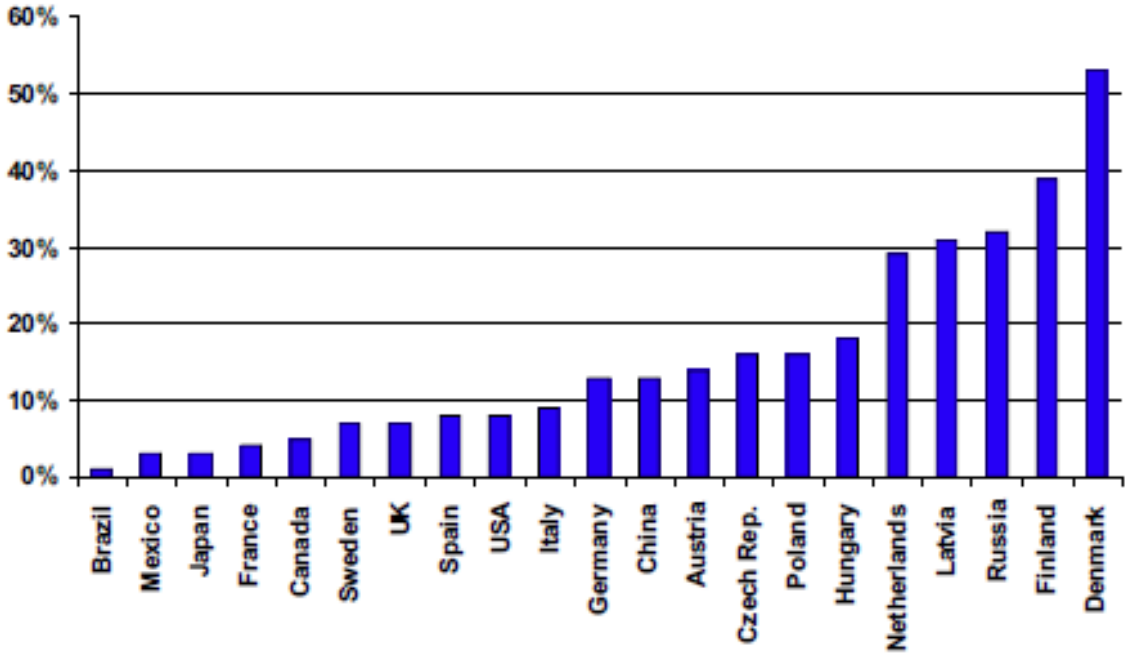

Fig. 2.9 CHP share of total national power production (till 2006) [15]

2.3.3 Trigeneration market penetration

Packaged trigeneration units have been developed for use in variety of residential, commercial and institutional applications. Typical systems are in 1–100 kW size range.

Residential and small applications of CCHP require high efficiency, less maintenance, low noise and reduced emissions. Micro-CHP using IC engines for single-family residential application are built mostly in Germany, Japan, Switzerland, China and Italy.

The most known units are Senertec (5.5 kWe), Ecopower (4.7-2 kWe), Honda (below 2 kWe), Toyota (14.4 kWe) and Yanmar (up to 25 kWe) [1, 15, 19, 29].

Development of solar based systems is also being researched [3].

2.4 Motivators and Barriers in Micro-trigeneration

Key motivators in Micro-trigeneration development are: more choices for useful energy outputs; high energy conversion efficiency; utilization of low grade heat; need for higher quality power supply; energy security; vast reduction in CO_2 emissions; fuel flexibility; reduced concerns about system vulnerability; government support for CHP/CCHP; growth of a new market segment; enhanced economic activity; new employment potential; reliable and sustainable decentralised energy supply [14, 15].

In certain consumption structures, micro-trigeneration is already a comprehensive solution for energy supply. A household sized micro-trigeneration system is a good flexible energy solution for small social communities. Yet, its applicability to domestic users in individual households needs further development to be widely acceptable. The obstacles in development of CCHP market come from every direction: technology, performance, costs, policies, regulations and market demands.

Key barriers in Micro-trigeneration development are: high fuel/energy prices and price volatility; non-standardized grid access; non-standardised CCHP components; monopoly of energy utilities; unclear emissions standards in trigeneration; unclear government policy regarding CCHP; lack of monitoring and enforcement by the government ; less public awareness; insufficient incentive policies; non uniform design standards; difficulties in manufacturing equipment; immature technology; poor market acceptance; high capital costs; shortages of investment finances [2, 3, 15, 20].

2.5 Recent research trends in Trigeneration applications

Review of development, working, components and technologies of various cogeneration and trigeneration systems was conducted by various researchers. The reviews were mainly focussed on single-family applications. Environmental and economic issues were also considered. Worldwide status of the CCHP development, and management,control, sizing and system optimization were also analysed [1, 2, 3].

Energy, exergy, and exergoeconomic analysis was conducted for diesel engine powered cogeneration system and omponents. Specific Exergy Costing (SPECO) method was used for cost analysis to maximize the benefit and/or to minimize the cost [4].

Study of a trigeneration application was carried out based on the data of a currently active insulated pipe production plant situated in Istanbul, Turkey. Feasibility study was carried out to calculate the profitability and payback period [5].

A household size tri-generation based on a H_2 fuelled diesel engine generator was investigated for performance and emissions using ECLIPSE simulation software. Results showed enormous potential for fuel savings and reductions in CO_2 emissions in cogeneration and trigeneration as compared to single generation [6].

Another household size trigeneration based on a small-scale diesel engine-generator set, vapour-absorption unit and heat exchanger was designed and realized in laboratory. Experimental test results show that the total thermal efficiency of trigeneration is much higher, and the CO_2 emission is much lower than that of the original single generation [7].

Testing, performance and economic evaluation for a utility company of a new prototype, gas-fuelled, 4-kW cogenerator has been reported. With an overall efficiency of 45%, this unit is targeted for use by a small business or homeowner [8].

Performance assessment of various building cogeneration systems was conducted under identical conditions, through energy and exergy efficiencies. The diesel engine and geothermal systems appeared to be thermodynamically more attractive with higher exergy efficiencies than steam-turbine and gas-turbine systems [9].

The energy available from an LPG fuelled IC engine was utilized to run the compressor of conventional air-conditioner and an electric generator for cooling, illumination

with running a fan inside a cabin and to charge a battery, along with hot water production using a heat exchanger. Overall efficiency of 96% was achieved, along with economical and environmental benefits [10].

Modulating flow cascade heat recovery system was introduced to recover waste heat with minimum exergy destruction. Over 13% rise in COP of the absorption chiller at 50% engine load was obtained over conventional fixed flow system [11].

Experiments were conducted on a small-size (3.7 kW) diesel engine based micro-trigeneration system realised in a lab. Performance and emission results showed that for trigeneration, the total thermal efficiency is much higher, and the CO_2 emission is much lower than that of single generation [13].

A review of Micro combined heat and power (MCHP) technologies and applications also conducted a comparison among the MCHP systems for the prime mover technology, electrical and thermal power, efficiency and emissions [14].

In another review, strategies for development, demonstration, and commercialization of integrated CHP systems for residential applications were evaluated. Energy conservation, environmental impact, economics (both capital cost and operational costs), scalability, flexibility, reliability, and security of the proposed configurations were discussed [15].

Transient and stationary operation of a natural gas fuelled ICE based cogeneration unit (6 kWe & 11.7 kWth) was performed and analysed. The results were compared with base-case data and also that obtained from simulation model developed within IEA/ECBCS Annex 42 framework [16].

Thermodynamic and exergy analysis of the existing diesel engine cogeneration system was performed. The thermal efficiency of the overall plant was found to be 44.2% and the exergetic efficiency was 40.7% [17].

Literature on energy balance of internal combustion engines operating on alternative fuels was reviewed. Effects of engine variables and design factors on energy balance, using thermodynamic models were explored [18].

POLYSMART (POLYgeneration with advanced Small and Medium scale thermally driven Air-conditioning and Refrigeration Technology) is a project partly funded by the EU,

to develop technical solutions for micro-CHCP systems (Deliverable D1-7 of Work Package 1). It has conducted detailed survey and analysis of trigeneration systems [19].

A comprehensive review of the latest developments in the field of CCHP generation along with supporting mechanisms, prime movers, cooling technologies, system configurations, fuels employed etc were presented and discussed [20].

IC engine exhaust gas as energy source for an ammonia–water absorption system was experimentally studied. The refrigerator reached a steady state temperature of 4-13 ^{o}C about 3 hours after system start up. Emissions of HC increased and CO reduced but CO_2 emissions remained unaltered [21].

A 10.55 kW absorption chiller was modified for exhaust gas intake from a 2.8 L V6 IC engine. System performance was enhanced. The concept could be used in transportation vehicles. However, transient operations, scalability and reliability require further investigation [22].

A review has been conducted on heat powered sorption techniques. High potential of emission saving exists using distributed poly-generation units for space heating /cooling [23].

Potential benefits of radiant panels coupled to ground-source heat pumps were analyzed using a new engineering metric based on Rational Exergy Management Model. Different scenarios were compared with a radiant panel system.

As per IEA Annex 49 for low-exergy buildings, actual benefits in controlling CO_2 emissions could be generated if heat pump is driven by renewable energy sources, or optimally matched with CHP systems, preferably running on alternative fuels [24].

In a study, emissivity and the roughness of a wall behind a radiator were altered and effect on the radiator heat output was observed. Presence of large roughness and a high emissivity of surface increase the heat flow rate by about 26 % compared to a smooth shiny surface [28].

A prototype small-size ammonia–water refrigeration plant (20 kW) was developed. It was driven by the exhaust gas of a microturbine or a reciprocating engine to realize a cooling-heating-power system. A good response on part load was observed through simulation

results, and it shows the possibility of working at varying generation and evaporation temperatures [29].

An experimental investigation and energetic analysis of a natural gas and LPG-fired micro-CCHP system using a small-scale silica gel–water adsorption chiller was conducted. With evaporation temperature at 13 ^{o}C, the COP of the adsorption chiller and overall efficiency were found to be 0.3, and 70% respectively [30].

A thermodynamic analysis was performed for the case of tri-generation with an absorption chiller. Limits for the best energetic performance of tri-generation were established [31].

Energy and exergy analyses were conducted for space heating in the buildings, based on a pre-design analysis tool [32].

Energy-conservation opportunity in cogeneration with double-effect absorption chiller in an institutional building in Bangkok was studied. Technical and economic feasibility was evaluated, and cash-flow analysis was done. Cogeneration with and without thermal energy storage (TES) were studied and compared.

A potential of 13% and 23% peak demand reduction, 16% and 21 % savings in energy consumption and 21% and 25% Internal Rate of Return (IRR), respectively, were obtained [33].

Energy and exergy analysis of a novel biogas powered 1 TR single-effect NH_3–H_2O absorption refrigeration system was carried out using a computational model.

For the generator temperature range of 50-70 ^{o}C, the COP was in the range of 0.159–0.33, whereas exergy efficiency was in the range of 0.29–0.80. The highest and the lowest exergy loss was found to be in the generator and the condenser, respectively [34].

The design of a system of trigeneration was presented. A regenerative-cycle cogeneration system and a new trigeneration system were studied, showing benefits as well as the operation criteria for both processes [35].

A water stream heated by the hot exhaust gases was utilized for comfort heating of the passenger compartment of a commercial minibus with an air-cooled engine. Comfortable compartment temperatures were obtained with above 0 ^{o}C ambient temperatures [36].

A parametric model for design and techno-economic evaluation of internal combustion engine (ICE) based residential cogeneration systems was presented.

Results of sensitivity analyses, obtained using the model with a building simulation program provides an insight into the energetic performance of ICE based cogeneration systems [37].

Cooling costs in a hospital trigeneration system for electric, heat and cooling power were calculated using energy and exergy approach [38].

Environmental impact resulting from the combustion of biodiesel fuel in thermoelectric power plants utilizing CHP has been evaluated and quantified. The ecological efficiency for pure biodiesel fuel (B100) is 98.16%, and for conventional diesel is 92.18%, considering thermoelectric power plant thermal efficiency to be 55% [39].

A mathematical model based on second law analysis on the heat transfer of a horizontal concentric tube heat exchanger was developed, and the results were presented. Reasonable agreement in results was found with measured data [40].

A trigeneration test rig with a microturbine, an absorption chiller, and a display cabinet was set up in the laboratory. Based on heat and mass balance and flow paths, various component simulation models were developed and validated with test results. System performance was investigated for application feasibility into a supermarket energy control system [41].

Performance of a compression ignition engine was theoretically investigated using DIESEL-RK software. Engine parameters were calculated using diesel–ethanol and diesel–ether mixtures as fuel.

Highest thermal efficiency was obtained with 15% ethanol–diesel blend [42].

An overview of the energy-use characteristics of the Chinese housing stock was portrayed. Draft building-energy standard was described. Potentials for energy conservation were also evaluated using a computer program [43].

Low temperature and conventional radiator heating system were studied for both detached houses and apartment buildings in North and Central Europe climates. Heating

curve of 45/35 ^{o}C for detached houses and 40/30 ^{o}C for apartment buildings were recommended [44].

It was concluded that most of the literature on trigeneration is based on theoretical/simulation methodologies like, SPECO method, ECLIPSE software, thermodynamic analysis, exergy analysis, REMM model, computational model, parametric model, economic/environmental theoretical analysis, etc. Very little experimental investigations were conducted on trigeneration systems.

On the other hand, majority of studies were related to medium/ large scale CCHP systems, like hotels, hospitals, pipe production plant, institutional buildings, apartment buildings, or, on different systems, like transport systems, design of system, etc.

Little experimental research has been conducted on real size micro-trigeneration system. Also, very little experimental work has been conducted using straight vegetable oils or biodiesels in micro- trigeneration with space cooling/heating as well as fuel pre-heating.

Hence, in order to fill the gap, in the proposed work, it was planned to develop a demonstration unit for alternative fuel based micro-trigeneration system with fuel preheating, space cooling/heating and power generation for residential applications. Exhaust driven modified electrolux vapor absorption system for space cooling along with fuel preheating provided a novel approach to the proposed micro-trigeneration system.

2.6 Straight Vegetable Oil

For the developing countries of the world, like India and in case of agricultural applications, fuels that can be produced in rural areas in a decentralized manner, near the consumption points are favoured.

Straight vegetable oils (SVO) can provide a solution to problems of environmental degradation, energy security as well as rural employment and agricultural economy.

Since India is not self sufficient in edible oil production, hence some non-edible oil seeds available in the country are required to be tapped for use as fuel. Non-edible vegetable oils from jatropha, karanj, linseed, mahua, rice bran, neem etc. are potentially effective diesel substitute [47, 51, 55, 57, 63, 65, 68, 70, 72, 73].

2.6.1 Production, composition and characteristics of SVO

SVO Production stages

Vegetable oil produced on small scale usually for local use in natural form, simply filtered unlike industrially produced refined vegetable oils is called Straight Vegetable Oil.

SVO is biodegradable, non-toxic and safe in storage and transportation. It can be used in diesel engines with minor modifications, either as an extender or as complete replacement to diesel fuel.

The fuel quality of SVO depends on the nature of the oil-seeds and their treatment. SVO displays highly variable physico-chemical characteristics depending on the nature of the oil-seeds, and on extraction and drying conditions.

SVO production has three major stages: Oilseed storage after harvest; Seed crushing; Oil processing. The successive operations for SVO production require a press, filters and/or decantation tanks, and storage tanks.

SVO production process is given in Fig. 2.10.

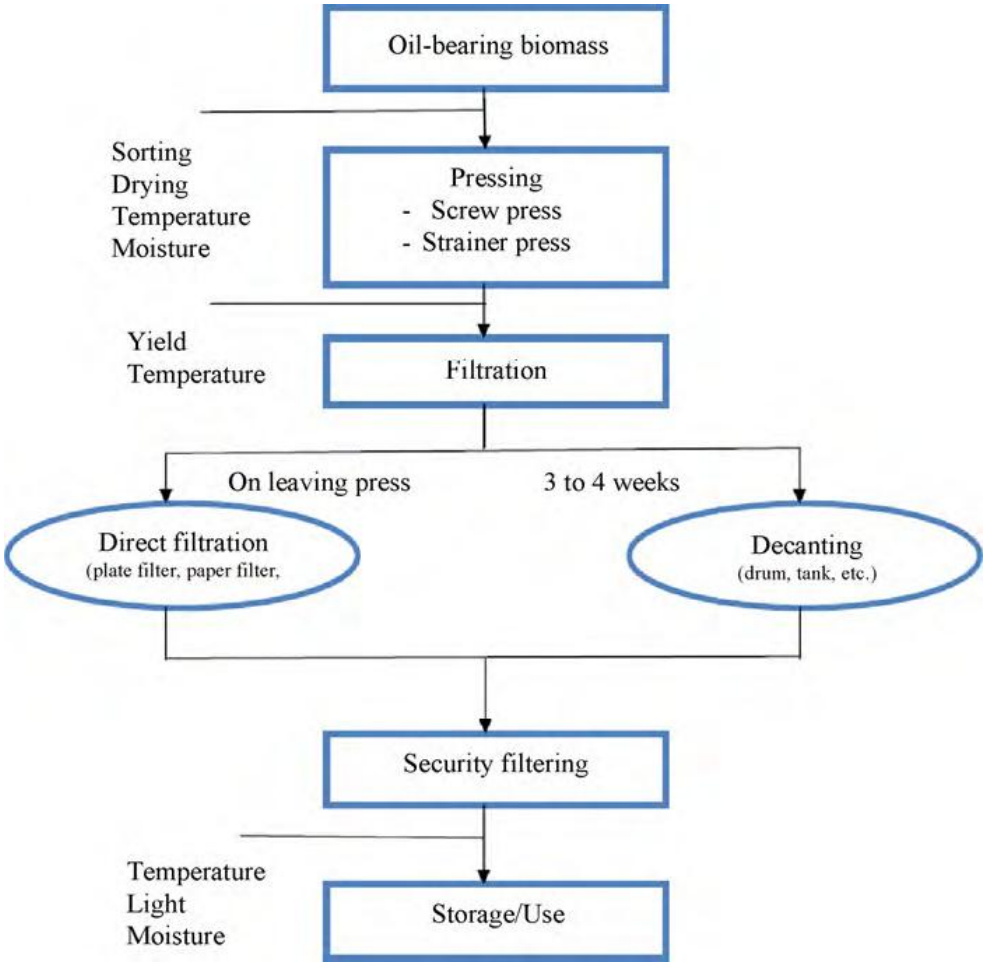

Fig 2.10 Technical process for SVO production [45]

Vegetable oil composition

Vegetable oils are lipid material derived mainly from plants, with only carbon and hydrogen atoms in straight or branched chain structures, and aromatic configurations.

They consist of about 90-98% triglycerides; the remaining as diglycerides, monoglycerides and free fatty acids. Triglycerides contain three fatty acid molecules and a glycerol molecule.

The structure of typical vegetable oil molecule is given in Fig. 2.11. Here R^1, R^2 and R^3 represent straight chain alkyl groups [51, 55, 72, 75]

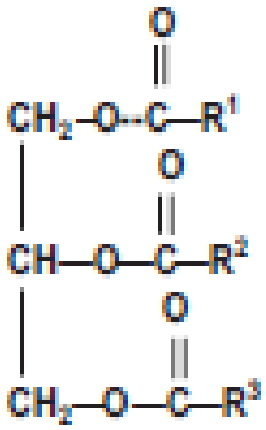

Fig. 2.11 Vegetable oil molecule structure

Characteristics of Straight Vegetable Oils

Chemical characteristics

Nature of fatty acids - The nature of fatty acids largely determines their ability to burn correctly in an engine. Low iodine value indicates high degree of saturation of oil, and is propitious to good combustion. Combustion quality decreases with unsaturation.

Phospholipids content- They are undesirable constituents, and vary in concentration depending on pressing and filtering techniques. They are responsible for the gumming phenomenon in engines.

Wax content- Waxes are long-chain fatty acid-esters and alcohols, and are problematic in engine when run in cold conditions.

Peroxide value- It determines the oxidation level of the oil, and thereby also its degree of stability [45].

Physical characteristics

Most of the properties of vegetable oils fall within a narrow range and are closer to those of diesel.

Kinematic viscosity - SVOs have 10–15 times higher kinematic viscosity (~ 30-40 cSt at 38 ^{o}C) than diesel, due to larger molecular mass (600-900 g/mol) and chemical structure.

Density- SVO density is 10% higher, on average, than that of diesel oil.

Calorific value (CV) - The CV of vegetable oils is lower than that of diesel (~ 45 MJ/kg), by around 10–15%. Low CV is due to presence of fuel-bound oxygen, carbon chain, triglycerides, and free fatty acids present in the vegetable oils.
The CV is not specified in ASTM D6751 and EN 14214 biodiesel standards, but prescribed in EN 14213 with a minimum value of 35 MJ/ kg.

Flash point - It is the minimum temperature at which the vapours of oil, under standardized conditions, ignite when exposed to a flame. Flash point is a measure of flammability of fuels and thus an important safety criterion in transport, handling and storage.
Generally, it is much higher for SVOs (158-318^{o} C) than for diesel (55-60^{o} C).

Cetane number - The cetane number for most SVOs (29-43) is lower than that for diesel (45-55). It results in difficult cold start-up and increased noise. Proportion and location of double bonds affects cetane number of vegetable oils.

Cloud and Pour point - The cloud and pour points are cold flow properties of fuel and important in low-temperature applications.
The cloud and pour point of vegetable oils are generally higher than that of diesel fuel, but vary significantly with feedstock.

Miscibility with diesel - SVOs are completely miscible with diesel and blending in any proportion is possible to improve the fuel viscosity and cold-flow properties. The most common blend is found to be a mix of 20% biofuel with 80% diesel in recent scientific investigations [47, 51, 55, 57, 61, 75-78].

Standards for SVOs

Currently, there is lack of quality standards for vegetable oils as fuel. A pre-standard DIN 51605 (German origin) exists for checking quality of SVOs. But, it involves complex analytical tools difficult to implement, especially in rural sectors of developing countries.

Renewable fuel standard (RFS) program of US Environmental Protection Agency is planning to ensure that transportation fuel sold in the United State contains a minimum volume of renewable fuel required to be blended into transportation fuel. However, some common practices are followed. The impurities must be less than 2% and moisture content less than 9% in weight. The oil must be filtered to 5 mm with a H_2O content of 750 and 30

ppm phosphorus. Upstream adaptations (dual fuelling, blending, preheating, etc.) or engine modifications (injection settings, etc) may be required for SVO use in diesel engines [45].

2.6.2 Recycling of Carbon-dioxide by SVO

SVOs and BD have short carbon cycle period (a few years) as compared to millions of years for petroleum fuels. Plants while growing absorbs more carbon dioxide (CO_2) from the atmosphere during the process of photosynthesis than is added by the SVO later during combustion, leading to net atmospheric CO_2 reduction. Thus, CO_2 emitted during combustion of SVO/BD is recycled in the photosynthesis process of the plants in the following crop cycle. This helps in mitigating global warming, and is in accordance with the goals of the Kyoto Protocol. A biodiesel life cycle study in 1998 jointly sponsored by the US Department of Energy and the US Department of Agriculture has also concluded that biodiesel decreases net CO_2 emissions by 78.45% compared to conventional diesel [45, 68, 78, 79, 80, 81].

2.6.3 Advantages and limitations of SVO

SVO as fuel for diesel engines offers many advantages:
Local production in rural areas can contribute to the local economy; biodegradable, non-toxic and renewable fuel; characteristics similar to those of pure diesel; low sulphur content; flash point higher than that of diesel, thus safer in use; higher reduction of most of the emissions as compared to diesel; possibility of small-scale production for power generation/irrigation; reduction in crude oil import; employment generation; improvement of CO_2 balance, etc [47, 58, 72].

But, there are many limitations of SVO as fuel use:
Direct use as fuel not satisfactory; SVO quality affected by nature of oilseed, soil, climate etc; high viscosity, poor volatility, polyunsaturated character interfere with the injection process; poor fuel atomization, improper mixing of fuel with air, leading to incomplete combustion; loss of power and economy; operational problems; engine durability issues like severe engine deposits, injector coking, gum formation; problems during cold weather, etc [47, 51, 57, 58, 72, 82].

2.6.4 Methods for SVO use as fuel

Two strategies can be employed to overcome high viscosity problems - modifying the engine, or processing the fuel. Modification of engine requires new injector, glow plugs, filter

and heat exchangers etc. Fuel modification is more practical especially in rural community, as it is a cheaper and simpler option [57, 55, 82].

Fuel modification is mainly aimed at reducing the viscosity to eliminate fuel atomization related problems. Major techniques to reduce the viscosity of vegetable oils are discussed below:

Dual fuelling

For direct SVO use, 'dual fuelling' is recommended. Duel fuelling consists in starting up the engine with diesel, then injecting vegetable oil once the engine load is sufficient to give a high temperature in the combustion chamber (~ 500^{o} C).

This enables total fuel combustion. Finally, the engine is stopped with diesel, so the feed circuit is well cleaned again. In dual fueling, SVO is heated up in combustion chamber and becomes more fluid and less viscous leading to better combustion [45].

Preheating

Preheating the vegetable oils prior to injection reduces its viscosity, and improves the spray characteristics of the fuel–air mixture, which results in improved performance and reduction in emissions [47, 72].

Blending

Viscosity, density and NCV of SVOs generally decrease in line with the quantity of vegetable oil in the blend. Vegetable oil blend up to 10% does not require engine modifications. Most of the research studies concluded that Diesel engine with 20% SVO/BD blend with diesel would run without major engine problems, and performs similar to diesel, with good performance, emissions and endurance results [45, 47, 72, 76].

Micro-emulsification

A micro-emulsion is a colloidal equilibrium dispersion of optically isotropic fluid microstructure with dimensions generally in the range of 1–150 nm range, formed spontaneously from two normally immiscible liquids, and are capable of reducing NOx and

PM. But, fuel emulsification may lead to corrosion, derated power and other engine problems. Micro-emulsions of vegetable oils with solvents, like methanol, ethanol and butanol have been investigated [47, 72].

Pyrolysis/Cracking

Pyrolysis is application of heat in the presence of a catalyst, and in absence of oxygen/air. Cleavage of chemical bonds occurs to yield small molecules. The pyrolised material can be vegetable oil, animal fats, or fatty acids methyl esters [47, 72].

Transesterification

Transesterification of vegetable oil involves reaction of triglycerides (fat/oil) with alcohol in presence of a catalyst, to form esters and glycerol. It is the process of exchanging the alkoxy group of an ester compound by alcohol and the reaction often catalyzed by an acid or a base. The fuels produced by transesterification of the oils are called biodiesel [47, 72].

Undoubtedly, transesterification is well accepted and best suited method, but it requires expertise and costly processing.

Vegetable oils can play a vital role in decentralized power generation for irrigation and electrification in remote agricultural areas. Blending with diesel, dual fuel operation or fuel preheating can be good options, particularly in rural and remote areas of developing countries, where it may not be possible to chemically process locally produced vegetable oils due to logistics problems in rural settings. These methods reduce viscosity substantially, leading to reduced emissions and improved performance [63, 72].

2.6.5 Fuel preheating and engine optimization

2.6.5.1 Fuel preheating

High viscosity of vegetable oils leads to poor atomization and cause incomplete combustion and more fuel consumption. Preheating is an important modification for engines running on vegetable oils. Preheating of inlet fuel reduces viscosity, and can lead to good mixture formation and lower HC emissions. Fuel preheating can be done by installing a

heater (electrical or using hot exhaust gases) and to maintain adequate fuel temperature, which may lead to a three to fourfold decrease in the viscosity. Preheated vegetable oils show similar performance to diesel with increased peak pressure and reduced ignition delay when compared to the straight vegetable oil [56, 63, 75, 82].

2.6.5.2 Engine optimisation with varying IOP and IT

The transesterification process although most effective method, adds to extra cost. Fuel modification reduces the viscosity but other problems due to the differences in the properties like cetane number still exist.

Minor modifications in engine operating parameters can be an effective method to improve the combustion of SVO and their blends. The design and operating parameters of available engines are standardized for diesel only. For all other fuels, the engine parameters must be optimized in view of the specific fuel properties [73, 74].

Increased injector opening pressure and advancing the Injection timing has a significant effect on the performance and emission characteristics of diesel engines. Such settings enhance the atomization of fuel, resulting in a more distributed vapour. Better mixing during the ignition delay period and improved combustion reduces HC and smoke levels.

But, a very high injection pressure and too much advanced Injection timing can adversely affect fuel distribution in air. On the other hand, retardation of the injection timing leads to lower temperature, the NOx emissions may also reduced, but it may lead to increase in smoke emissions [61, 63, 73].

2.6.6 NOx in diesel engines

In diesel exhaust, NOx is primarily composed of NO, with lesser amounts of NO_2, and negligible N_2O, N_2O_5 and NO_3.

2.6.6.1 Mechanism of NOx formation

In general, there are three NOx formation processes: Thermal NOx, Prompt NOx and Fuel NOx.

Thermal NOx is the primary contributor to total NOx in diesel engines. NOx is formed when nitrogen and oxygen (from air) react at the extremely high temperatures reached during combustion [67, 70].

2.6.6.2 NOx reduction techniques

Common techniques to reduce NOx emission from diesel engines include retarded fuel injection timing, exhaust gas recirculation (EGR), fuel modification, staged injection of fuel, exhaust catalysts, fuel-water emulsification, water injection, inlet-air cooling, and after-treatment approaches etc.

NOx reduction by altering fuel properties is highly limited. Cetane improving additives are expensive, and promote auto oxidation in biodiesel. Also, inadequate reduction of NOx using them has been reported. Retarded injection leads to increased fuel consumption, reduced power, increased HC and excess smoke. Water injection is prone to corrosion, and maintaining a water storage tank adds weight to engine system.

After-treatment approaches employed to reduce NOx emissions involves two approaches-use of a NOx adsorber catalyst (NAC), and use of selective catalytic reduction (SCR), but they are costly.

Exhaust gas recirculation (EGR) is an effective and low cost technique for NOx control. The major effect of EGR is reduced temperature, and reduced oxygen content in the cylinder. Cooled EGR (exhaust gas cooled to room temperature) is effective but expensive due to requirement of gas cooler, which adds to weight and cost, apart from corrosion. HOT EGR is a low cost and effective technique to reduce NOx [66, 70, 71, 74].

2.6.6.3 EGR

Controlling the NOx emissions primarily requires reduction of in-cylinder temperatures and reduction of oxygen concentration of the intake mixture.

EGR involves diverting a fraction of the exhaust gas into the intake manifold where the recirculated exhaust gas mixes with the incoming air before being inducted into the combustion chamber. Exhaust gases possess high specific heat and act as a heat sink. Thus specific heat capacity of the mixture in the cylinder increases. All these factors lead to lower

the NOx formation. But, EGR can significantly increase the BSFC, and also HC, CO and smoke emissions unless suitably optimized. EGR can also adversely affect lubricating oil quality and engine durability [62, 65-69].

Many researchers agreed that EGR is a very effective method to reduce NO_x emissions up to 50–75% in bio-diesel-fuelled engines.

Biodiesel with 15% EGR showed a NOx reduction up to 74% with 20% increase in smoke. Increasing the quantity of EGR by more than 15% generally results in increase in smoke and fuel consumption [47, 84].

2.7 Biodiesel

Biodiesels are mono alkyl esters of long chain fatty acids derived from renewable sources like vegetable oils and animal fats. They are produced through the bio-chemical process of transesterification. Low production costs and large production scale are main requirements of SVO for biodiesel production. Biodiesel composition and properties depends on the nature of the feedstock. Therefore, biodiesel must meet the fuel specifications, EN 14214 or ASTM D6751 [47, 58, 68, 78, 85].

2.7.1 Transesterification process

Transesterification is an effective process of bio-diesel production. It is a reversible reaction of fat or oil (triglyceride) with a primary alcohol in presence of a catalyst to form esters and glycerol.

The typical transesterification reaction is shown in **Fig. 2.12**. Here, R1, R2 and R3 represent the long hydrocarbon chains.

In transesterification, alcohol combines with triglycerides to form glycerol and esters. So, it is also known as alcoholysis. Methanol and ethanol are used commercially because of their low cost and their better physico-chemical properties. Triglycerides quickly react with them and are easily dissolved in them.

Stoichiometrically, 3:1 molar ratio of alcohol to triglycerides is needed. Yet, higher alcohol to oil ratio is generally employed to obtain biodiesel of low viscosity and high conversion.

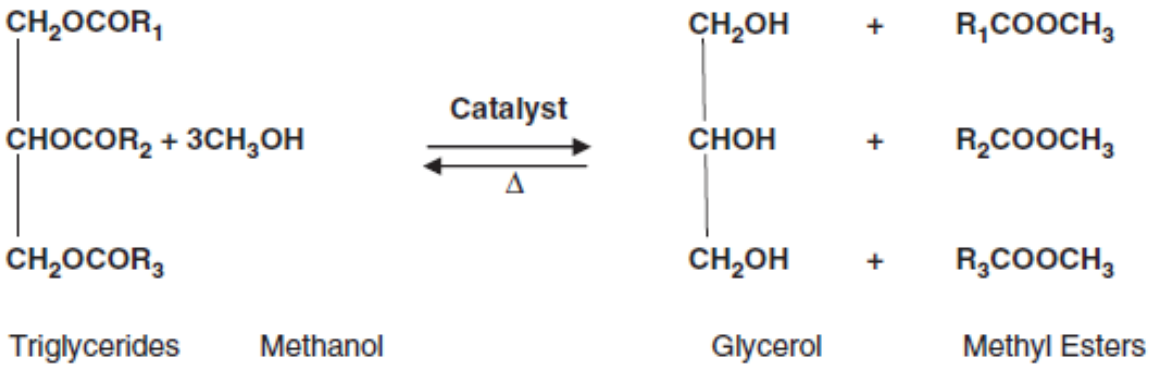

Fig. 2.12 Transesterification reaction [68]

Effect of different parameters like temperature, molar ratio of alcohol to oil, catalyst, reaction time have been investigated by several researchers. It was found that the yield was maximum for base catalyzed transesterification at atmospheric pressure, 55–65^{o} C temperature, 45 min to 1 h reaction time and 6:1 molar ratio of alcohol to oil. Glycerin is a by-product which is used in pharmaceutical and cosmetic industries [52, 68, 79, 83, 85].

2.7.2 Advantages and limitations of bio-diesel

Advantages of bio-diesel

Various researchers reported the following advantages with bio-diesel:

Non-toxic, biodegradable, renewable nature; Blending of bio-diesel with diesel increases engine efficiency; Lower viscosity, higher volatility, and lower un-saturation than SVOs; Higher flash point than diesel, making it safer to handle, transport and store; Oxygen content of bio-diesel improves the combustion process; More lubricity than diesel; Energy content close to diesel; Decrease in acid rain and greenhouse effect; Carbon neutral; Can be blended in any ratio with diesel; Supports domestic crops; Promotes new employment; Biodiesel

contains no sulphur, aromatics or PAH compounds; Glycerol is a byproduct used in medical and industrial chemicals; Low emission profile, etc [47, 50, 77, 79].

Limitations of bio-diesel

A few researchers have reported the following limitations of biodiesels:
Higher viscosity and density than diesel; Higher copper strip corrosion; Lower energy content (about 10% less than diesel); Unfavorable cold flow properties; More prone to oxidation, acid formation in the fuel, to form insoluble gums and sediments; More expensive than vegetable oil or diesel, etc [47, 50, 77, 79].

Table 2.3 and Table 2.4 show the fuel properties of selected inedible vegetable oils and their biodiesels respectively.

Table 2.3 Fuel properties of selected inedible vegetable oils [80]

Property	***Jatropha***	***Karanj***	***Mahua***	***Linseed***	***Rubber seed***	***Cotton seed***	***Neem***	***Diesel***
Density (kg/m^3 at 40 ^oC)	901-940	870-928	891-960	865-950	910-930	911-921	91.2-96.5	-
Viscosity (mm^2/s, 40 ^oC)	24.5-52.7	27.8-56	24.6-37.6	16.2-36.6	34.0-76.4	32.8-36.0	20.5-48.2	2.0-2.7
Flash point (^oC)	180-280	198-263	212-260	108-242	144-198	210-243	34-285	45 min^m
Pour point (^oC)	-3 to5	-3 to 6	12-15	-15 to -4	-1	-10 to 16	-	-20 to 5
Cloud point (^oC)	8-10	13-15	12	1.7-2.0	14	-8.7 to1.7	-	-
Cetane number	33.7-51	45-67	43.5	28-35	37	41.2-59.5	51	45 min^m
Calorific value (MJ/kg)	38.20-42.15	34.0-38.8	35.6-38.9	37.7-39.8	37.5	39.5-40.1	33.7-39.5	-

Table 2.4 Fuel properties of selected biodiesels and American standards [80]

Property	*JOME*	*KOME*	*MOME*	*LOME*	*ROME*	*COME*	*NOME*	*Diesel*
Density (kg/m^3 at 40 ^oC)	862-886	865-898	828-865	874-920	858-900	872-885	820-942	870-900
Viscosity (mm^2/s, 40 ^oC)	3.0-5.65	3.8-9.6	2.7-6.2	3.36-8.91	1.9-6.0	3.6-5.94	3.2-10.7	1.9-6
Flash point (^oC)	180-280	110-187	56-208	161-181	130-174	70-200	-	> 130
Pour point (^oC)	2-6	-6 to 14	1-6	-18 to 14	-15 to 10	-15 to 6	-	-15 to 10
Cloud point ^oC)	4-10	-2 to 24	3-5	-3.5	-3 to 12	-	-	-
Cetane number	43-59	36-61	47-51	48-59	49-57	45-60	51-53	47 min^m
Calorific value (MJ/kg)	37.2-43.0	36.0-42.1	36.8-43.0	37.5-42.2	36.5-42.1	40.1-40.8	39.6-40.2	-

2.8 Policies and trends in SVO/BD use in diesel engines

2.8.1 Bio-fuel Policy and government incentives

Many countries have already used targeted policies to increase the production and use of bio-fuels. EU (Directive 2003/30/EC) planned an increasing share of bio-fuels from 2-5.75% of total energy supply. USA and Canada governments have also implemented similar directives. According to the International Energy Agency's (IEA) report, global biodiesel production increased tenfold from 2000 to 2008 and almost doubled to 21.8 billion liters by 2012 [48].

2.8.1.1 Energy scenario in India

India depends solely on non-edible feedstocks for biofuels, to avoid a possible fuel vs. food conflict. High yielding perennial non-edible feedstocks that can be grown using low

inputs on degraded/marginal or wastelands not suited to agriculture is recommended by Indian government. Rehabilitation of wastelands is also ensured in this manner.

Even with abundance of forests, and plant based non-edible oils being available in India, not much attempt has been made to utilise these non-edible oils as substitute for diesel. National Policy on Biofuel has been prepared by the Ministry of New and Renewable Energy (MNRE), which is the body governing the usage of renewable energy resources. MNRE targets 20% blending of biofuels with the fossil-derived mineral fuel by 2017. To start with, 5% of biodiesel from non-edible oil extracted from jatropha and pongamia, would be mixed with diesel during trial runs. At a later stage, in phases, blending is to be increased to 20%. The Oil Marketing Companies–IOCL, BPCL, and HPCL have plans to purchase bio-diesel that meets the fuel quality standards, through select purchase centers [77, 81].

2.8.2 Recent research trends in SVO/BD use as fuel

A review regarding influence of the type and quality of vegetable oils as fuel in diesel engines was conducted. Dual fuelling and blending with diesel was also discussed [45].

Impact of untreated SVO application on fuel consumption and emissions on a Euro 3 common rail diesel passenger car was assessed. Three vegetable oils (sunflower, cottonseed and rapeseed) were blended with diesel fuel for this study [46].

Various methods of biodiesel production along with a brief discussion of performance and emissions of biodiesel sources were analysed. EGR was also discussed [47].

In another study, development of biodiesel, challenges of biodiesel and environmental and social impacts were discussed. Government incentives and public awareness for biodiesel were also portrayed [48].

Detailed statistical investigation was conducted for the assessment of all properties of the 26 biodiesels found in available literature. The results were compared with the US and European specifications. Feedstock unsaturation and its effects on biodiesels was also considered. Trends observed were explained on the basis of fuel chemistry [49].

Empirical models were developed to predict the density and viscosity of biodiesel and biodiesel blends in a wide range of temperatures [50].

Performance and emission characteristics of linseed oil, mahua oil, rice bran oil and linseed oil methyl ester (LOME) in a stationary diesel engine was investigated. Economic analysis showed that vegetable oil has similar cost as that of diesel [51].

In another study with mahua biodiesel, power loss was about 13% and increase in fuel consumption was 20% at engine full load. Emissions such as CO and HC were less than that from diesel by 26% and 20% respectively. Also, 4 % less NOx was produced [52].

Neem oil extraction, refining and transesterification process variables were evaluated and biodiesel was produced using base-catalyzed transesterification. It was found that Neem oil could be almost completely converted to biodiesel [53].

Suitability of Rice bran oil methyl ester-ethanol blends as fuel in terms of fuel properties was also evaluated in a study [54].

In a study, results with preheated jatropha oil as fuel showed that brake thermal efficiency of engine increased and brake specific energy consumption decreased. Emissions of NOx increased and CO, HC, CO_2 emissions decreased. Optimal fuel inlet temperature was found to be 80 ^{o}C [55]. Preheating of rapeseed oil and blends by heating up to100 oC lowered the viscosity, improved the fuel flow and showed positive effects on engine performance and emissions [56].Waste frying oil was preheated to two different inlet temperatures (75 and 135 ^{o}C). The engine performance improved and CO and smoke emissions reduced with preheating [57]. Cottonseed oil methyl ester was preheated to 30, 60, 90 and 120 ^{o}C temperatures. Results revealed that 90 ^{o}C preheating leads to improved BTE and CO emissions but with higher NOx emissions. But, at 120 ^{o}C, decreased fuel viscosity caused excessive fuel leakage and brake power dropped considerably [58].

Mahua biodiesel and blends were tested in Ricardo E6 engine at varying compression ratio (CR) and injection timing (IT). With increase in the CR and advancement of IT, brake specific fuel consumption and exhaust gas temperature decreased but brake thermal efficiency increased [59].

Simultaneous reduction of NOx and smoke in a diesel engine fuelled with biodiesel blend was attempted with combination of retarded fuel injection timing and increased injection pressure [60].

Effect of four different injection pressure on characteristics of a diesel engine has been investigated using canola oil methyl esters (COME) and its blends with diesel. The brake specific fuel consumption and brake specific energy consumption for COME are higher, and brake thermal efficiency is lower than that of diesel fuel at increased injection pressure [61].

Tests were carried out on engine with three different injection pressures (250, 300 and 350 bar) and fuelled with rapeseed and soybean oil methyl esters. The performance and emission values of engine for these fuels were found to be nearly the same as those of diesel at injection pressure of 300 bar [62].

Injection timing, injector opening pressure, injection rate and air swirl level were changed to study their influence on performance, emissions and combustion of a diesel engine operated on neat Jatropha oil. Advancing the injection timing and increasing the injector opening pressure increased the brake thermal efficiency and reduced HC and smoke emissions significantly [63].

Investigations were conducted to optimize the use of 20% blend of Mahua methyl ester (MME) in a diesel engine at various nozzle opening pressures (225, 250,275 bar) and static injection timings (19, 21, 23, 25, 27 ^{o}bTDC) in accordance with ISO 8178 D2 cycle, intended for homologation. Increased pressure of 275 bar or retarded injection timing of 21 ^{o}bTDC conformed to the stringent emission norms of Central Pollution Control Board (CPCB) stage-I. Obtained emissions were lesser than CPCB limits [64].

A single cylinder diesel engine fuelled with JBD was operated under HOT EGR levels of 5–25%. EGR level was optimized as 15% based on reductions in NOx, CO and HC emissions with reasonable brake thermal efficiency, but smoke emissions were slightly higher. Combustion parameters were found to be comparable with diesel [65].

Application of cooled EGR (optimised at 20%) on a diesel engine with waste plastic oil also depicted similar results [66].

EGR was found to be effective technique for reducing NOx emissions from a diesel engine using jojoba methyl ester. A better trade-off between HC, CO and NOx emissions could be attained with 5–15% EGR rate. The effect of cooled EGR with high ratio was also examined [67].

Biodiesel and EGR simultaneously employed in a two-cylinder, air-cooled diesel engine resulted in reductions in NOx emissions without any significant penalty in PM emissions or BSEC [68].

Emission tests in low pressure EGR system were conducted in a diesel EURO IV engine. NOx and fuel consumption decreased and HC and CO increased [69].

A review paper summarized the relevant literature and presented the theories to explain the biodiesel-NOx effect. Mitigation strategies by modifying engine control settings with injection timing and and exhaust gas recirculation were discussed [70].

2.9 Selection of oils for present investigation

Mahua oil, Ricebran oil and Neem oil were selected as base fuels for microtrigeneration in the present investigation. Oil blends with 20% oil and 80% diesel were used. Also, Mahua biodiesel (Mahua oil methyl ester) was prepared and used. A brief description of these oils is given in the following paragraphs.

Mahua oil (Madhuca indica)

Mahua (Madhuca indica) tree is widely available in India producing tree-borne mahua oil. It has an estimated annual production potential of 181 thousand metric-tons in India. But, not much investigations on usage of mahua oil as fuel has been reported.

Two major species found in India are Madhuca Indica (or, Madhuca latifolia) and Madhuca longifolia. Mahua is a medium to large tree found in most parts of India, but mainly distributed in tropical forests of India. M. Latifolia is deciduous, while M. Longifolia is semi ever-green tree.

Table 2.5 Fatty acid profile of Mahua oil [89]

Properties	***Values (weight %)***
Oleic	41.0-51.0
Palmitic	16.0-28.2
Stearic	20.0-25.1
Linoleic	8.9-13.7
Arachidic	0.0-3.3

Fatty acid profile of mahua oil is given in Table 2.5. The oil has a relatively high percentage of saturated fatty acids such as palmitic (17.8 wt.%) and stearic (14.0 wt.%) acids. The remaining unsaturated components are oleic (46.3 wt.%) and linoleic (17.9 wt.%) acids. The mahua oil generally contains about 20% FFAs.

Fresh oil from properly stored seeds is yellow in colour, while commercial oils are generally greenish-yellow. Mahua tree and mahua seeds are shown in **Fig 2.13.**

Fig 2.13 Mahua tree and mahua seeds

Most of the fuel properties of mahua biodiesel were found to be comparable to those of diesel, and mostly conforming to both the American and European standards. Calorific value of mahua oil (Madhuca Indica) is lower by 14–15% as compared to Diesel. But, its kinematic viscosity is about 12 times higher than that of diesel. So, mahua oil is converted into biodiesel to improve the properties as fuel. Mahua oil methyl ester is a biodiesel produced by transesterification process from Mahua oil [52, 64, 81, 85].

Neem oil (Azadirachta indica)

The neem tree can be found in Asia, Africa, Central and South America etc, but is mainly native to South Asia, particularly India and Burma. In India, Neem is scattered all around, but mainly in the states of Rajasthan, Uttar Pradesh, Madhya Pradesh, Andhra Pradesh, Tamil Nadu and Delhi.

Fig 2.14 Neem tree, fruits and seeds

It grows almost in all types of soils including clay, saline, alkaline, dry, stony, shallow soils and even on pan-forming and high calcareous soils. Neem tree can tolerate extreme conditions like high temperature of 45^{o} C and scanty rainfall of less than 35 cm per year.

A mature tree can produce 30–50 kg of fruit every year and can continue up to 150–200 years. Out of this high production potential, only 20-25 % is utilized, mainly in soap, cosmetics and pharmaceutical industries. Remaining large untapped source can be a potential biofuel source. Fig 2.14 shows the photograph of Neem tree, fruits and seeds.

Neem oil (Azadirachta indica) is low cost non-edible oil available in huge surplus quantities in India with estimated oil production of 30,000 tons. Oil yield from seeds is 30–60% of the weight of the kernel. It is light to dark brown in colour, and contains sulfurous compounds which result in pungent odor. Azardiratchi is the main biochemical component of Neem used for medicinal purposes. Traditionally it has been used on an industrial scale for manufacturing of soaps, cosmetics, pharmaceuticals and other non-edible products. Neem oil contains high moisture content and high free fatty acids (FFA), and undergoes fast oxidation with rapid increase in its acid value. Due to its high FFA content, problems are encountered in transesterification process to efficiently convert it into neem biodiesel [53, 81, 85, 87].

Rice bran oil (Oryza sativum)

Non-edible rice bran oil is a post-harvesting agricultural by-product obtained from outer layer of brown rice kernel. Estimated yield potential of crude rice bran oil is about 8 million metric tons globally.

Fig 2.15 Rice plant (paddy) and its seed

Rice grain consists of the edible portion covered with an outer layer called husk or hull. After removing the protective husk, a thin bran layer is seen surrounding the starchy

white rice kernel. The rice milling process produces rice husk and rice bran as by-products. The rice bran is about 10% of the weight of rough rice.

Rice plant (paddy) and its seed are shown in Fig 2.15.

The crude non-edible rice bran oil is extracted mostly by solvent extraction process. It contains 15-23% lipids, depending on the milling procedure and the rice variety. Active lipase in bran reacts with lipids to decompose into FFA, making it unstable and generally unsuitable for edible purpose. After a month's time of storage, the FFA content may reach even up to 70%.

Crude rice bran oil is a non-conventional, inexpensive, low-grade vegetable oil, and can be used as a feedstock for biodiesel. However, its use has not been standardized, although it has a potential as a fuel because of its mineral diesel like properties.

Advantages of rice bran as fuel are: generally non-edible, local and widely available, no large distance transportation needs, no large processing infrastructure required, cheaper fuel source, etc. Transesterification of rice bran produces valuable by-product, the defatted bran, which is rich in active antioxidant compounds, proteins and carbohydrates and has good market value. The rice bran wax has cosmetic and pharmaceutical uses.

Its main limitations are high density, very high viscosity and presence of suspended particulates. Although poly unsaturated fats are less, high viscosity and saturated fatty acids prevents its widespread use as fuel. Efficient dewaxing and degumming is very necessary for its use as fuel [54, 86, 88].

CHAPTER 3

MATERIALS AND METHODS

The entire research work was divided into five phases; First phase was related to selection of oil, preparation of biodiesel, optimization of Mahua oil/biodiesel blends with diesel, determination of optimum preheat temperature and fuel characterisation; Second phase was to experimentally optimize the engine performance and emissions with varying injection pressure, injection timing and EGR using alternative fuel; Third phase included procurement and fabrication of different components to realize the real sized micro-Trigeneration system; Fourth phase was to operate the developed micro-Trigeneration system with alternate fuel blends to evaluate the performance and emissions while working in single, cogeneration, and trigeneration modes. Next phase was related to development of simulation model for predicting the performance of micro-Trigeneration system, and validating it with experimental results. It also includes a simple economic analysis of the developed micro-trigeneration system.

3.1 Base Vegetable oils

Three base vegetable oils were adopted for the experimentations: Mahua oil, Neem oil and Rice bran oil. All three are abundantly available in India, and can be used as fuel source. Mahua is non-edible oil. Neem is also non edible oil with medicinal value. Rice bran oil is a cheaper fuel substitute, widely available, and lies in the borderline of edible and non-edible oils.

The quality of expelled oils depends largely on the storage conditions of seeds and the oils. Fresh oils from properly stored seeds have better characteristics. The crude mahua, rice bran and neem oils that were freshly extracted were procured from the local market. They were filtered with cloth and also with filter paper mainly to remove dirt. High speed diesel was procured from pump station of Indian Oil Corporation in Jaipur. It was used for blending with vegetable oils for further experimentations. It was also used as reference fuel for comparison of performance and emission characteristics of the engine with the prepared blends. Initial acid number was determined to decide about further processing or refining of crude oil.

Various alternative fuel blends with diesel were used in the investigation: mahua oil-

diesel blend; rice bran oil-diesel blend; neem oil-diesel blend; mahua oil methyl ester-diesel blend; pure mahua oil.

3.2 Biodiesel preparation

Mahua oil methyl ester production

Transesterification is a process of producing a reaction between a triglyceride and alcohol in presence of a catalyst to produce glycerol and ester. Crude mahua oil (CMO) contains high free fatty acids (FFA ~ 20 %). In transesterification process, high FFA (>1 % w/w) form soap with alkaline catalyst and can prevent separation of the biodiesel from the glycerine.

Hence, Mahua biodiesel (Mahua oil methyl ester) was produced in two stages, namely acid esterification followed by alkaline transesterification. Mahua oil methyl ester (MOME) from mahua oil was prepared in Biodiesel lab in Mechanical Engineering Department of MNIT Jaipur.

FFA content was found to be 17.6 % in CMO. Hence, standard two step 'acid–base' process was followed, i.e. acid pre-treatment followed by main base transesterification reaction, using methanol as reagent and H_2SO4 and KOH as catalysts for acid and base reactions respectively to produce biodiesel from crude mahua oil on laboratory scale. Standard procedure was followed.

The set up consisted of an electric hot plate with magnetic stirrer, 1000 ml 3-necked round bottom flask, digital temperature controller, condenser with guard tube which prevents moisture entering into the system, water and pump, thermometer and separating funnel. The set up for biodiesel production on lab-scale is shown in Fig 3.1 (a).

L. R. grade Methanol (99% pure) was used as reagent, and the sulphuric acid (98% pure) and potassium hydroxide (97% Pure) as shown in Fig. 3.1 (b) were used as catalysts for the esterification and transesterification processes, respectively. These reagents and 1 litre of filtered crude Mahua oil was heated at 110^{o} C for 15 minutes to drive out residual moisture, and then cooled up to 70^{o} C. A solution of H_2SO4 (10 ml), and methanol (60 ml) was prepared and mixed thoroughly. This solution was added to the oil. The solution was heated at 60^{o} C for 2 hours, and magnetic stirring was done continuously, to complete the reaction. After 2 hours, the reaction was complete, and the mixture was transferred to separating funnel

and left for 12 hours. Two distinct layers were formed; the upper layer was the esterified oil and was separated under gravity, and used for further processing.

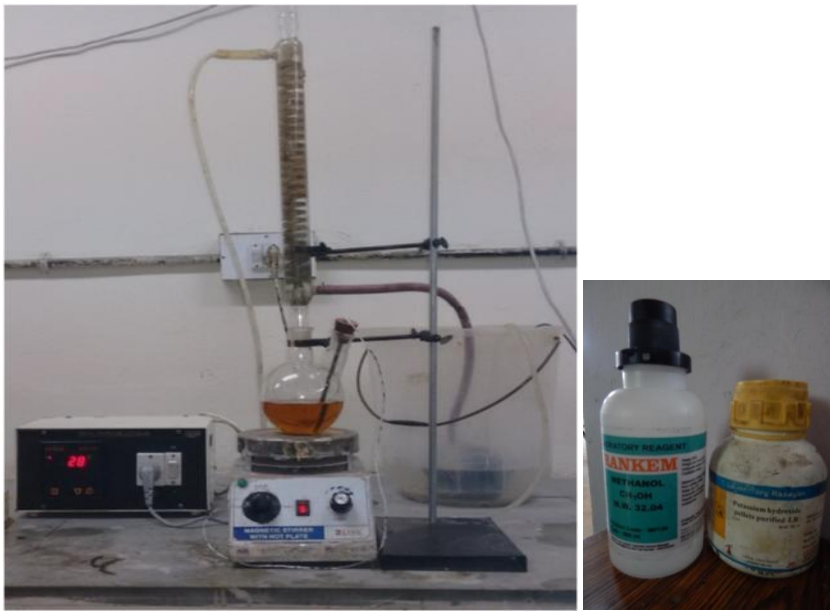

(a) **(b)**

(c) **(d)**

Fig. 3.1 (a) Transesterification set up (b) Methyl alcohol and Potassium hydroxide (c) Biodiesel and glycerol layers (d) Water washing of biodiesel

The esterified oil has reduced FFA content. It was used for the next step, i. e., the transesterification process. The esterified oil was again heated up to 110 ^{o}C and cooled up to

70^{o} C. A solution of KOH (5 g) and methanol (40 ml) was mixed to form a solution and mixed in the esterified oil. The final solution was heated at 60^{o} C for 1 hour, along with continuous stirring, and then left for 24 hours. Again, two layers were formed-the upper layer was mahua oil methyl ester (mahua biodiesel), and the lower layer was mainly glycerol, which was separated under gravity.

Separate layers of biodiesel and glycerol can be seen after base transesterification in Fig.3.1 (c).

Methanol content , if any , left in the biodiesel was removed easily by heating the biodiesel up to 75^{o} C (since, the boiling point of methanol is only 64.5^{o} C). Next, water washing of biodiesel was carried out to remove the traces of catalysts. Water at 35-40^{o} C was mixed from top in the separating funnel in the biodiesel, to absorb any catalyst, and left for 2 hours, as can be seen in Fig. 3.1 (d). The water with dissolved catalyst in it, were removed under gravity. This step was repeated 3-4 times.

Biodiesel was again heated for 15 minutes at 110^{o} C to drive out traces of moisture, and then left to cool down to room temperature. Biodiesel was filtered using filter paper to remove sediments if any, before storage. About 91 % biodiesel yield could be obtained following the above steps.

3.3 Fuel characterisation

The physico-chemical properties of vegetable oils are highly sensitive to the variety of feedstock used. Depending on the nature of the oil-bearing biomass from which SVOs are obtained, and on extraction and drying conditions, SVOs display highly variable physicochemical characteristics and combustion properties [45, 90].

Hence, a detailed characterisation of fuel properties must be conducted before experimentations if straight vegetable oils are used. Fuel characterisation for major properties of test fuels was done as per ASTM standards in Biodiesel labs in Mechanical and Chemical Engineering Departments of MNIT Jaipur.

Major physico-chemical properties of the test fuels were determined. Viscosity of all the vegetable oils was measured at room temperature. Viscosity of Mahua oil was also measured at different temperatures from 30^{o} C to 120^{o} C to find the effect of temperature on viscosity. Relative Density was determined by Relative density bottle, Kinematic viscosity by Redwood viscometer and calorific value by using Bomb calorimeter.

(a) **(b)**

(c) **(d)**

Fig. 3.2 Setup for measurement of fuel properties (a) Redwood Viscometer (b) Bomb calorimeter (c) Cloud and Pour point apparatus (d) Flash and Fire point apparatus

For Acid value estimation, standard titrimetry was adopted. Flash and Fire point point was determined by Pensky Marten apparatus, while Cloud and Pour point was determined by Cloud and Pour point apparatus. The ash content in the fuels was decided by testing in a muffle furnace. The tests were performed according to ASTMD 6751 standards.

Fig 3.2 (a) - (d) shows some of the set ups used for various tests.

3.4 Heat Exchangers

Heat exchangers perform two main functions. These act as waste heat recovery equipment and also reduce environmental warming. Maximum heat is generally available at engine full load. In the developed micro-trigeneration system, heat exchangers were installed in the passage of exhaust gases and coolant water to extract maximum possible heat.

3.4.1 Heat Exchanger for Generator of Electrolux VA refrigeration units

The generators of all the four Electrolux Vapour Absorption refrigerators used in this investigation were modified to utilize the waste exhaust gas heat. A parallel flow pipe in pipe heat exchanger was designed, fabricated and installed. The inlet/outlet temperatures, overall heat transfer coefficient and the geometry of the heat exchanger are used in the design procedure. The vertical generator tube was considered as inner tube and the encircling tube was designed as outer tube. A square cross-section was selected for the ease of fabrication in the lab, and other constraints.

The cross sectional area (A_c), the wetted perimeter (P_w) and the hydraulic diameter (D_h) for the flow was given by,

$A_c = A_{outer} - A_{inner} = a^2 - \pi/4 * d^2_{inner}$

$P_w = 4a + \pi\, d_{inner\ pipe}$, where 'a' is the side of the square cross section of the outer pipe.

$h_D = 4A_c/P_w$

Reynolds Number (Re), and friction factor (f) is given by,

$Re = \rho V h_D/\mu$

$f = (0.790 \ln Re - 1.64)^{-2}$

The Prandtl Number (Pr) was assumed as Pr=0.7, Nusselt number (Nu) was determined by the Dittus-Boelter equation, as shown below,

$Nu = 0.023 Re^{\frac{4}{5}} Pr^n$, where, for heating, n= 0.4 and for cooling, n=0.3.

Convective heat transfer coefficient (h_{conv}) was calculated as,

$h_{conv} = Nu*k/ h_D$

The main heat transfer resistance (R_{ther}) was due to the generator tube, and was given by,

$R_{ther}=1/\pi d_{inner} * l * h_{conv}$

The UA value was given by,

$UA=1/R_{ther}$

If the minimum heat capacity rate is C_{min}, then the Number of transfer units (NTU) was calculated as,

$NTU=UA/C_{min}$

Effectiveness (ϵ) was given by using the capacity ratio ($C= C_{min}/C_{max}$) in the following equation,

$$\varepsilon=\frac{1- \exp\{-NTU(1+C)\}}{(1+C)\}} \text{ (for parallel flow)}$$

The heat transfer through generator (Q_{gen}) was calculated as,

$Q_{gen}= \epsilon *C_{min} * (T_{hi}- T_{co})$

Since the generator tube is of fixed length of 0.21 m, so the length of the outer square pipe was also fixed equal to that, which is the maximum possible length in that space. But, the outer pipe cross-sectional dimensions were evaluated by designing in such a way so as to adjust in the limited space available, with maximum heat transfer at the generator end.

Also, some space was considered for effective insulation of the outer pipe. The side of outer square pipe was estimated to be, a= 4.5cm. Schematic diagram and the fabricated heat exchanger for generator of VAR unit can be seen in Fig. 3.3 (a) and (b).

The layered insulation with total thickness of 1.5 cm could be applied, using asbestos rope, glass wool and aluminium foil to prevent heat transfer to the evaporator end of the tube.

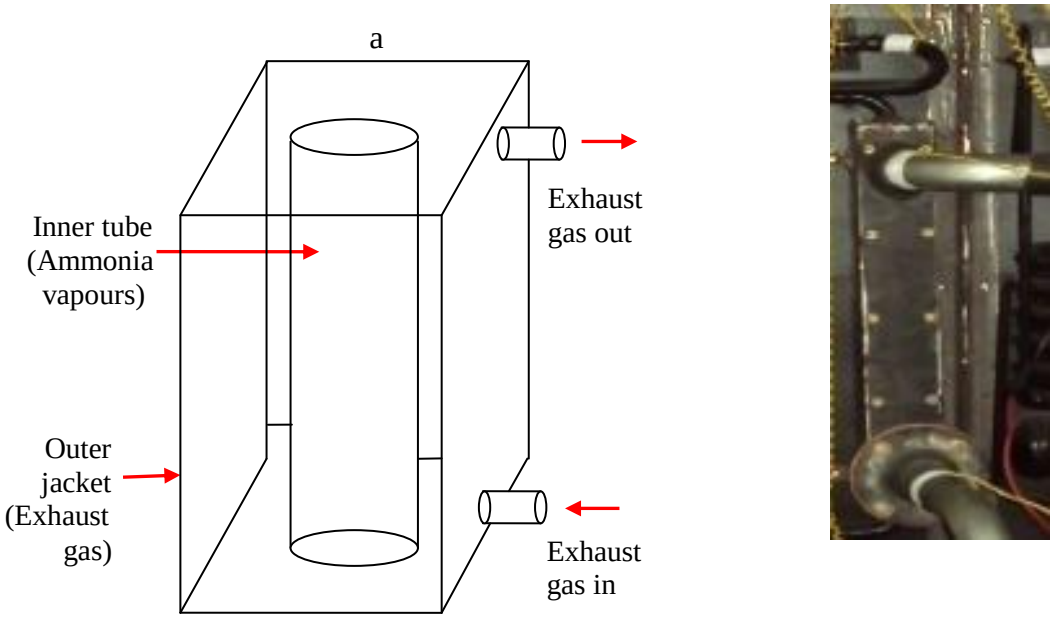

Fig. 3.3 (a) Schematic diagram and (b) Photograph of the fabricated heat exchanger for generator of VAR unit

3.4.2 Heat Exchanger for Fuel Preheating

The heat exchanger for fuel preheating transfers the heat from the engine exhaust to the fuel to lower its viscosity before it enters the engine cylinder through the fuel pump and fuel injector. A counter flow pipe in pipe heat exchanger was designed, fabricated and installed in exhaust line to preheat the vegetable oil using waste heat of the exhaust gases.

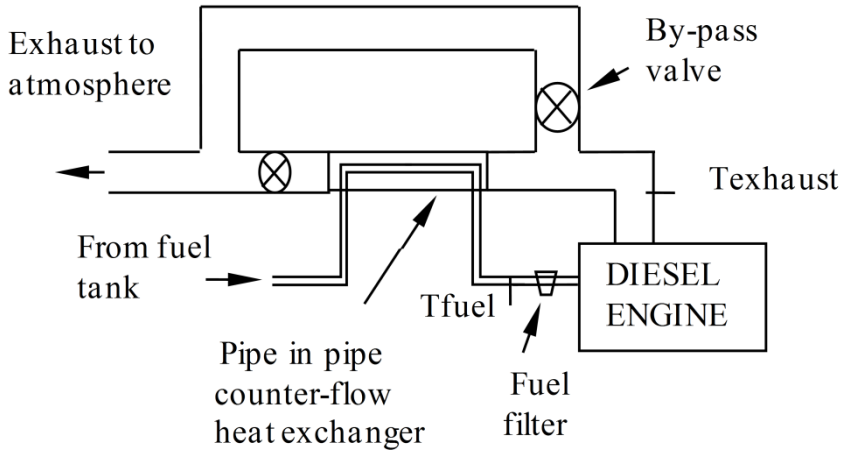

Fig. 3.4 Line diagram of the fuel preheating arrangement

(a) (b) (c)

Fig. 3.5 Photograph of (a) copper tube for fuel (b) outer pipe with inserted fuel tube (c) the side view of heat exchanger

Due to ease of fabrication and installation, outer GI pipe of length 30 cm and diameter 5.1 cm was used and inner copper tube of 0.95 cm diameter was inserted. It was found to be suitable taking into consideration the limited space available, and simplicity in construction. The length of the inner tube was estimated from the design for effectiveness and maximum heat transfer.

The procedure followed is similar to that in previous one, except two main differences: the outer pipe is also of circular cross section and the flow is counter flow.

For counter flow, effectiveness (ϵ) was given by using the capacity ratio ($C= C_{min}/C_{max}$) in the following equation,

$$\varepsilon = \frac{1- \exp\{-NTU(1+C)\}}{1+C \exp\{-NTU(1+C)\}}$$

The heat transfer (Q_{fp}) was calculated as,

$$Q_{fp} = \epsilon * C_{min} * (T_{hi} - T_{ci})$$

The copper tube was inserted in the outer GI pipe, and the ends of the tube were connected to fuel tank and fuel pump of the engine, respectively. The length of the tube inside the pipe was determined to be 25 cm using design principles. The fuel line was thermally insulated to minimize the heat loss. Preheating was carried out next to the fuel pump of the engine. The temperature of the fuel was measured just at the engine inlet.

A bypass valve was used to control the temperature of fuel within a range of $\pm 5^{o}$ C by adjusting the amount of exhaust gases to preheat the oil. Thermocouples were provided in the exhaust line as well as in fuel pipe just before the fuel pump to measure the exhaust and the

fuel temperatures. The line diagram of the fuel preheating arrangement and photographs of the heat exchanger are shown in Figs. 3.4 and 3.5 respectively.

3.4.3 Heat Exchanger for Water-Heating

A compact heat exchanger (previously designed and fabricated for use in conjunction with 3.7 kW water cooled engine) was utilised for heating of water in this study. This heat exchanger is cross flow, multi-flattened tube and finned type, and is made of brass tubes and copper fins. It transfers heat from the exhaust gases to the water coming from engine jacket water coolant-loop. A very large heat transfer surface area per unit volume can be achieved with this type of compact heat exchanger. The dimensions of the heat exchanger were obtained using Energy balance and Effectiveness (ε)-NTU method.

The dimensional measurements were:

Height	=	340 mm
Width	=	300 mm
Thickness	=	60 mm
Number of tubes	=	64
No. of fins	=	152
Tubes height	=	2.54 mm
Tubes depth	=	18.71 mm

Overall length of convergent-divergent duct was 750 mm [91].

Heat exchanger shell was fabricated from G.I. sheet. The heat exchanger was placed on a wooden frame at 1.2 m height from the ground. At the top and bottom of the drum, ports were provided for entry and exit of cold and hot water respectively. The exhaust gas entry side of the heat exchanger was insulated by tightly covering the jacket with glass wool and wrapping it with asbestos ropes and thick aluminium foils. The photograph of this heat exchanger is given in Fig. 3.6.

The cooling water was circulated using a 1 HP pump. The mass flow rate of cooling water can be varied with the help of a valve and checking the flow in water meter and a rotameter installed in the cooling water circuit.

The heat exchanger could heat water up to about 85-90 º C using heat of engine exhaust gases with an average temperature of 370 º C. The exhaust gases were expected to

cool down to 150 -180º C. This heat exchanger was used to generate hot water which was used in one set of experiments in micro-trigeneration for space heating.

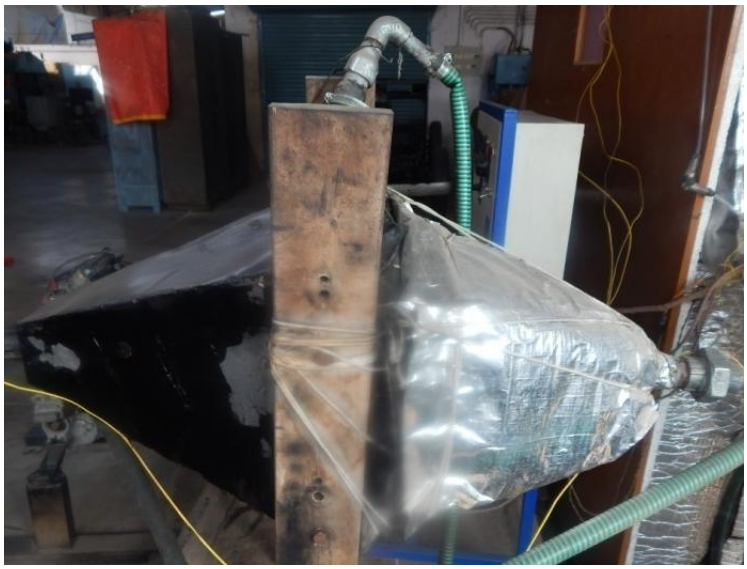

Fig. 3.6 Heat exchanger with diverging- converging duct

3.4.4 Various layouts for Heat Exchangers

A. In case of space cooling arrangement, the exhaust gases leaving the engine pass through a counter-flow heat exchanger for preheating of alternate fuel, and then enter the heating jacket of the generator of the modified VAR system to produce cooling effect in the cabin.

B. In case of space heating arrangement, two options were considered:

1. Direct exhaust fired space heating:

The exhaust gases leaving the engine pass through a counter-flow heat exchanger for preheating of alternate fuel, and then enter the cabin through the piping arrangement to produce heating effect in the cabin.

2. Hot-water fired space heating:

The exhaust gases leaving the engine pass through a counter-flow heat exchanger for preheating of alternate fuel, and then enter another heat exchanger to produce hot water, and then the hot water is used in the cabin through the piping arrangement to produce heating effect in the cabin.

The cabin could be comfortably heated by sending the exhaust gases, or hot water stream to a finned pipe located inside the cabin to exchange heat with the cabin air. An electric fan was used to increase the heat transfer rate. Globe valves were located to bypass the hot exhaust gases/hot water stream to the outdoor coil, if needed; the case usually encountered in mild winter conditions.

3.5 Finned pipes for space heating set up

Experiments were conducted using bare pipe as well as annular and longitudinal finned pipes in the final space heating set up. The total surface areas of the fins were kept equal in both finned pipes for comparison. The length and diameter of the base pipes in all three cases were also kept equal. The fabrications of the finned pipes in the lab were based on the ease of manufacture, available resources and other constraints. The fin efficiency and fin effectiveness were calculated for the annular as well as longitudinal finned pipes. Actual heat transfer during experiments in space heating also was found to be in accordance with these values. Fig 3.7 (a) to (c) show the bare pipe and the finned pipes used in the study.

3.5.1 Various dimensions in finned pipes

The various dimensions for the pipes are as given below:

Bare pipe-

Length = 600 mm

Inner diameter = 25.39 mm

Outer diameter = 34.10 mm

Annular finned pipe-

Total length of pipe with fins = 460 mm

Base diameter of fins = 34.10 mm

Maximum diameter of fins = 73.14 mm

Fin thickness = 1.8 mm

Number of fins = 20

Longitudinal finned pipe-

Total length of pipe with fins = 460 mm

Base diameter of fins = 34.10 mm

Fin height = 46.12 mm

Fin thickness = 1.8 mm

Number of fins = 5

3.5.2 Fin effectiveness and fin efficiency

For Annular fin-

Circumference of fin (C_{fin}),

C_{fin}= л * (do – di)

area of fin, A_{fin} = w x b

For Longitudinal fin-

Circumference of fin (C_{fin}),

C_{fin}= 2(w + b)

Cross-section area of fin, A_{fin} = w x b

For both types,

Fin area available for heat transfer ($A_{fin\text{-}avail}$)

$A_{fin\text{-}avail}$ = C x H_{fin} x n

Bare pipe area available for heat transfer (A_{pipe})

A_{pipe} = (л D – nb) w

Total available heat transfer area,

A_{total} = A_{pipe} + $A_{fin\text{-}avail}$

Total heat transfer in finned pipe,

Q_{total} = m* $c_{p\text{-}exh}$* dT , where, $c_{p\text{-}exh}$ = specific heat of exhaust gas

Bare tube film heat transfer coefficient,

h_{bare} = Q_{total} / A_{bare}* dT

or, h_{bare} = Q_{total} / лDL* dT,

where, dT = T_{exh} - T_{am}b

$mL = \sqrt{\frac{hCfin}{KA}} * L$

Quantity of heat actually dissipated by fin,

$Q_{fin} = Q_{total} - (A_{pipe} * h * dT)$

Quantity of heat that can be dissipated by ideal fin,

$Q_{fin\text{-}ideal} = A_{fin\text{-}avail} * h * dT$

Fin efficiency,

$\eta_{fin} = Q_{fin} / Q_{fin\text{-}ideal}$

Fin effectiveness,

$\epsilon_{fin} = Q_{fin} / Q_{bare}$

(a)

(b)

(c)

Fig. 3.7 (a) Annular finned pipe (b) Longitudinal finned pipe (c) Bare pipe

3.6 Electrolux Vapour Absorption System

Absorption chillers play an important role in the CCHP systems by recovering waste heat for cooling which is a higher exergy application. They reduce the fuel consumption along with the carbon footprint. But, low coefficient of performance is the inherent disadvantage of a single effect absorption cycle.

Li-Br refrigerant mixture pose problems like very low working pressure, crystallization etc.But the ammonia-water mixture is free from such problems. This pair has more stability and easier control with the possibility to produce sub-zero temperatures.

Four units of Electrolux vapour absorption-refrigerators (Dometic RH440-LD) were modified, assembled and installed for space cooling application in this study. Dometic RH440-LD is a commercially available, electrically operated NH_3-H_2O Electrolux absorption refrigerator (single effect) with a capacity of 41 L and heat input of 95 W.

It is also called triple fluid absorption system, the three fluids being ammonia, hydrogen and water. Ammonia is used as refrigerant and water as an absorbent.

The third fluid, hydrogen is used to increase the evaporation rate of liquid ammonia. The refrigeration circuit comprises of an evaporator coil, an air-cooled absorber, an upright generator, an air-cooled condenser. The refrigeration unit was hermetically sealed.

3.6.1 Principle of operation

The triple fluid vapour absorption system cycle of operation is described below. From the condenser, low pressure saturated liquid ammonia enters the evaporator. In accordance with Dalton's theory, hydrogen creates a change in partial pressure, and liquid ammonia evaporates at low pressure and temperature by absorbing the latent heat from the cooling space, thus creating the cooling effect. Ammonia - hydrogen mixture returns from the evaporator; ammonia enters back to absorber where it is absorbed by a weak solution of water and ammonia, and hydrogen rises upwards. Now, absorber contains a strong solution of ammonia in water that passes to the generator to be heated by exhaust gases. In generator, ammonia vaporises and along with the traces of water vapour pass to the water separator. Water is separated from ammonia and a weak solution of ammonia returns to the absorber by gravity, where it can absorb ammonia coming from the evaporator.

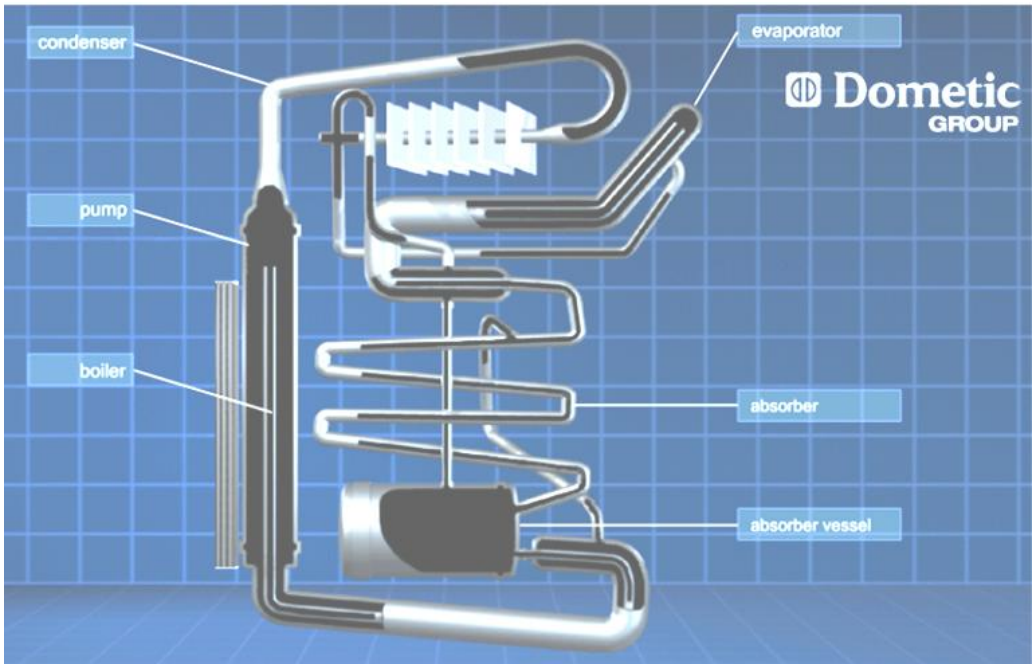

(a)

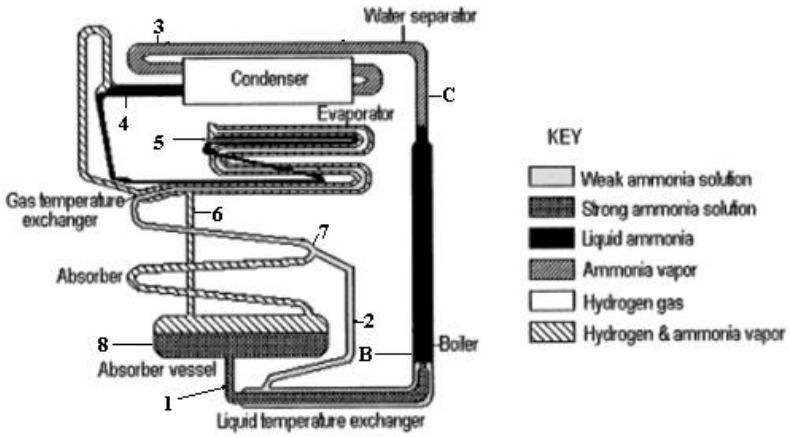

(b)

Fig. 3.8 (a) Components of an Electrolux vapour absorption system [92]
(b) VAR showing flow of refrigerant [93]

High pressure ammonia vapours entering the condenser are condensed and the latent heat of condensation is released to the surroundings. The process continues to produce the refrigerating effect.

Fig. 3.8 (a) shows the various components of an Electrolux vapour absorption system. Fig. 3.8 (b) shows the ammonia-water-hydrogen flows in the vapour absorption unit.

3.7 Analysis of micro-trigeneration system

3.7.1 Experimental plan

Blends of mahua oil (M) and mineral diesel (D) in various proportions were prepared by mixing different volumes of filtered mahua oil and diesel. Blends were designated by the letter 'Mxx'. For example, M20 indicates that it contains 20 % of mahua oil and remaining 80 % is diesel. Similarly, blend of mahua biodiesel (Bxx) with diesel was also prepared.

A series of tests were designed to evaluate the performance and emissions of engine in various modes using different alternative fuels. For M20, comparison was also made between rated and optimised engine settings. Various parameters were recorded in order to evaluate the following:

- Engine generator power output, BSFC, BTE and EGT in all modes of operation;
- Heat recovered from heat exchangers, fuel preheating unit and the engine cooling system;
- Coefficient of performance (COP) of the space cooling unit;
- Different temperatures, relative humidity and the time taken to reach comfort state.
- Total useful energy output
- Total thermal efficiency
- Exhaust emissions.

A detailed experimental plan was designed to evaluate the performance of the entire micro-trigeneration system.

1. In the first place, in single generation and at rated engine settings (196 bar and 23 ^{o}btdc), mahua oil and its various blends with diesel were tested to find the optimum blend considering maximum BTE, minimum BSFC and emissions at full load condition. After the blend was finalised, further experimentations were conducted using this optimum blend only.

2. Mahua oil methyl ester (mahua biodiesel) was prepared through transesterification process from Mahua oil. It was followed by the characterisation of fuel properties of all test fuels, viz, diesel, mahua oil, ricebran oil, neem oil, mahua biodiesel and their blends with diesel.

3. Now, Mahua, Ricebran and Neem oils and their blends with diesel along with mahua biodiesel blend with diesel were tested as fuels in single generation at rated engine settings in

the entire load range to find the performance and emission characteristics of the engine. Baseline values of diesel were also generated.

4. Next step was to conduct experiments with fuel preheating. Mahua blend with diesel (M20) and pure mahua oil (M100) were used as fuels and preheated using exhaust gases to 30, 60, 80 and 90^{o} C to find the best preheat temperature for maximum BTE, and minimum BSFC and emissions. This preheat temperature was used in further experimentations in cogeneration and trigeneration modes. At this preheat temperature, performance and emission characteristics of the engine for entire load range were determined using M20 as fuel.

5. A set of experiments were conducted to find the optimum values of fuel injection opening pressure (IOP),fuel injection timing (IT), and exhaust gas recirculation (EGR) using M20 blend considering maximum BTE and minimum BSFC and emissions at full load condition.

6. Next, the following sets of experiments were conducted with space heating arrangement:-

a. Tests were conducted at rated settings for the engine in micro-cogeneration and micro-trigeneration modes, using various fuels with following variations-

i. Use of unfinned pipe, longitudinal finned pipe and annular finned pipe for space heating in the cabin.

ii. Exhaust gas fired and hot water fired settings.

iii. Combined power and fuel preheating(C-P-FP) and combined power and space heating (C-P-SH) modes.

iv. Combined power, fuel preheating and space heating (C-P-FP-SH) mode (Direct exhaust fired)

v. Combined power, fuel preheating, water heating and space heating (C-P-FP-WH-SH) mode (Hot water fired)

b. Similar tests were also performed with M20 fuel at optimised engine settings and EGR.

7. The following sets of tests were conducted with space cooling arrangement:-

a. Tests were conducted at rated settings for the engine in micro-cogeneration and micro-trigeneration modes, using various fuels with following variations-

i. Combined power and space cooling(C-P-SC) mode

ii. Combined power, fuel preheating and space cooling (C-P-FP-SC) mode

b. Similar tests were also performed with M20 fuel at optimised engine settings and EGR.

8. Energy analysis was done to find out the parameters of micro-trigeneration and compared with that of single generation and cogeneration. Exergy analysis was also done to determine the exergetic efficiencies.

9. Simulation of the alternate fuel operated micro-trigeneration system was also conducted. A simplified simulation model was developed using Diesel RK software for alternate fuel operated Micro-trigeneration and the results were validated with experiments.

10. Finally, Economic analysis was conducted for the micro-trigeneration system. Energy balance was estimated and the energy savings were determined. A comparison was made with separate production.

3.7.2 Energy and Exergy analysis

The engine generator performance and emissions were evaluated when it was run on single generation mode with alternate fuels in both rated as well as optimised engine settings. The performance and emissions of the system in cogeneration and trigeneration modes were also evaluated. In all cases, the parameters were recorded for the entire engine load range.

In various experiments, the required parameters were measured to evaluate the power, heat recovered from coolant and exhaust, the refrigeration effect, total useful output, total thermal efficiency, emissions etc. Relevant data were recorded and performance characteristics (BTE, BSFC and EGT) and emission values (CO, HC, CO_2, O_2, NOx and Smoke) were recorded as required in the above experiments. Tests were conducted and repeated thrice, and averaged values were recorded to increase the reliability of the results. The results were displayed in appropriate graphs and analysed.

Exergy analysis (or, second law analysis) is concerned with energy degradation and entropy generation during a process. It defines maximum available energy in an energy system through interaction of the system with its surroundings, as it reaches thermal, mechanical and chemical equilibrium. Magnitude of losses and irreversibility in components, and also the whole system can be determined using exergy analysis.

Chemical exergy of the fuel was used as the Primary exergy input to the micro-trigeneration system. Exergy destruction in system components was calculated and then

related to the exergy of the fuel and to the total exergy destruction in the system. Exergy recovered from engine cooling, engine exhaust, VA system and exergy losses were determined. Exergy efficiencies were also determined. The reference dead state in the exergy analysis was considered as the atmospheric pressure and temperature.

3.7.3 Mathematical formulations

Fuel input energy: $Q_f = m_f * LHV$

Heat available in engine exhaust, $Q_{exh} = m_{exh} * c_{pexh} * (T_{engine\text{-}exh} - T_{amb})$

Heat available in generator of the VAR ($Q_{ava\text{-}gen}$), $Q_{ava\text{-}gen} = \epsilon$ HE-gen * Q_{exh}

Coefficient of Performance (COP_{cool}), $COP_{cool} = \frac{Q_{RE}}{Q_{ava}}$

Heat available for space cooling ($Q_{ava\_space\ cool}$), $Q_{ava\_space\ cool} = Q_{RE} = COP_{cool} *.Q_{ava}$

Heat available for fuel preheating ($Q_{ava\_fuel\text{-}preheat}$) $Q_{ava\_fuel\text{-}preheat} = \epsilon$ HE fuel- preheat $*Q_{exh}$

Heat available for hot water ($Q_{ava\_hotwater}$) $Q_{ava\_hot\ water} = \epsilon_{engine\text{-}jacket} * Q_{engine\text{-}jacket}$

Heat available for space heating ($Q_{ava\_space\ heat}$), $Q_{ava\_space\ heat} = \epsilon_{finned\text{-}pipe} * Q_{ava\text{-}sh}$

Useful energy output of micro-trigeneration, $E_{useful} = Q_{RE} + Q_{ava\_hot\ water} + BP$

Thermal efficiency of micro-trigeneration ($\eta_{trigeneration}$), $\eta_{trigeneration} = \frac{\text{Useful energy output}}{\text{heat supplied}}$

3.7.4 Assumptions and limitations

In the thermodynamic analysis of the micro-trigeneration, the following assumptions have been made:

- Internal energy demands of the micro-trigeneration unit are neglected.
- Reciprocating diesel engine has been considered as prime mover.
- Only steady-state and steady-flow processes are assumed
- Heat transfers and pressure drops in pipings and ductings are ignored.
- Ideal gas principles have been applied to air and exhaust gas treatment.
- Combustion reaction in diesel engine is assumed to be complete.
- The kinetic energy and potential energy changes are assumed to be negligible.
- The dead (environmental) state values are taken as the actual ambient conditions.
- Lower heating value (LHV) of the fuel is used for calculations.

3.8 Simulation of micro-trigeneration system

For internal combustion engines, the theoretical models can be thermodynamic or fluid dynamics models. Further, they are also classified as single-zone and multi-zone models. Multi-zone models are based on the calculations of mass, momentum, energy and species conservation equations, and can be applied for the simulation of the internal combustion engines. [42]

Out of several software that were commercialized for the simulation of diesel engines, like ProRacing engine simulation, Virtual engine DYNO, etc, very little work has been reported using Diesel-RK program to simulate a diesel engine running on SVO–diesel blends.

Diesel RK software was chosen due to its close agreement with experimental results. In this software, the database for fuel properties can be modified according to the fuel used. Properties such as temperature, pressure, etc at each stroke or crank angle were used to calculate the parameters for SVO blend.

Using the energy and mass balance, and interfacing with DOS based file, the proposed trigeneration was simulated in Diesel RK software. Fundamental operating conditions were defined for the simulation model: the heat source temperature and power, the useful cold temperature and ambient temperature. The waste heat recovery system and the vapour absorption refrigeration system in the trigeneration, including engine working

processes were simulated. In this study, the Diesel-RK software was used to evaluate the performance of micro-trigeneration using a diesel engine with pure mahua oil (M100) as fuel. The obtained results were validated with experimental results with M100 as fuel in trigeneration mode at rated engine settings.

3.9 Economic analysis of micro-trigeneration system

For the economic analysis of the micro-trigeneration system, both heating and cooling seasons were considered in a year. A simple calculation methodology is adopted for economical analysis and payback period calculation.

Separate production of energy (Traditional System) -

For comparison, a system without trigeneration has been described. The electricity is purchased in single generation to perform the necessary services. An electric heater of 2000W heating element, with 85% efficiency would be used for space heating. Air conditioning is assumed to be provided by vapour compression machine of 0.5 ton capacity, and a COP of approximately 3.5, which is matching the requirements of the test cabin. Domestic hot water is assumed to be provided by an electric water heater (electric geyser), as it is the most common mode of hot water supply among the residents in India. A 3000 W capacity electric geyser with 90 % efficiency is chosen to compare with the hot water produced in trigeneration. Many other factors would influence the analysis, but these are not included in this simplified analysis.

Experimental micro-trigeneration system-

The strategy utilized for the economic analysis is thermal load following without thermal storage. Due to time and other constraints, thermal storage was not included in the set up. It is also assumed that all electricity generated in the micro-trigeneration is fully utilised. There are neither any shortages, nor any surpluses of electric energy.

In order to assess the economical feasibility, necessary input data like fuel costs, water costs, carrying charges, and operating and maintenance expenses etc, all have been considered. During the life of the micro-trigeneration system, the cost components may vary significantly. So, the levelized annual values for all cost components have been used. Various cost components have been described in the following paragraphs.

Fuel cost-

Assessment of direct material costs of diesel, Mahua oil and its biodiesel was conducted. Direct material and energy costs of transesterification process were assessed for mahua biodiesel. These costs include the actual costs of mahua oil, alcohol, KOH etc, and energy consumed in the transesterification process. Labour costs were estimated according to prevalent labour rates. Other costs include transportation, storage, wastages and losses, and are assumed to be negligibly small. Prevalent average costs (for bulk purchase) at the time of investigations were used for all cost calculations in the economic analysis. The fuel is used by the micro-trigeneration system, and its annual total cost is considered.

Total fuel cost in trigeneration operation/year = Fuel cost (Rs/kg) *BSFC (kg/kWh) * kWh generated/year

Investment cost (IC)-

The investment cost in trigeneration is the initial payment to be made at the time of purchase and installation of the unit and its components. It includes the costs of engine-generator set, absorption chiller cost, costs of heat exchangers, site preparation, installation, commissioning, etc. Also included are the associated costs of necessary raw materials to fabricate the overall set up, like plumbing and piping costs, insulation costs, cabin fabrication cost, various smaller set ups like, fuel preheating set up cost, VAR generator modification cost, EGR set up cost etc.

The cost of engine-generator set was taken from the supplier's quotation price.
Since the space cooling unit was designed and fabricated in the laboratory, cost data cannot be specifically ascertained, and only general cost estimations are made.

Lubricating oil cost-

It was calculated taking the specific lube oil consumption of 1.2 g/kWh as recommended in catalogue.

Maintenance and spare parts (inventory) cost-

The maintenance cost includes the costs of periodic maintenance and overhauls. The maintenance cost (MC) is based upon a factor of the electricity generated, and on hours of

operation as well as the life of the prime mover. It was generally assumed to be a total of Rs 1.00/kWh of power generated.

Electrical Energy Cost-

The average cost of electricity for residential consumer in India is utilized for this analysis. It will be used in separate production of energy only for the period when micro-trigeneration is shut down for maintenance; it is assumed that the micro-trigeneration set up will be shut down for maintenance for a period of roughly 2-3 % of total operational time (based on the experience with this set up).

Avoided costs (AC)-

These are based upon the energy that would have been utilized by the traditional separate production system. These are mainly based upon the electricity price purchased to provide for the power, cooling and heating needs.

Avoided costs = Cost of total energy required in separate production – cost of total energy required in micro-trigeneration

Annual savings (AS)-

These are based on yearlong operation of the micro-trigeneration unit and includes both the heating and cooling seasons, and is calculated as given by the equation given below,

Net annual Savings = {Avoided costs} – {Maintenance costs}

AS= AC-MC

Pay-back period (PBP) of the micro-trigeneration unit-

In the economic analysis, the important result is the pay-back period of the micro-trigeneration unit. This is that point of time after which the higher initial capital costs for the micro-trigeneration system has paid for itself, and starts saving money from the reduced annual operational expenses when compared to the traditional separate production system.

Payback period = Net micro-trigeneration investment costs/annual savings

PBP= IC/AS

CHAPTER 4

EXPERIMENTAL SETUP AND INSTRUMENTATION

For the realisation of the alternative fuel operated micro-trigeneration experimental test-rig, various smaller set ups were designed, fabricated and incorporated in the main test-rig. A number of duly calibrated measuring instruments were also attached to obtain the values of important parameters.

In addition to the basic test-rig for single generation, this chapter also deals with space heating and space cooling set up, EGR set up etc. Proper and necessary instrumentation for measurement of electric power, air flow, fuel flow, water flow, various temperatures etc and measurement techniques are also included.

A brief description of exhaust analyser and smoke meter to measure exhaust emissions is also given. It also includes the structure of experiments and the engine optimisation procedure with varying injection pressure, injection timing and EGR.

4.1 Diesel engine as Prime Mover

Prime mover selection for trigeneration application depends on the power requirement, performance, availability of fuel and price. Reciprocating engines have high efficiency, power and reliability with the ability of load variation and flexibility to run with different bio-fuels.

It was found that stationary diesel engines for agricultural applications can be operated at a particular speed and loading conditions for a longer time. Also, single cylinder diesel engines with mechanical fuel injection systems are more suitable for SVO/biodiesel fuel operation in the long run [1, 5, 33, 64].

So, a stationary, single cylinder, water cooled, four stroke 3.7 kW diesel engine with electric generator was selected and procured to be used as prime mover for micro-trigeneration test-rig. This engine is an agricultural engine widely used in rural India for irrigation and electricity generation. The overall set up has the facility for testing in all modes of operation-single generation, cogeneration and trigeneration.

The photograph of the procured engine-generator set is given in Fig. 4.1. The technical specifications of the engine and dynamometer are summarized in Table 4.1 and Table 4.2 respectively.

Fig. 4.1 Engine-generator set

Table 4.1 Major Specifications of the Engine [94]

S.No	***Components***	***Unit***	***Description***
1.	Engine Make and Model	-	Kirloskar Oil Engine, AV1
2.	Type of engine	-	Vertical, Single Cylinder, Water-Cooled, Four-Stroke , CI Diesel Engine
3.	Rotation		Clockwise (while looking at flywheel)
4.	Power rating as per IS: 11170	kW (bhp)	3.7 (5.0)
5.	Rated speed of engine	RPM	1500
6.	Bore X Stroke of engine	mm	80 X 110
7.	Cubic Capacity of engine	Litres	0.553
8.	Compression Ratio (CR)	-	16.5 : 1
9.	Torque at full load (Crankshaft drive)	k N m (kg m)	0.024 (2.387)
10.	Recommended fuel	-	Diesel (IS : 1460)
11.	Specific fuel consumption	g/kW/hr (g/bhp/hr)	245 (180)
12.	Fuel injection	-	Direct injection type
13.	No. of Injection Pumps Type of injection	-	1 number for single cylinder Flange mounted without camshaft
14.	Fuel injection timing	Degree crank angle	23^0 (before top dead centre)
15.	Fuel injection opening pressure	kgf/cm^2 (bar)	200 (196)
16.	Fuel Tank Capacity	Litres	6.5

17.	Apparatus for starting of engine Starting method	- -	Extension shaft; Starting Handle; (Decompression arrangement) Flywheel end Hand start
18.	Engine overloading capacity	-	10 % of rated output of engine
19.	Filter type Air Fuel Lubricating Oil	 - - -	 Dry oil bath (paper element) Bypass filter (paper element) Bypass filter (paper element)
20.	Governor type and class	-	Mechanical centrifugal type; Class A2/B1
21.	Method of Cooling Coolant flow rate	- Litre/min	Cooling Water (run through system, attached water flow meter) 7
22.	Lube-oil specification	-	HD- type 3 (IS : 496–1982)
23.	Lube-oil consumption	-	0.8% of SFC
24.	Lube-oil sump capacity	Litres	3.7
25.	Maximum permissible back pressure	kPa	2.5
26.	Maximum permissible intake depression	kPa	1.0
27.	Overall Dimensions of the engine (L X W X H)	mm	617 X 504 X 843
28.	Engine Weight (dry)	kg	130

Table 4.2 Specifications of the dynamometer [94]

S. No.	***Specifications***	***Description***
1.	Make	Power star
2.	kVA	3.5
3.	Voltage	230 Volt
4.	Current	14 Amperes
5.	Frequency	50 c/s
6.	Rating	Continuous
7.	RPM	1500

4.2 Single generation set up

The set-up for single generation includes the diesel engine, an electrical load bank, two fuel tanks-one each for diesel and alternative fuels, an air box, a panel displaying

different thermocouple temperatures, a tachometer and various flow meters and valves, along with exhaust analyzer and smoke meter for emission measurements.

The engine was coupled to a single phase, 220 V AC alternator, with electrical load bank, consisting of 37 electric bulbs of 100 W each for load application.

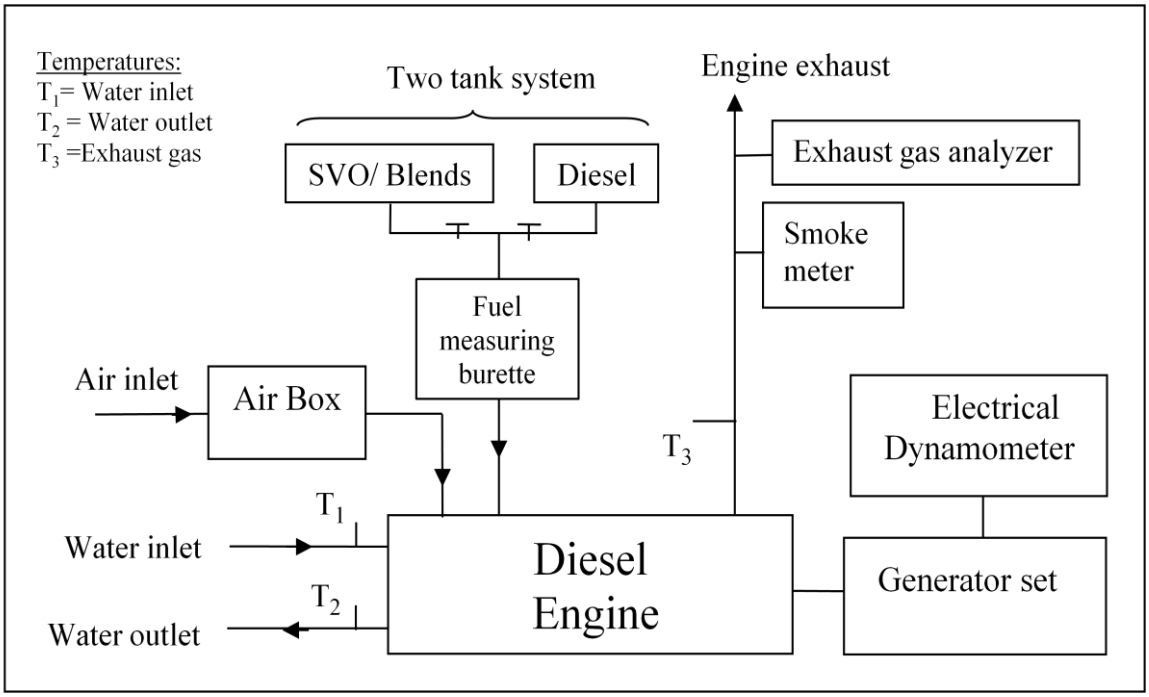

Fig. 4.2 Schematic diagram of experimental set up for single generation

The performance and exhaust emission tests were carried out on a single cylinder, four stroke, constant speed, water cooled, direct injection diesel engine. Fresh lubricating oil was filled in the oil sump before conducting experiments. The schematic diagram of the experimental setup for single generation is shown in Fig. 4.2.

4.3 Micro-trigeneration setup

The micro-trigeneration set-up is an extension of single generation set up with the addition of few more components. It consists of mainly a diesel engine with electricity generator, dual fuelling arrangement, an EGR set up, heat exchangers for fuel pre-heating/space heating and water heating, an exhaust gas driven modified Electrolux (four units) absorption chilling machine interfaced with the engine and a test cabin.

Fig. 4.3 Micro-trigeneration set up

Hence, the test facility provided electric power along with fuel pre-heating, water preheating and space heating/cooling.

The entire micro-trigeneration system was erected in I.C. Engines laboratory at MNIT Jaipur. The components and piping in the micro-trigeneration test facility was properly insulated to prevent the heat losses and extract maximum heat from the exhaust gases and the coolant. A multi-layered insulation was provided. All pipings were covered with asbestos ropes, glass wool and foils. The outer back wall of the cabin was covered by a thick layer of nitrile rubber.

Fig. 4.3 shows the micro-trigeneration set-up. Fig. 4.4 shows the insulation of various components of trigeneration unit.

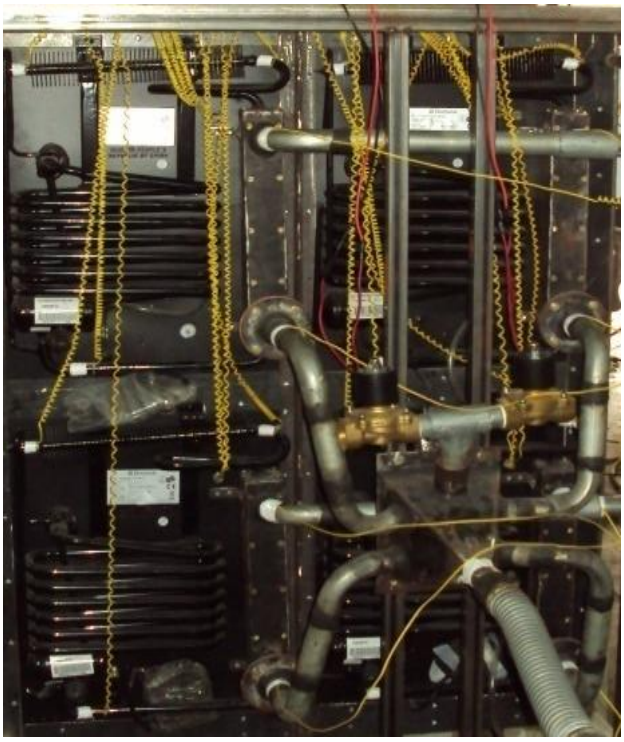

(a)

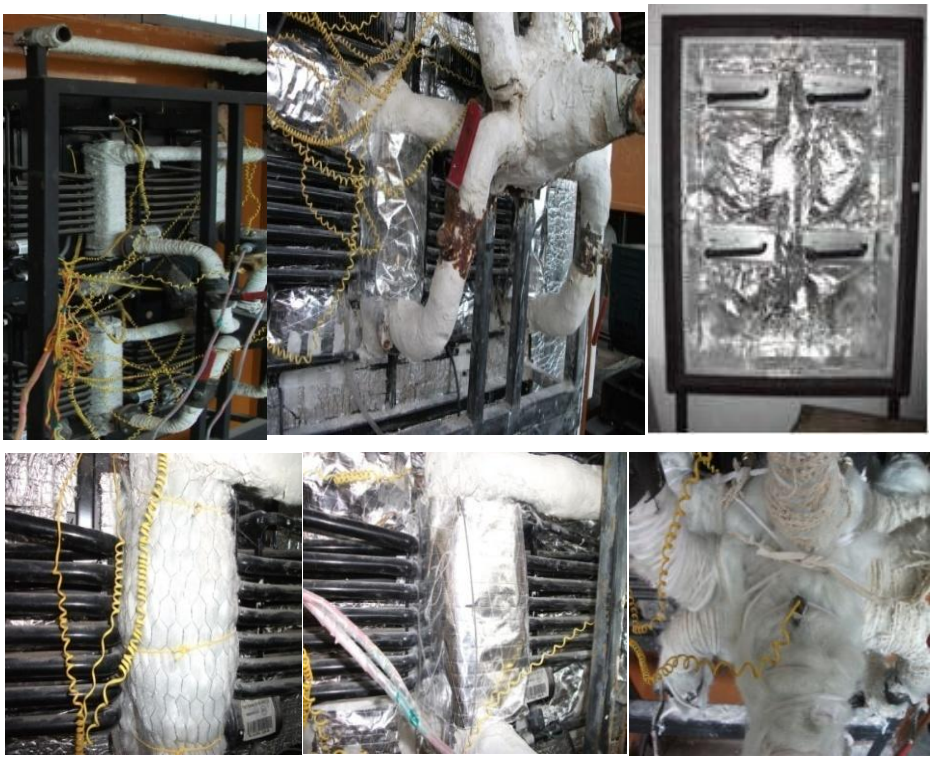

(b)

Fig. 4.4 (a) Uninsulated space cooling unit (b) Insulation of components of VAR unit

4.4 Measurement parameters

Various instruments were used for measuring the parameters such as engine load, rpm, fuel consumption, air flow rate, coolant, air and fuel temperatures and exhaust emissions.

4.4.1 Brake power-Electrical Load Bank

The engine-generator was coupled to an electrical load bank for providing load on the engine. The engine load was varied to 0, 1, 2, 3 and 3.7 kW, by operating the desired number of bulbs in the Electrical load bank. Voltmeter of range 0-230 V connected in parallel circuit, and the ammeter of range 0-30 A in series circuit were also installed to monitor the electrical power output. Fig. 4.5 (a) shows the electrical load bank and Fig. 4.5 (b) shows the air box with orifice.

(a) **(b)**

Fig. 4.5 (a) Electrical load bank (b) Air box with orifice

4.4.2 Air flow measurement

Air was supplied to the engine through an air box of size 45*45*50 cm^3 to dampen the pulsation of air, as shown in Fig 4.5 (b). It was having a sharp edged orifice plate of 20 mm diameter(d_o), and the discharge coefficient C_d = 0.6. The orifice was fitted on side wall of airbox. The air supply to engine was from the bottom of the air box. The air consumption was determined with the help of a U-tube water manometer, fitted on one side of the air box.

Mass flow rate of the air is given by the equation,

$m_{air}=\rho_{air}*C_d*A_{orifice}*(2*g*h_{water}*\rho_{water}/\rho_{air})^{1/2}$

where,

m_{air} = mass flow rate of air (kg/s)

ρ= density of air (kg/mm^3)

C_d= Coefficient of discharge (for orifice) = 0.6

$A_{orifice}$= Area of orifice=$A_{orifice}=л/4*d_o^2= 3.1416*10^{-4}$ (m^2)

h_{water} = manometric difference in water columns (m)

ρ_{water} = density of water = 1000 (kg/m^3)

ρ_{air} = density of air (kg/m^3)

4.4.3 Fuel flow measurement

Fuel flow rate was measured on volumetric basis, using 100 ml glass burette and a stop-watch. The glass burette was having graduated scale for measurement. Time elapsed for a fixed quantity of fuel (20 ml) before feeding to engine was measured, and simultaneously stop watch was operated to calculate the volumetric flow rate of fuel. The mass flow rate was calculated using fuel density and volumetric flow rate. A three way Tee valve was used as shown in Fig. 4.6 (a), in which one end was connected to the fuel tank, another to the burette and yet other to the fuel supply to the engine. Dual fuel tank system was used for intake of SVO or biodiesel as shown in Fig. 4.6 (b). Fig. 4.6 (c) shows the burette for fuel quantity measurement.

(a) **(b)** **(c)**

Fig. 4.6 (a) Three way Tee valve (b) Two fuel tank system (c) Burette for fuel flow measurement

4.4.4 Exhaust gas flow measurement

The total mass flow rate of the exhaust gas was estimated by mass balance, which is equal to the mass flow rate of air and mass flow rate of fuel. It was also verified by calculations using the fuel air ratio as displayed in the exhaust gas analyser.

4.4.5 Water flow measurement

Globe valves were used to control the flow of cooling water and exhaust gases. Mass flow rate of the coolant water was measured with a turbine type flow meter and a rotameter. Rahul make digital water meter was installed in the inlet water pipeline to the engine. The digital domestic water meter is of dry dial inferential type suitable for measuring the flow of water at a nominal pressure of 0.1 mPa and ambient temperature. It is of size 15 mm, class B type, with flow of 1.5 kl/h, and metering accuracy of ±2% to ±5%. This meter works according to ISO: 4064/ IS: 779 (1994) [95].

Further, a rotameter of range up to 10 l/s, was also installed just before the inlet to engine, to directly check the flow rate of water. The diagrams of both types of installed water flow meters are shown in Fig. 4.7 (a) and (b). Fig. 4.7 (c) shows the valve used to control the flow of water.

(a) **(b)** **(c)**

Fig. 4.7 (a) Digital water flow-meter (b) Rotameter
(c) Valve used to control the water-flow

4.4.6 Temperature measurement

K-type thermocouples with range of 0-600°C and coupled with an eight-channel selector switch (digital display) was used to measure the temperatures at several locations on

the engine, the components of the vapour absorption units, heat exchangers, and inside of the cabin. Water and exhaust gas temperatures, and ambient temperature were also measured. Fig. 4.8 (a) and (b) show the thermocouple wire, and Fig. 4.8 (c) shows the 8 channel selector switch.

A mercury-in-glass thermometer having range of 0-150°C with least count of 1°C was used to measure the engine jacket water temperatures and the ambient temperature.

(a) (b) (c)

Fig. 4.8 (a) Thermocouple wire bundle (b) Prepared thermocouple wire for use (c) 8-channel selector switch

4.4.7 Measurement of psychrometric parameters

Wet bulb temperature, dry bulb temperature, relative humidity and air velocity were recorded during experimentations with space cooling system.

Mercury in glass dry and wet bulb thermometer having a range of 0-100 ^{o}C and least count of 1°C were used to measure ambient and cabin temperatures. Air velocity was measured with the help of anemometer. Relative Humidity was measured by a thermo-hygrometer having range of 0-100% with a resolution of 1%. Relative Humidity was measured both for air inside the test cabin as well as for the ambient air.

The velocity of air leaving the evaporator could be varied, and was recorded by an anemometer with range for velocity 0.4 –30 m/s and having the least count of 0.1m/s.

4.4.8 Exhaust Emission Measurements

The major pollutants in the diesel engine exhaust are smoke and oxides of nitrogen. The exhaust gases were sampled from exhaust line using the probe of the gas analyzer, and the gas-composition was digitally displayed on its screen.

Prior calibrated five gas analyser (AVL DiGas 4000 light) was used to measure CO, HC, O_2, CO_2 and NOx in the exhaust gas.

Measurement of CO_2, CO, and HC emissions is based on the principle of non-diffractive infrared radiation (NDIR) and that of O_2 and NOx on electrochemical method. CO, CO_2 and O_2 were measured in volume percent, while NOx and HC were measured as n-hexane equivalent ppm. The five gas analyser is shown in Fig. 4.9 (a).

(a) **(b)**

Fig. 4.9 Exhaust gas composition measurements (a) five-gas analyser (b) Smoke meter

Prior calibrated smoke meter (AVL 437), as shown in Fig. 4.9 (b) was used to measure the smoke level of the exhaust gas as percent opacity. It is a filter-type smoke meter for measuring the soot content in the exhaust of diesel engines. This smoke meter is based on light extinction principle. Light is passed in a standard tube containing the sample from the engine exhaust. Then, intensity of transmitted light is measured by a photovoltaic device at the other end.

Major specifications of five gas analyzer and smoke meter are shown in Table 4.3 and Table 4.4 respectively.

Table 4.3 Major specifications of Five gas analyser [96]

	Measurement Principle	***Measurement range***	***Resolution***
CO	Infrared measurement	0-10 % Vol	0.01 % Vol
CO_2	Infrared measurement	0-20 % Vol	0.1 % Vol
HC	Infrared measurement	0-20000 ppm Vol	1 ppm
NOx	Electrochemical measurement	0-5000 ppm Vol	1 ppm
O2	Electrochemical measurement	0-25 % Vol	0.01 % Vol
λ-calculation	-	0-9.999	0.001
Oil temperature	-	0-150 °C	1 °C

Table 4.4 Major specifications of Smoke meter [96]

Measurement principle:	Measurement of filter paper blackening
Measured value output:	FSN (filter smoke number) or mg/m³ (soot concentration)
Measurement range:	0 to 10 FSN
Resolution:	0.001 FSN or 0.01 mg/m³
Sample flow:	~ 10 l/min
Repeatability:	Standard deviation 1 s = ± (0.005 FSN + 3 % of the measured value @ 10sec intake time)

4.5 Modified space cooling set up

Due to the small amount of waste heat available from the engine, the generators of the VAR systems were modified to direct exhaust fired systems instead of a hot water or steam fired.

Instead of the conventional cylindrical electrical heater, and to suit the space and orientation limitations, a one through heating jacket fabricated from G.I. sheet and consisting of a parallel flow, double pipe heat exchanger, was fabricated and installed external to the generator pipe, to receive the exhaust heat.

High temperature exhaust heat could be transferred in any or all of the assembled units simultaneously. The generator was insulated by tightly covering the jacket with glass

wool and wrapping it with asbestos ropes and thick aluminium foils. Fig. 4.10 depicts the micro-trigeneration set-up for space cooling.

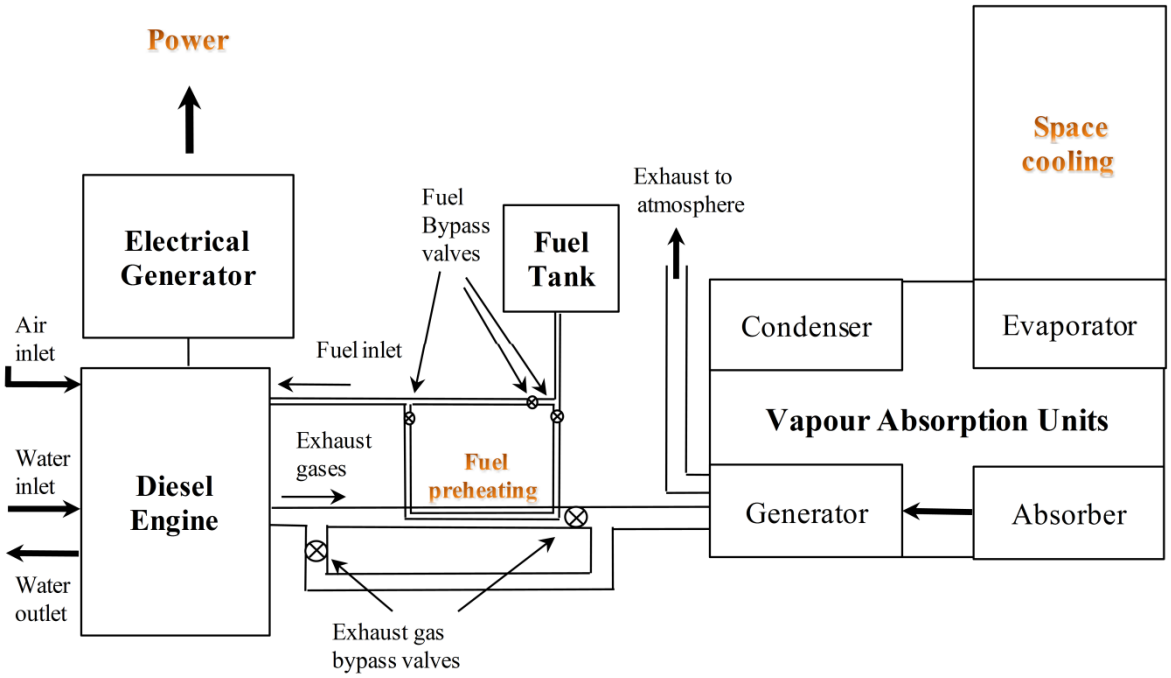

Fig. 4.10 Schematic diagram of the micro-trigeneration with power, fuel preheating and space cooling options

Four identical Electrolux VAR units (VAU, 1-4) were assembled with two on top and two on bottom side of the back wall of the cabin. Quantity of the exhaust gases flowing towards the generator were controlled using four globe valves located in exhaust gas line at the entry to the four generators of the VAR units. The generators of all the units were connected with common exhaust gas piping.

Two convective fans (100W each) were used to drive away excessive heat from top two condensers as shown in Fig. 2(d). Two fans (100W each) were also used in the cabin near the evaporator coil to maintain air-flow in the cabin.

The evaporator coils of the modified space cooling unit were mounted inside a cabin in which the space air temperature, humidity and velocity were all measured during the tests.

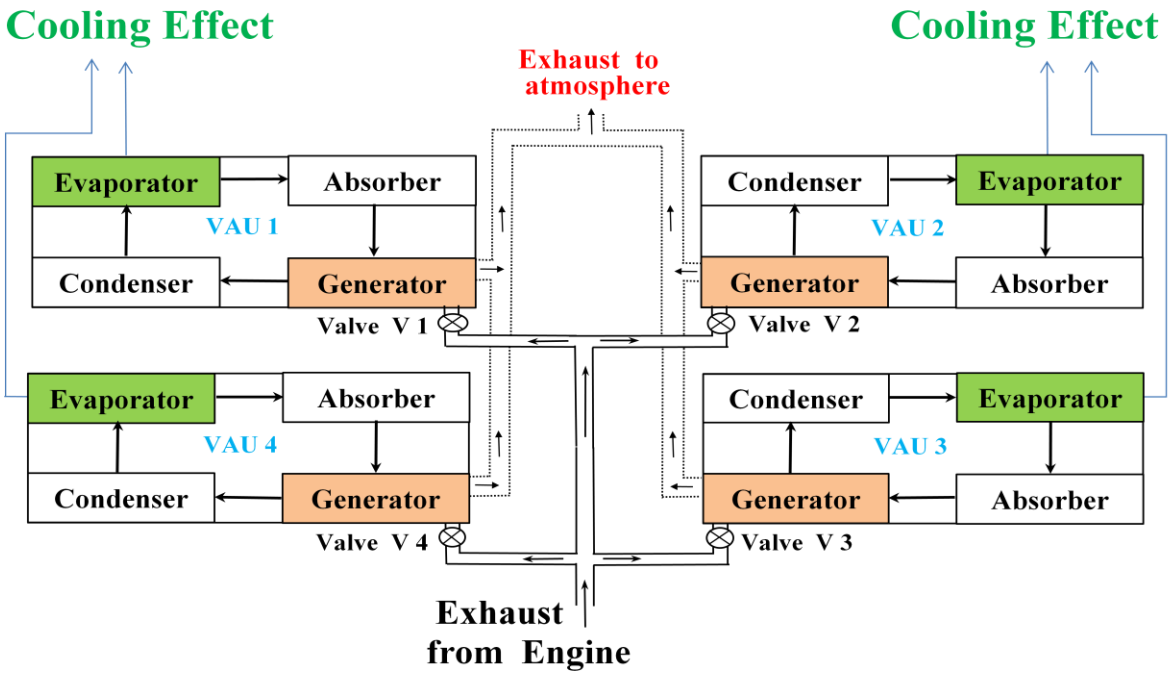

Fig. 4.11 Arrangement of the four vapour absorption units in the space cooling set up

K –type thermocouples (range~ 600 °C) were mounted at different points on the components of the space cooling system (all 4 assembled VAR units). Proper thermal insulation was adopted for the components of the space cooling unit. It was also ensured that all components were leak proof. Fig. 4.11 shows the schematic arrangement of the four VAR units.

4.6 Space heating set up

A simplified space heating system using direct exhaust gas as well as hot water was employed in this study.

Two cases were considered, as shown in Fig. 4.12 and Fig. 4.13 respectively.

i. The exhaust heat is directly passed in the pipe passing through the cabin for space heating.
ii. The exhaust heat is passed through a gas/water heat exchanger to heat the water, which is then pumped in the pipe to the cabin for space heating.

In case of direct exhaust fired system, the quantity of the exhaust gases could be varied with the help of a by-pass valve. In case of hot water fed system, the hot water was circulated by a pump, and controlled by a valve.

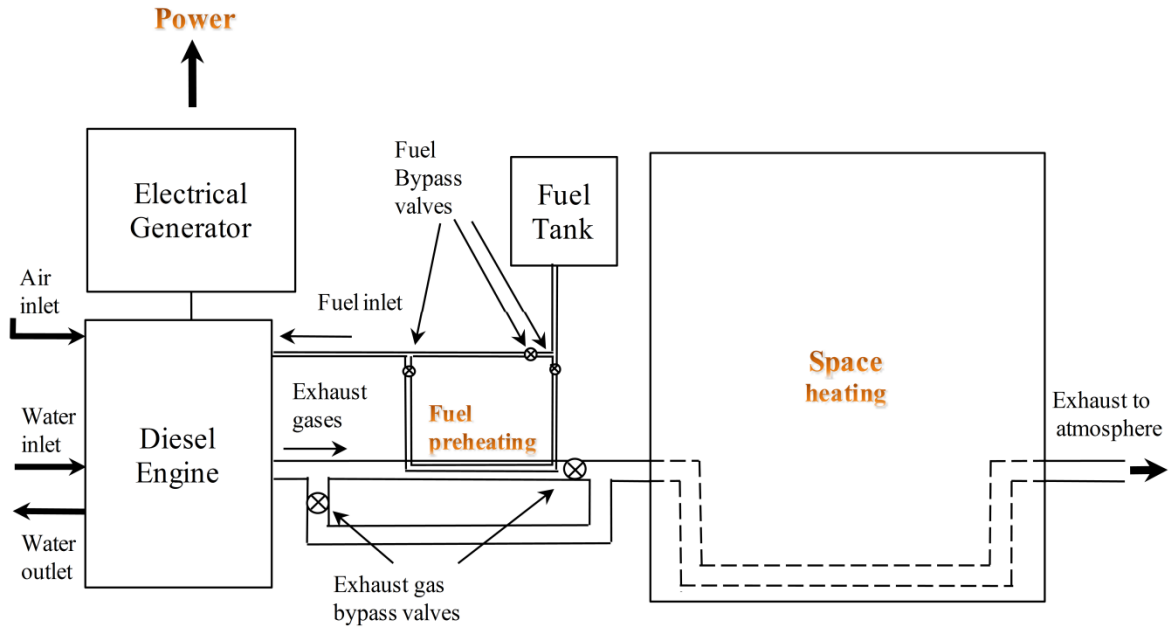

Fig. 4.12 Schematic diagram of direct exhaust fired space heating set up

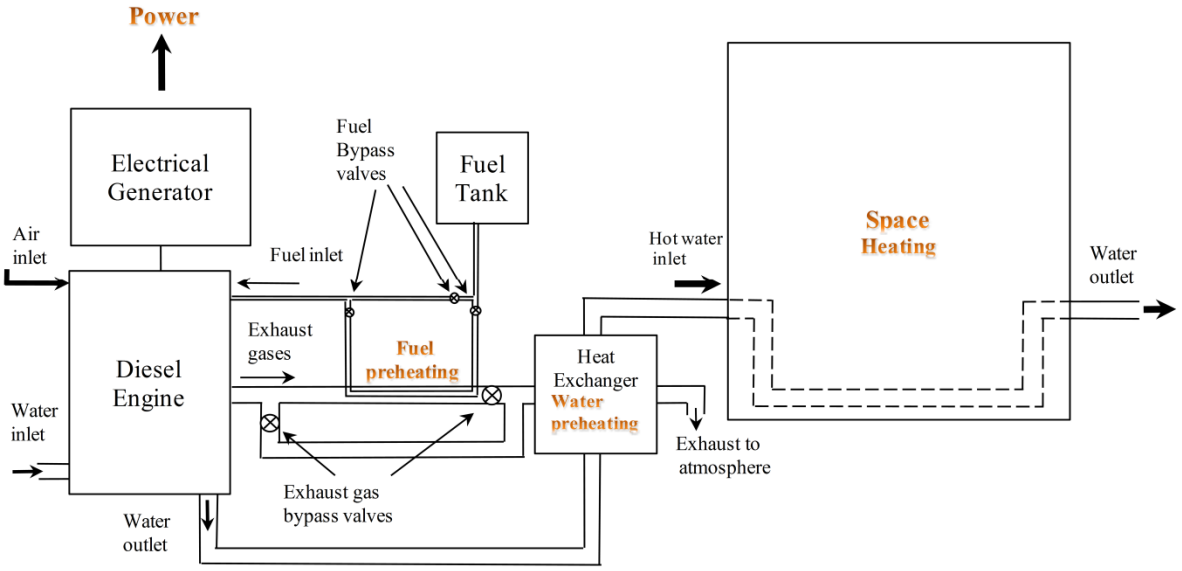

Fig. 4.13 Schematic diagram of hot water fired space heating set up

Convective heating with pipe emitters was used in the system. Experiments were conducted with three types of pipes- Bare pipe, annular finned pipe and longitudinally finned pipe, as shown in Fig 4.14 (a) and (b). Pipe lengths and surface area of fins were kept equal in case of finned pipes. The space-heating pipe arrangement is 0.4 m above the ground level and 0.2 m from the rear wall inside the test cabin. The effective length of test pipe emitter for

heating inside the cabin was 60 cm. For connecting pipes, layered insulation of 10 mm thickness with glass wool, asbestos ropes and aluminium foil was provided. Connecting pipe was not used for heating purpose, and so was properly insulated.

(a) **(b)** **(c)**

Fig. 4.14 Photographs showing (a) Annular finned pipe (b) longitudinal finned pipe (c) convective fan in the cabin

Bypass valves were used to shut off the energy supply to cabin, if not needed. Two small convective fans of 0.07 W each were also employed to create air flow in the cabin, as shown in Fig 4.14 (c). The exhaust gas/water temperature before and after the emitter pipe was measured with K-type thermocouples attached to the surface of the pipe. The cabin wall was constructed from 18 mm thick particle board of thermal conductivity (U= 0.17W/m-K).

The cabin wall was insulated using expanding foam insulation with a thermal conductivity of 0.04W/mK. This meant that most of the heat transfer occurred only from the test pipe section. Thermocouples were placed at the centre of each wall and also suspended in air in the middle of the cabin. The average temperature was calculated and recorded. The water flow rate was set to 7 litres/min.

4.7 Test cabin

A cabin of size 1.65 m Length x 0.53 m width x 2.22 m height was constructed using 18mm ply wood sheets and wooden battens. Two glass windows were provided for observation. The four evaporators of the four VAR units modified for space cooling were installed inside the cabin. The other components of the modified four units i.e. condenser, absorber, generator and the pipes etc, were assembled outside the cabin.

(a) **(b)**

(c)

Fig. 4.15 Photographs showing (a) front side and (b) back side of the cabin (c) insulation of walls of the cabin

Cabin air quality was monitored throughout the experimentations. Layered insulation was adopted to insulate the exhaust piping, the components of the VAR units and the rear wall of the cabin. Nitrile rubber, then glass wool and finally the aluminium foils were pasted at proper places at cabin walls to minimise the heat losses.

The side exterior walls and roof of the cabin was thermally insulated by 75 mm thick thermocol sheets. The internal walls and ceiling of the cabin was also insulated with high grade XPS sheets of 25 mm thickness. The photographs of the cabin and insulation of the walls are shown in Fig. 4.15 (a)-(c).

4.8 Fuel preheating- set up and experiments

The problem of using Mahua oil in diesel engine due to its high viscosity was solved by simultaneously blending and heating.

The engine fuelling system was modified for fuel preheating. Main components of the fuel preheating setup consisted of two fuel tanks (Diesel and Mahua oil), heat exchanger for fuel preheating, exhaust gas line, by-pass line, and performance and emissions measurement equipment. The fuel preheating arrangement installed in the exhaust passage is shown in Fig. 4.16. Engine was run with preheated mahua–diesel blend (PM20) and preheated mahua oil (PM100), and performance and emission characteristics were determined.

The engine was started using diesel for at least 20 minutes. After the engine warmed up, it was switched over to Mahua oil or blends, using a three way valve, whose one end was connected to Mahua oil tank, the other to diesel tank, and the third to the fuel pump of the engine. Also, the engine was run at idling for at least 20 minutes on diesel before stopping to ensure that all Mahua oil in the fuel line, fuel filter and injection pump was purged out, to prevent deposits and cold starting problems. Fuel passed through fuel measuring unit, and then entered the heat exchanger followed by fuel filter before entering the engine.

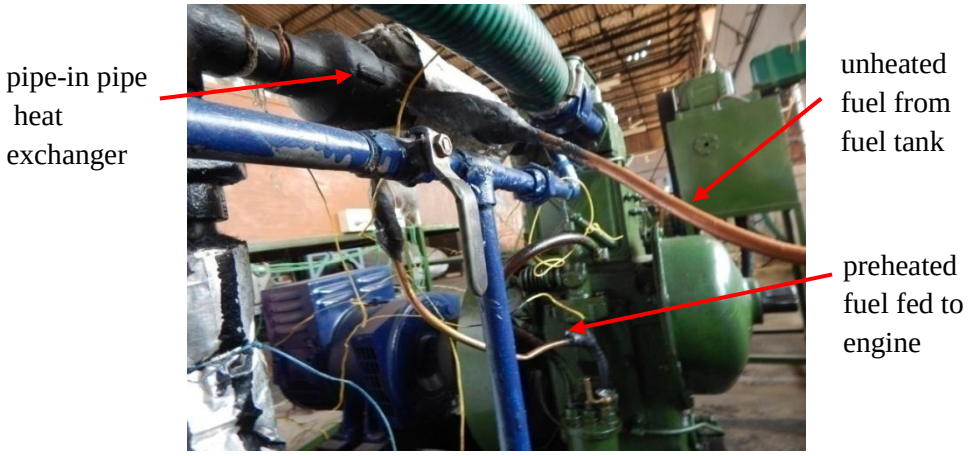

Fig. 4.16 Fuel preheating arrangement

The engine was tested with unheated diesel fuel, M20 and M100. Then, M20 was preheated at different fuel inlet temperatures and the performance and emission characteristics of the engine were evaluated. Engine was operated with fuel at four different temperatures, 30, 60, 80 and 90 ^{o}C, to find the optimum value of degree of preheat for M20. Effects of preheated fuel on brake power, brake specific fuel consumption, brake thermal efficiency, exhaust gas temperature, and emissions like CO, HC, NOx and smoke were observed.

The engine was run at a constant speed of 1500 rpm. The engine speed in rpm was recorded by mechanical contact type tachometer. The air and oil filters were replaced prior to each series of experimentations.

The system was allowed to reach the steady state before taking measurements. In all test runs, the desired load was applied to the engine for approximately 20 minutes so as to achieve steady state, and then various readings were recorded.

4.9 Engine optimisation for alternate fuel used

The optimum combination of injection opening pressure (IOP) and injection timing (IT) was desired while working with M20 as fuel in diesel engine, so as to obtain maximum BTE and minimum BSFC.

4.9.1 Injection Opening Pressure

The IOP is the opening pressure of fuel nozzle. Optimum IOP is that value in which maximum BTE and minimum BSFC is obtained. IOP was varied by testing the injector assembly in a nozzle tester, as shown in Fig. 4.17 (a). The spring tension of the injector needle with setting screw was varied to get different fuel injection pressure values. Some of the researchers have recently used this technique to vary the IOP for investigations in a diesel engine [63, 74, 97, 98, 99, 100]. Initially, one lower and one higher injection pressure was selected to identify the trend.

To start with, the tests were carried out using diesel and M20 on the engine with manufacturer recommended fuel injection pressure of 196 bars and injection timing of 23 ^{o}bTDC and at the rated speed of 1,500 rpm. These values were considered as baseline values throughout the experimentation. The engine tests were carried out at 0, 1, 2, 3 and 3.7 kW loadings. IOP was varied to 181, 196, 211, 226 and 240 bar (corresponding to 185, 200, 215, 230 and 245 kgf/cm^2 respectively).

To overcome the problem of high fuel viscosity, the engine was always started and run for 20 min, using diesel fuel and then switched to vegetable oil/blends. Similarly, while

shutting down, reverse was done to ensure that only diesel fuel was left inside the fuel system. At each load, after the engine reached the stabilized condition, the performance and emission parameters were recorded. The best IOP for the engine for improved performance and emissions at full load were determined.

4.9.2 Injection Timing

Injection timing influences the mixing quality of the air–fuel mixture and, consequently, the combustion process.

(a) **(b)**

Fig. 4.17 (a) Fuel injector pressure tester (b) Shims to set injection timing

In a mechanical pump-nozzle system, the start of fuel delivery from pump depends on the start of injection, which can be easily set to preferred value that leads to the highest BTE and lowest BSFC, along with reduced emissions.

Static fuel injection timing can be varied by varying the number of shims between the fuel injection pump body and engine body. To advance the IT, the shims under the pump were removed, and to retard the IT, additional shims were added below the fuel injection pump. Fig. 4.17 (b) shows the shims used to vary the injection timing of the engine.

Spill method was used to find the beginning of fuel injection. The flywheel is slowly rotated, and the crank angle at which the fuel spills out from the disconnected fuel injection pump outlet is determined, which shows the beginning of fuel injection.

Shims of 0.22 mm thickness were procured from the engine supplier. It was found that for addition or removal of each shim, the IT differed by 2 degree of crank rotation.

The tests were carried out using M20 on the engine with optimised fuel injection pressure at 0, 1, 2, 3 and 3.7 kW loadings. IT was varied to 21, 23, 25 and 27 ^{o}bTDC. Initially, one lower and one higher injection timing was selected to identify the trend. At each load, after the engine reached the stabilized condition, the performance and emission parameters were recorded.

For the engine set at optimised value of IOP, the best IT for improved performance and emissions at full load were determined.

Lubricant oil level was checked prior to all the tests. For each test, the engine was run for at least 20 minutes to allow the engine to achieve steady-state, before recording the data. All the experiments were replicated three times and average values were taken. Each reading was also averaged for values during loading and unloading.

4.9.3 Exhaust Gas Recirculation

Two predominant factors for formation of NOx are in-cylinder temperature and oxygen availability during combustion. EGR reduces oxygen availability, decreases the temperature in the combustion chamber and curbs NOx formation.

Some modifications in the engine set up were made to incorporate the EGR arrangement. The schematic diagram of the EGR setup is shown in Fig. 4.18 (a) and (b).

The experimental set up for EGR consists of the engine-generator set, exhaust bypass arrangement, pipes, exhaust-particulate filter, an exhaust gas control valve, air box, U-tube manometer, fuel metering systems, and exhaust gas analysers. Filter was used for particulate reduction in the recirculated exhaust gas. Exhaust gases were tapped from exhaust pipe and connected to inlet airflow passage for recirculation. The exhaust gas control valve installed in the pipe enabled manual control of the flow rate of EGR to inlet manifold.

Proper mixing of fresh air and exhaust gases were ensured by maintaining sufficient distance. A piping arrangement of total 3 m length was provided to connect the exhaust pipe and inlet air flow passage. Further, the exhaust gases were allowed to enter the engine inlet manifold about 2 m away from the engine. This caused a reduction in the temperature of the

exhaust gases without any additional cooling system. Especially in cogeneration and trigeneration, the temperature of the exhaust gases after the space heating/cooling exit in such a small agricultural engine is of the order of 150^{o} C, so this arrangement ensures the EGT at inlet manifold to be close to ambient air value.

(a) **(b)**

Fig. 4.18 (a) Valve to vary the EGR flow (b) EGR set up

Recycled exhaust gas temperature was measured just before its entry into the combustion chamber by using a K- type thermocouple.

Pressure difference obtained from the U-tube manometer was used to calculate the volume of air replaced by exhaust gases from which the percentage EGR was calculated on volume basis.

$$\text{EGR \%} = \frac{(\text{volume of air without EGR} - \text{volume of air with EGR})}{(\text{volume of air without EGR})} \times 100\%$$

EGR percentages during the tests were varied in steps, i.e., 5, 10, 15 and 20%.

With optimised settings of IOP and IT previously determined, the engine was tested with M20 at various rates of EGR, to find an optimum ratio of EGR as regards NOx, BSFC and other emissions. The engine was also run with M20 at rated settings and without EGR to generate baseline data.

CHAPTER 5

RESULTS AND DISCUSSION

After conducting the experiments according to the test plan as described in Chapter 3 and 4, various measured and calculated parameters were documented, and displayed in graphs and tables for analysis, and are discussed in this chapter.

This chapter is divided into two parts. The first part (Part-I) concerns basically with fuel properties characterisation, blend selection, fuel preheating and engine optimisation using M20 as fuel with varying IOP, IT and EGR. The second part (Part-II) is related to engine performance and emission analysis at rated and optimised engine settings with alternate fuels in various modes: single generation, cogeneration and trigeneration. It deals with energy balance, fuel preheating, space heating/cooling, useful energy outputs, total thermal efficiencies, emission analysis, exergy analysis, simulation, and economic analysis.

Comparisons of parameters were made while using various fuels in cogeneration and trigeneration modes at rated settings, and also when M20 was used at optimised engine settings.

The various fuels employed in the study include M20, R20, N20, MB20, M100 and MB100, along with base case diesel (D) for single generation at rated settings.

Part-I

5.1 Fuel properties characterisation

Fuel characterisation for major physico-chemical properties of test fuels was conducted as per ASTM standards in Biodiesel labs in Mechanical and Chemical Engineering Departments of MNIT Jaipur, and the property values, procedure followed and the instruments used are recorded in Table 5.1.

Acid value of Crude Mahua oil (M100) was 35.4 mg KOH/g; but, after esterification, it reduced to 1.35 and for mahua biodiesel (MOME, or MB100), it was only 0.38. The biodiesel yield was high at 91 %.

Table 5.1 Fuel properties of various fuels with ASTM limits and methods used

Fuel property	***Unit***	***Diesel***	***M100***	***MB100***	***ASTM D 6751***	***Method / apparatus***
Density at 15 ^{o}C	kg/m^{3}	832	912	882	*	Relative density bottle
Kin. viscosity at 40 ^{o}C	mm^{2}/s (cSt)	2.61	37.84	5.24	1.9–6.0	Redwood viscometer
Calorific value	MJ/kg	43.51	38.65	39.43	*	Bomb calorimeter
Acid value	mg KOH/g	–	35.40	0.38	< 0.8	Standard titrimetry
Flash point	^{o}C	62	227	198	>120	Pensky martens closed cup Flash and Fire point apparatus
Fire point	^{o}C	71	239	195	*	
Cloud point	^{o}C	-11	16	5	*	Cloud and Pour point apparatus
Pour point	^{o}C	-20	11	2	*	
Ash content	%	–	0.88	0.02	< 0.03	Muffle furnace

* Not mentioned

It was found that all vegetable oils and Mahua biodiesel were completely miscible with diesel. Most of the properties of vegetable oils, mahua biodiesel and their blends with diesel were comparable to diesel fuel.

The lower calorific values of M100 and MB100 were found to be 38.65 and 39.43 MJ/kg, respectively, which were 11 and 9.5 % less than diesel respectively. This may be due to the difference in chemical composition, different percentage of carbon and hydrogen atoms and the presence of oxygen molecule in mahua oil and biodiesel.

The flash and fire points of all test fuels were quite high making them extremely safe in transportation, storage and handling.

Density and viscosity varied linearly with increasing concentration of mahua oil/biodiesel in the blends. The kinematic viscosity of Mahua oil reduced from 37.84 to 5.24 cSt after transesterification. The densities of M100 and MB100 were 9.5 % and 6 % higher than that of HSD, may be due to the higher molecular weights of triglyceride molecules present in the oil.

Viscosity of M100 decreases remarkably with temperature. Preheating of M100 at a temperature of 90^{o} C, lowered its viscosity to 6.12 cSt, which was close to the level of viscosity of diesel. Influence of temperature on viscosity of Mahua oil is shown in Fig. 5.1.

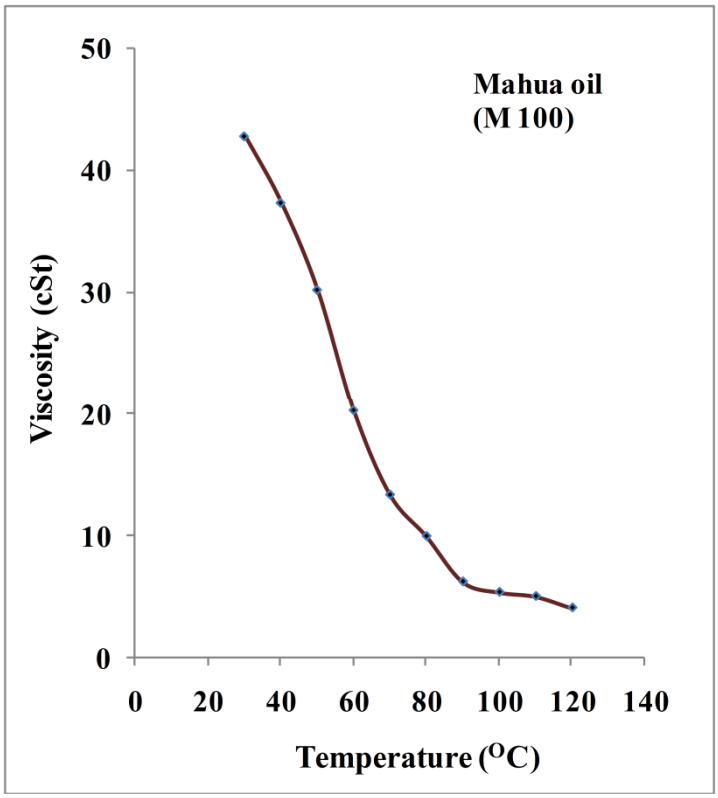

Fig. 5.1 Variation of viscosity with temperature for mahua oil

Table 5.2 Fuel properties of various fuel-blends with ASTM limits and methods used

Fuel property	*Unit*	*Diesel*	*M 20*	*MB20*	*R20*	*N20*	*ASTM D 6751*	*Method /apparatus*
Density at 15 ^{o}C	kg/m^{3}	832	848	842	851	853	*	Relative density bottle
Kin. viscosity at 40 ^{o}C	mm^{2}/s (cSt)	2.61	9.65	3.14	10.45	9.66	1.9–6.0	Redwood viscometer
Calorific value	MJ/kg	43.51	42.54	42.69	42.38	42.39	*	Bomb calorimeter

* Not mentioned

5.2 Blend selection

Tests were conducted to estimate the best Mahua blend regarding maximum BTE, minimum BSFC and emissions. The variation of engine performance (BSFC, BSEC, BTE, EGT) and engine emissions (CO, HC, NOx and Smoke) at engine full load for Diesel (D) and various mahua blends with diesel (M10, M20, M30, M50, M100) are shown in Fig 5.2 (a)-(h). All tests were conducted at rated engine settings of 200 bar injection opening pressure and 23^{o} btdc injection timing.

5.2.1 Brake specific fuel consumption and Brake specific energy consumption

The BSFC for M10, M20, M30, M50 and M100 at engine full load condition were 0.295, 0.292, 0.3, 0.318, 0.36 kg/kWh respectively, which were 10.9, 9.8, 12.8, 19.5 and 35.3 % higher than that of diesel.

As the BSFC was calculated on weight basis, obviously higher densities of blends resulted in higher values for BSFC, for the same volume at the same injection pressure. So, a better measure, BSEC based on energy consumption was also calculated.

To compare fuels with different calorific values, brake specific energy consumption (BSEC) is more effective, which is the product of BSFC and the calorific value of the fuel.

The BSEC for M10, M20, M30, M50 and M100 at engine full load condition were 12.45, 12.42, 12.46, 12.89, 13.39 kg/kWh respectively, which were still higher than that of diesel by 8.1, 7.8, 8.3, 11.9, and 16.2 %.

BSFC and BSEC slightly increased with increasing mahua concentration in the fuel blend because of the lower LCV and higher viscosity of mahua oil. LCV of the fuel affects the engine power. The effective power decreases with the increase of SVO quantity in the fuel mixture. Thus, the engine needs more fuel consumption to maintain the same amount of output power.

As can be seen, the minimum values were observed for M10 and M20 blends.

5.2.2 Brake thermal efficiency

BTE for M10, M20, M30, M50 and M100 at engine full load condition were 28.83, 29.02, 28.66, 27.94 and 26.88 % respectively, which were 8.1, 7.7, 8.3, 11.8, and 13.9 % lower than that of diesel. BTE in general, reduced with the increasing concentration of Mahua oil in the blends.

However, BTE of M20 was highest among blends and slightly (7.7 %) lower than that of Diesel. This could be attributed to the best trade-off between reduced calorific value and increased oxygen content in the M20 blend.

5.2.3 Exhaust gas temperature

EGT was found to increase with the increasing concentration of Mahua oil in the blends. EGT for M10, M20, M30, M50 and M100 at engine full load condition were 380, 384, 385, 390 and 395 ^{o}C respectively, which were 0.53, 1.6, 1.85, 3.17 and 4.5 % higher than that of diesel. EGT with M100 was highest among all blends.

5.2.4 Exhaust emissions

CO for M10, M20, M30, M50 and M100 at engine full load condition were 0.05, 0.05, 0.05, 0.04 and 0.03 % respectively, which were 0, 0, 0, 20 and 40 % lower than that of diesel. HC for M10, M20, M30, M50 and M100 at engine full load condition were 48, 44, 42, 39 and 31 ppm respectively, which were 7.7, 15.4, 17.3, 25 and 40.4 % lower than that of diesel. CO and HC emission decreases with increasing concentration of Mahua in the blend, probably as a result of extra oxygen molecule present in the fuel and more complete combustion at engine full load.

NOx for M10, M20, M30, M50 and M100 at engine full load condition were 1688, 1691, 1693, 1715 and 1745 ppm respectively, for which M10, M20 and M30 were 0.78, 0.59 and 0.47 % lower, and for M50 and M100 were 0.82 and 2.6 % higher than that of diesel. Mahua and its lower blends showed lower NOx emissions than diesel, but were slightly higher for higher blends.

A NOx-Blend trade off can be seen for M20 and M30 blends.

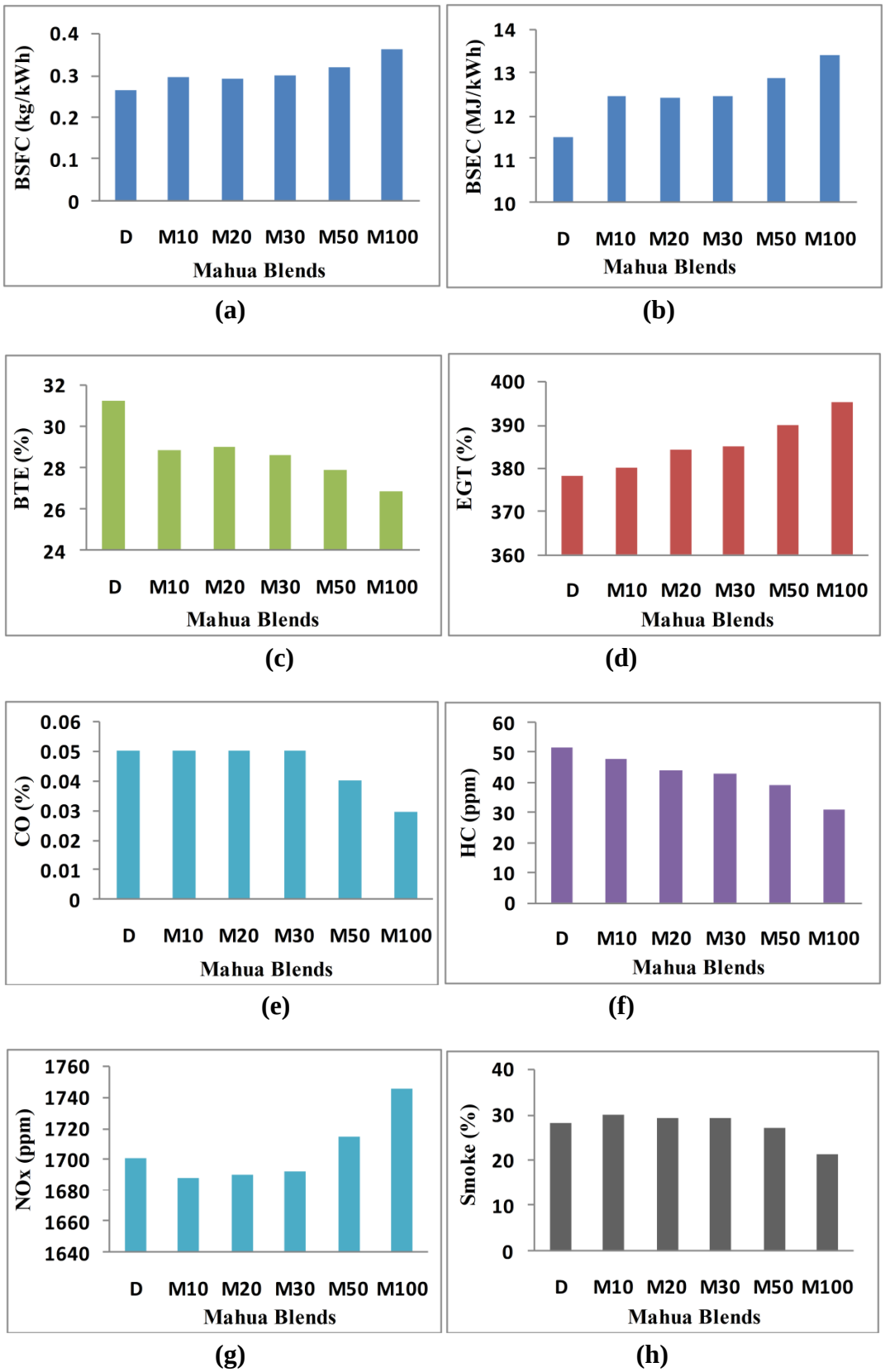

Fig. 5.2 (a)-(h) Engine performance and emission characteristics at engine full load for various mahua blends with diesel (rated engine settings)

The NOx emissions increase with higher blends due to more complete combustion with presence of oxygen in fuel.

Smoke opacity for M10, M20, M30, M50 and M100 at engine full load condition were 27.9, 26.8, 26.3, 22.7 and 19.3 % respectively, which were 1.4, 5.3, 7.1, 19.8 and 31.8 % lower than that of diesel. Smoke opacity for all blends were lower than that of diesel, and decreased with higher blends. This is possibly a result of better combustion of Mahua oil and blends at engine full load.

Viscosity of Mahua oil decreases after blending. The viscosity of M20 and M30 blends were 4.19 and 5.35 cSt respectively, and only slightly higher than diesel. NOx, CO and HC values of emissions were higher for higher blends. Considering the possible carbon deposits formed during long term usage of vegetable oils/blends [72], M30 as well as higher blends were not selected. BTE was highest, and BSEC lowest for M20 blend. Also, most of the emissions were lowest with M20.

A blend ratio of 20 % with diesel for SVOs and Biodiesels is also recommended by many researchers [59, 72]. So, 20 % blend was selected for further experimentations.

5.3 Fuel preheating

The optimum fuel pre-heat temperature at which the viscosity of M100 and M20 becomes comparable to that of diesel at 30 ^{o}C was determined. The performance and emission characteristics of diesel engine using these fuels at the optimum temperature were evaluated and the results were compared with those of unheated fuels and baseline diesel.

5.3.1 Preheat temperature determination

Higher viscosity is a major problem in using vegetable oil as fuel for diesel engines. Preheating of fuel reduces the viscosity.

But, there is discrepancy in the data concerning the optimal preheat temperature for a particular SVO to obtain improved combustion, probably because the temperature requirement depends on engine type and configuration. At least 60 ^{o}C preheating is needed for smooth flow and to avoid fuel filter clogging. At 90 ^{o}C, the viscosity is very close to that of diesel [82, 101, 102, 103].

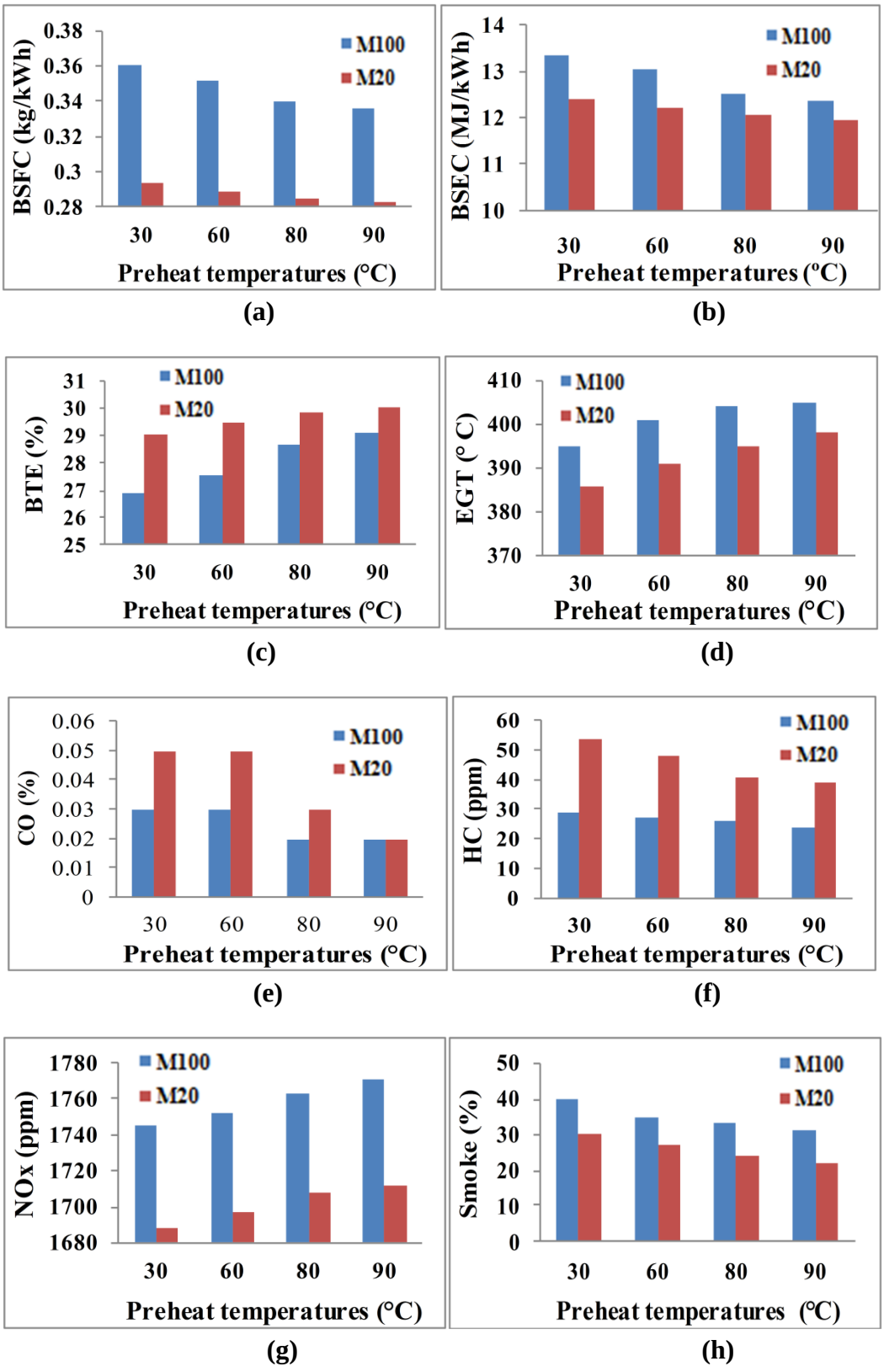

Fig. 5.3 (a)-(h) Engine performance and emission characteristics at full load with M100 and M20 at various preheat temperatures

Engine performance and exhaust emissions for engine full load operation, at fuel preheating temperatures of 60, 80 and 90 ^{o}C were evaluated for M100 and M20.

Fig 5.3 (a) to (d) shows the variation of BSFC, BSEC, BTE and EGT at full load, at various preheat temperatures.

BSFC was lower for both M100 and M20 at 90^{o} C, from their unheated values by 6.7 % and 3.7 % respectively. But either unheated or preheated its value was higher than that of diesel.

BSEC was also calculated for the fuels. With preheating the BSEC values for M100 and M20 were lowered by 7.5% and 3.5 %, respectively from their unheated values.

Similarly, BTE was higher at 90^{o}C, from their unheated values by 8.1% and 3.5% respectively. But either unheated or preheated its value was lower than that of diesel.

BSFC and BTE improved significantly by fuel preheating, may be due to reduction in viscosity, better spray atomization and improved combustion.

EGT increased with preheating of the fuel, may be due to increase in the combustion gas temperature with improved combustion.

Fig 5.3 (e) to (h) shows the variation of emissions of carbon monoxide (CO), unburnt hydrocarbons (HC), nitrogeneous oxides (NOx) and smoke opacity at various preheat temperatures.

At 90^{o} C, CO decreased by 33 % and 60 % respectively for M100 and M20 as compared to unheated values. HC emissions also decrease with preheating. The corresponding decrease in HC emissions was 17.2 % and 27.8 % respectively.

Decreased viscosity of oils due to preheating, and the higher oxygen content in these fuels promotes the combustion, leading to lower CO and HC emissions.

NOx for M100 and M20 increased with preheating, and at 90^{o} C preheat by 1.5 % and 1.4 % respectively from their unheated values. This is probably again due to better combustion and increased combustion gas temperature.

Similarly, Smoke opacity for M100 and M20 with preheating decreased and at 90^{o} C, it was 20.8 % and 27.2 % lower than corresponding unheated values respectively. This may

be due to the reduction in viscosity, and improved combustion. But it was still higher than diesel.

The values at and above 100^{o} C are not reported here. Beyond 100^{o} C preheating, a considerable decrease in BTE was observed, probably due to leakage of lube oil from the engine and excessive fuel leakage from the fuel pump and injectors, a result of decreased fuel viscosity. So, a lower viscosity limit is always imposed to prevent leakage [55, 58, 102, 104].

Therefore, 90^{o} C was considered as the optimal fuel inlet temperature, considering the BTE, BSFC and gaseous emissions, along with durability and safe operation of the engine.

5.4 Injection opening pressure, Injection timing and EGR

The results of the performance and emission tests of the engine with M20 fuel are presented in three subsections. The first subsection deals with the influence of varying the fuel injection opening pressure, the second subsection deals with the influence of varying the fuel injection timing, and in the third subsection the influence of different EGR rates is discussed.

All results were compared with the results obtained for diesel fuel and also M20 operation under the rated engine operating settings of 200 bar and 23 ^{o}btdc without EGR.

5.4.1 Injection opening pressure

Optimum fuel injection pressure was considered that nozzle opening pressure at which engine produces maximum BTE and minimum BSFC. Set of experiments were conducted with varying IOP in M20-fuelled engine. The IOP values selected were 185, 200 (rated), 215, 230 and 245 bar.

5.4.1.1 Effect of varying injection opening pressure on engine performance

Fig 5.4 (a)-(b) indicate the effect of varying IOP on BSFC and BTE respectively, at engine full load.

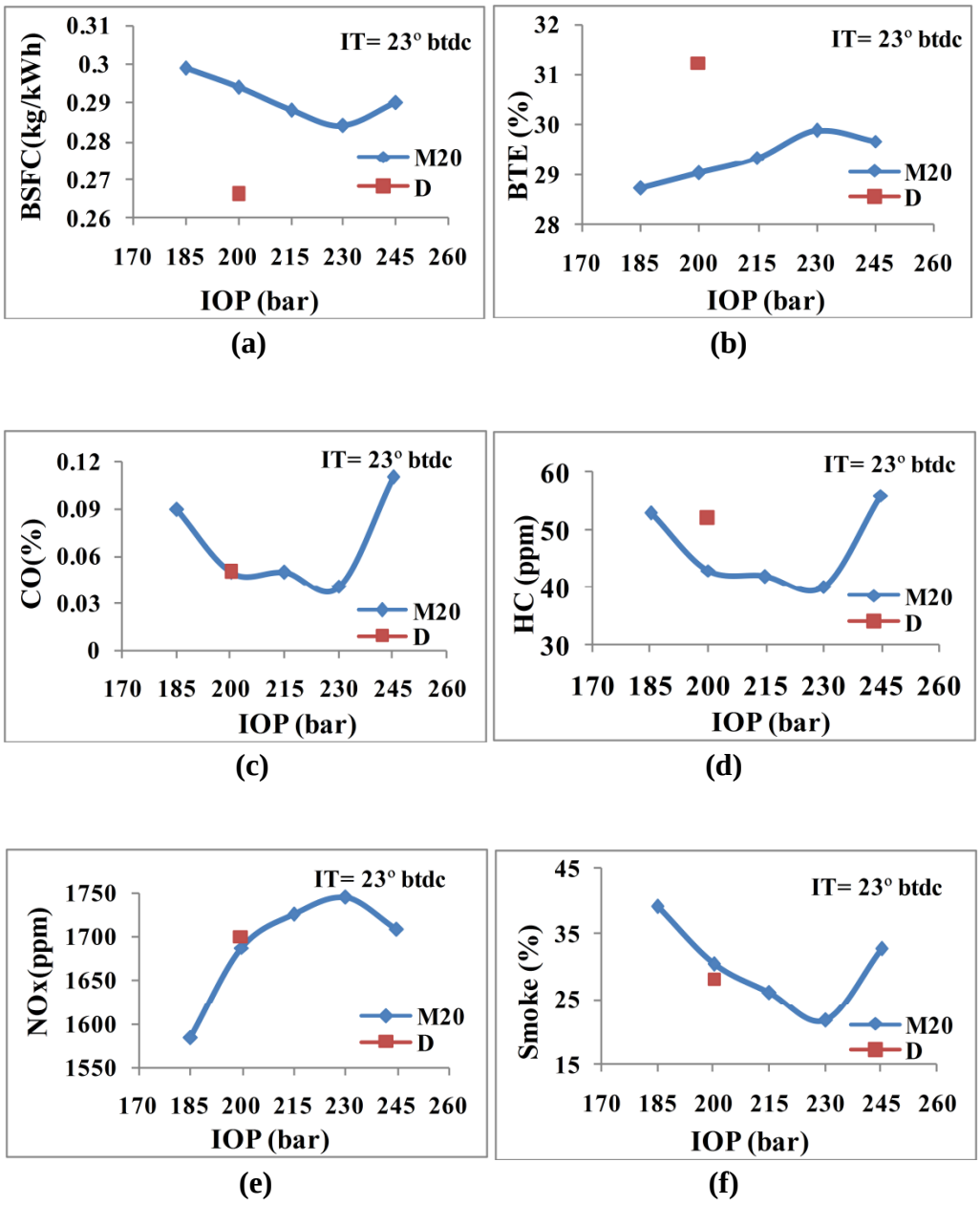

Fig. 5.4 (a)-(f) Effect of varying IOP on BSFC, BTE, CO, HC, NOx and Smoke

Maximum BTE of 29.89 % occurred at 230 bar, and decreased when fuel IOP was either decreased or increased from 230 bar. At 230 bar, BTE increased by 2.9 % than at rated setting, though still less than that of diesel by 4.4 %.

Similar trend was observed for BSFC, which was lowest, 0.284 kg/kWh at 230 bar, a decrease of 3.4 % from rated value, but still higher than that of diesel.

BTE increased and BSFC reduced with increase in IOP, probably due to better fuel atomization and mixing with air, leading to better combustion. Better utilization of the fuel enhances the combustion, improves the efficiency and reduces the fuel consumption. But, too high IOP leads to delayed injection with drop in efficiency and increased fuel consumption.

Effect of IOP on EGT was marginal in the case of M20.

5.4.1.2 Effect of varying injection opening pressure on engine emissions

Fig 5.4 (c)-(f) indicates the effect of varying IOP on HC, CO, NOx and Smoke at engine full load.

CO and HC reduced by 20 % and 6.9 % from the rated values respectively, and also were 20 % and 23.1% lower than that in case of diesel at 230 bar. Both CO and HC are the products of incomplete combustion and tend to decrease with higher IOP. But beyond 230 bar, CO and HC emissions increased.

NOx emission increased slightly at 230 bar, by 3.4 %, perhaps due to better mixture formation and improved combustion in the cycle, resulting in higher in-cylinder temperatures.

Smoke reduced sharply with increase in IOP, and was lowest at 230 bar, which was a decrease of 29.9 % from the rated value. It was also lower than that of diesel. This may be due to well-atomized spray and improved fuel-air mixing.

Higher IOP reduced the fuel droplet size and faster fuel vaporisation occurred. This improved combustion, thus reducing the smoke emissions.

In conclusion, the increased IOP provided better results for BSFC and BTE compared to rated and decreased IOPs. Based on decreased BSFC, increased BTE and lower emissions, 230 bar was found as optimum fuel injection pressure for M20 operation.

5.4.2 Injection timing

Optimum fuel injection timing was considered as that fuel injection timing at which engine delivers maximum BTE and minimum BSFC. Engine was run with M20 fuel at different fuel injection timings: 21, 23, 25 and 27^{o} btdc. Injection pressure was maintained at optimum value of 230 bar.

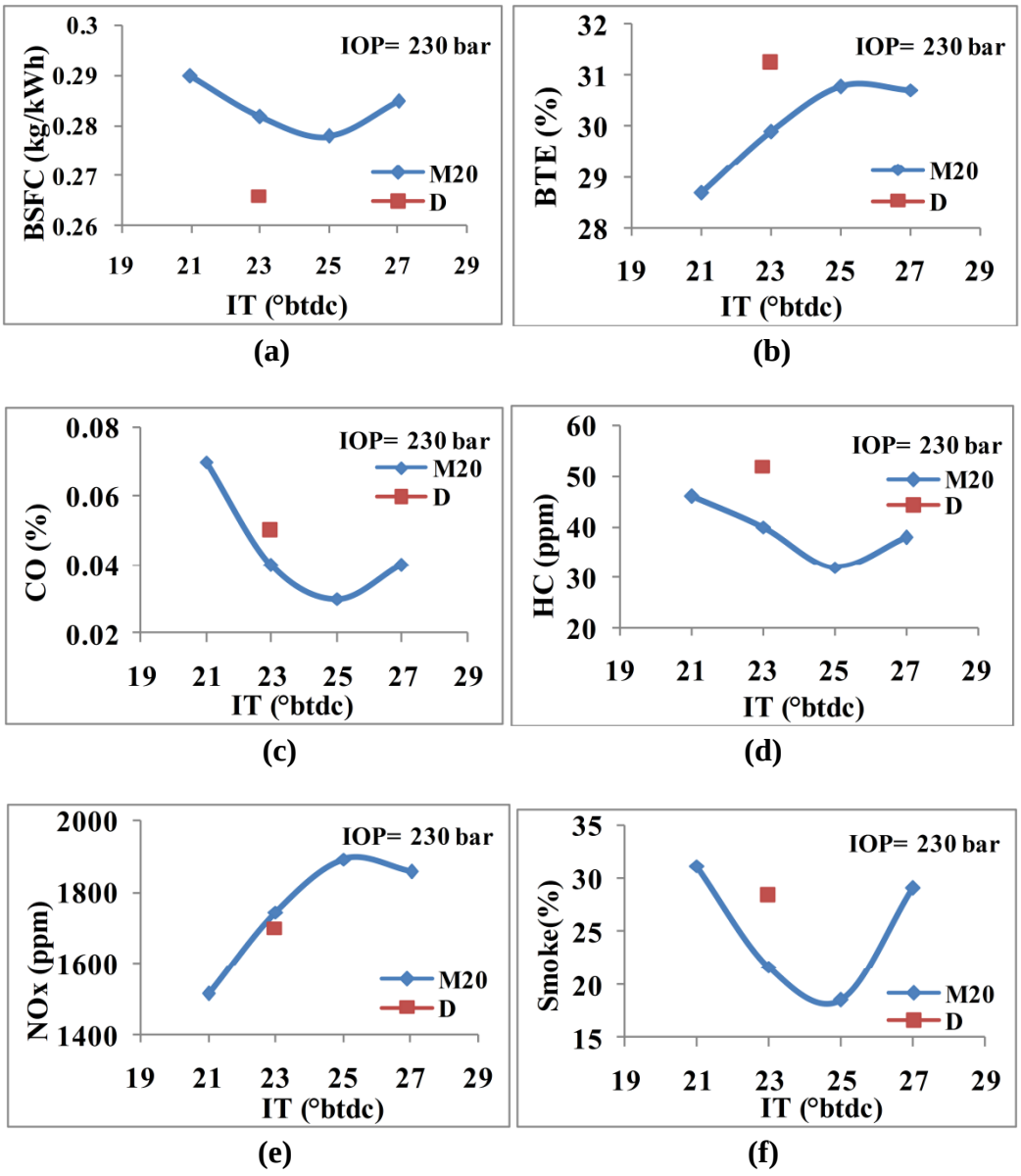

Fig. 5.5 (a)-(f) Effect of varying IT on BSFC, BTE, CO, HC, NOx and Smoke

5.4.2.1 Effect of varying injection timing on engine performance

Fig 5.5 (a)-(b) indicate the effect of varying IT on BSFC, BTE and EGT at engine full load.

BSFC was lowest, i. e., 0.278 kg/kWh at 25^{o} btdc. It decreased by 1.4 % from rated value, but was still higher than that of diesel by 4.5 %. BSFC increased when IT was either decreased or increased from 25^{o} btdc.

Similar was the observation in case of BTE. Amongst all the IT tested, the maximum BTE occurred at advanced setting of 25^{o} btdc, and its value was 30.79 %. It increased by 3.01 % from rated value, but was still lower than that of diesel by 1.5 %. BTE decreased when IT was either decreased or increased from 25^{o} btdc.

No definite trend for EGT with varying IT could be established. Also, the variations of EGT with IT were insignificant.

At advanced IT, the combustion occurs earlier in the cycle with more fuel burning before TDC, compensating the effect of slow burning of M20 fuel. Advanced IT increases the ignition delay with more prominent initial premixed phase of combustion. But with too much advanced IT, peak pressure and TDC could be incorrectly matched and cylinder temperature and pressure might be too low to cause auto ignition.

It was seen that the parameters responsible for giving best fuel economy also resulted in maximum BTE. So, 25^{o} btdc was considered the best injection timing for getting minimum BSFC and maximum BTE.

5.4.2.2 Effect of varying injection timing on engine emissions

Fig 5.5 (c)-(f) indicates the effect of varying IT on CO, HC, NOx and Smoke at engine full load.

At 25^{o} btdc, value of CO and HC were lowest i. e., 0.03 % and 32 ppm respectively, which were less than rated value by 25 % and 20 % and less than that of Diesel (rated settings) by 40 % and 38 % respectively.

Both CO and HC tend to decrease with advanced IT due to improved combustion. But beyond 25^{o} btdc, CO and HC emissions increased.

At advanced IT of 25^{o} btdc, NOx emissions increased significantly by 8.5 % from rated value. It was higher than that of diesel by 11.3 %. Influence on NOx is more may be due to the reason that fuel bound oxygen might have resulted in improved combustion. Thus, increased quantity of fuel burned with higher heat release rate resulting in higher combustion temperatures.

The smoke steadily reduced with advancement of IT, and at 25^{o} btdc, it was lowest at

18.5 % only, a reduction of 14.7 % from rated value, and 34.6 % from that of diesel.

This might be due to dominance of the premixed combustion phase, better fuel-air mixing and well-atomized spray. Owing to reduced fuel droplet size, the combustion improved and the smoke emissions reduced.

Based on decreased BSFC, increased BTE and lower emissions, 25 ^{o} btdc was found as optimum IT for M20 operation.

At optimised engine settings of 230 bar and 25 ^{o}btdc, BSFC reduced by 5.44 % and BTE increased by 6.13 % as compared to that of M20 at rated settings. CO, HC and Smoke decreased by 40%, 25.58% and 39.34%, but NOx increased by 12.14%.

BSFC and BTE of engine in general, were found to be a function of biodiesel blend, IOP and IT. A synergic effect was seen for the combination of 230 bar IOP and 25 ^{o} btdc IT when the engine was operated with M20 fuel. The BSFC was minimum, BTE was maximum and most of the emissions also reduced at this combination. Only NOx levels increased beyond limits, which can be controlled by employing EGR.

5.4.3 Exhaust gas recirculation

The NOx emission can be reduced significantly by adopting Exhaust Gas Recirculation (EGR) in which part of the exhaust gases from the engine is recirculated along with the intake air into the engine cylinder.

M20 fuel was experimentally investigated for various performance and emission parameters at optimised settings of 230 bar and 25 ^{o}btdc and EGR rates of 0, 5, 10, 15 and 20%. Diesel as well as unoptimised case for M20 at rated settings was also depicted for comparison.

The settings of fuels during the tests and as used in the graphs are shown below:

U-M20	*M20-unoptimised*	O-M20	*M20-optimised, no egr*
5-M20	*M20-optimised, 5% egr*	10-M20	*M20-optimised, 10% egr*
15-M20	*M20-optimised, 15% egr*	20-M20	*M20-optimised, 20% egr*
D	*Diesel at rated settings*		

(Optimised Settings- IOP-230 bar, IT=25°btdc)

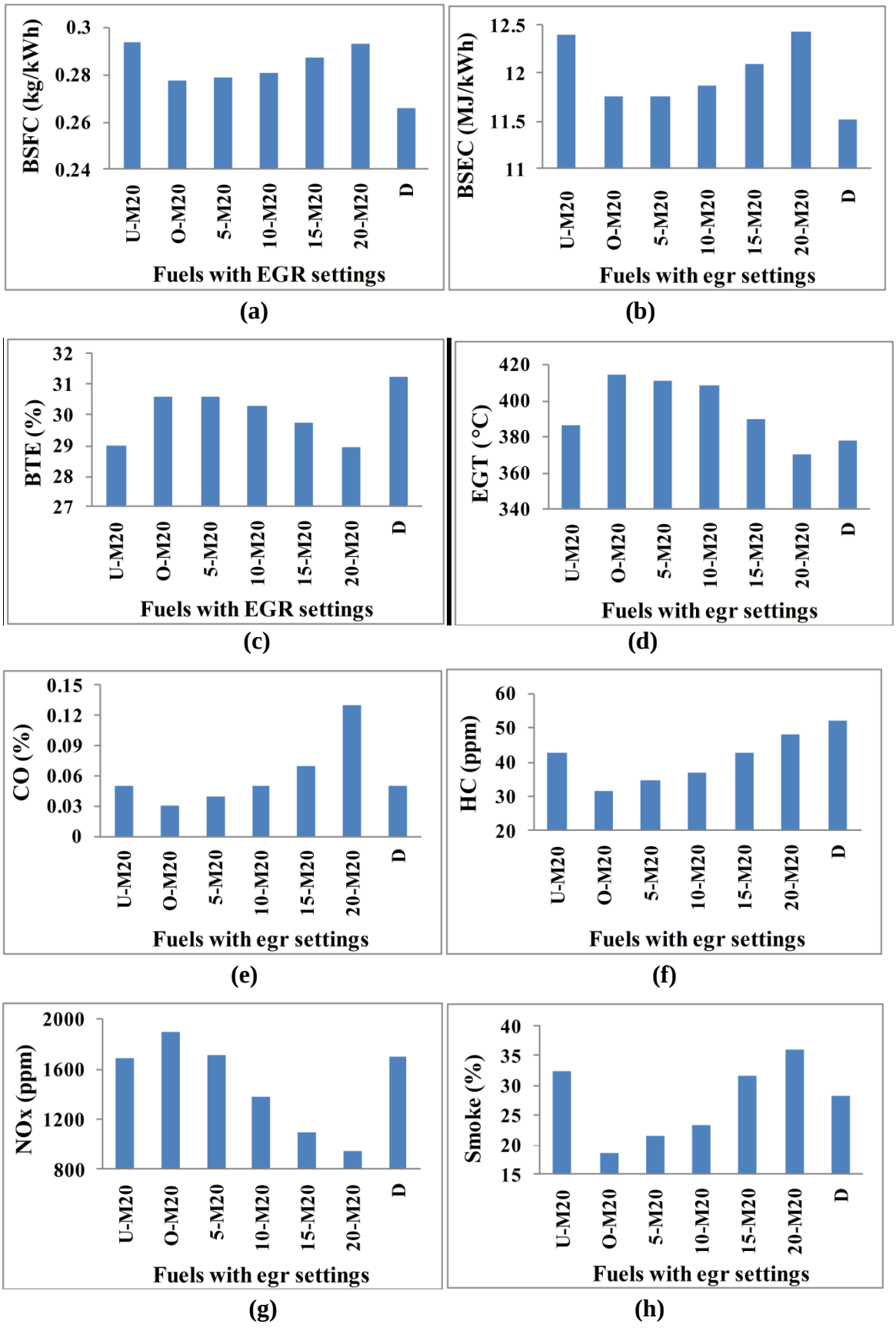

Fig. 5.6 (a)-(g) Effect of varying EGR with M20 as fuel on BSFC, BSEC, BTE, EGT, CO, HC, NOx and Smoke at engine full load.

5.4.3.1 Effect of varying EGR on engine performance

Fig 5.6 (a)-(d) shows the effect of varying EGR and optimised and unoptimised (rated) engine settings with M20 as fuel on BTE, BSFC, BSEC and EGT at engine full load.

Effect of EGR at 5% level on BTE was negligible. This is probably due to improved combustion with higher temperatures of EGR, which might have compensated for minor loss in efficiency due to dilution effects. With 10 and 15% EGR too, the reductions were very small, within 4%. Beyond 15% EGR level, BTE reduced significantly. This is possibly due to predominant dilution effect of EGR due to replacement of air by the exhaust gases, and resulting in oxygen deficient combustion process.

BSFC and BSEC showed similar trends. Both increased with increasing EGR rate. From optimised settings and no-EGR case, BSFC increased by 0.36%, 1.08%, 3.24% and 5.39 % for 5, 10, 15 and 20% EGR rates respectively, but was still lower than unoptimised value of BSFC for M20.

EGT decreased marginally with increase in EGR quantity. In EGR, CO_2 serves as heat absorbing agent and reduces the peak temperature during combustion, resulting in reduced EGT. The maximum decrease in EGT was 0.7 %, 1.4 %, 5.8 % and 10.6 % for 5, 10, 15 and 20 % EGR rates, respectively.

5.4.3.2 Effect of varying EGR on engine emissions

Fig 5.6 (e)-(h) shows the effect of varying EGR and optimised and unoptimised (rated) engine settings with M20 as fuel on CO, HC, NOx and Smoke at engine full load.

Both CO and HC are the result of incomplete combustion. Generally, diesel engine operates with lean mixtures and hence the CO and HC emissions are low. The effect of EGR on CO and HC emissions were similar. The increase in CO and HC with EGR rate was probably due to the reduction of oxygen during combustion in the cylinder, with rich mixture leading to incomplete combustion. Up to 10 % EGR, CO emissions were comparable to that of diesel. But, HC emissions were lower than that of diesel with even up to 15 and 20 % EGR rate.

The addition of exhaust gases into the inlet manifold results in a slight reduction of oxygen content in the cylinder, and rich mixture leads to higher CO and HC emissions.

EGR produces a large decrease in NOx emissions. NOx decreased from 1893 ppm at no EGR by 9.1 %, 26.78 %, 41.8 % and 49.8 % at 5, 10, 15 and 20 % EGR rates respectively. At 10 % EGR rate and beyond, the NOx levels were less than that of Diesel.

There is a rise in total heat capacity of gases in presence of inert gases (CO_2 and H_2O), which absorb energy released by combustion. EGR alters the A/F ratio, and due to decreased oxygen concentration of combustible mixture, cylinder temperature decreases and so does NOx.

But, application of EGR also resulted in some penalties like increase in HC, CO and smoke emissions, and higher BSFC. At higher EGR levels, NOx levels reduced significantly presumably due to the dominant dilution effect of fresh air by EGR. 15 % EGR and beyond could reduce NOx by a larger amount, but reduction in BTE and large increase in smoke, CO and HC emissions could not be prevented. At 10-15% EGR, all emissions including NOx and Smoke were below that of diesel.

At optimised engine settings, the smoke emissions were found to be lower for M20 compared to diesel at full load even without EGR, presumably due to good mixture formation and presence of oxygen in fuel leading to improved combustion.
Smoke emissions increased with increase in EGR percentage. The increase in smoke emission is due to partial replacement of air by exhaust gases, resulting in combustion instability.

Opacity value higher than diesel was unacceptable. So, optimum EGR rate with respect to smoke was found to be 10-15%, which gives lesser smoke compared to diesel and the NOx reduction is also higher.

From the emissions data presented above, optimum EGR level is 5–15% for engine full load considering a better trade-off between HC, CO and NOx emissions with little penalty on BSFC and BTE.

Part-II

5.5 Single generation

5.5.1Performance and emissions tests with various fuels at rated engine settings

Tests in single generation were conducted at rated engine settings for engine loadings at 0, 1, 2, 3and 3.7 kW (full load).

The variation of engine performance (BSFC, BTE, EGT) and engine emissions (CO, HC, CO_2, NOx and Smoke) for 20 % blends of Mahua, Ricebran and Neem (M20, R20, N20), 20% blend of Mahua biodiesel (MB20), Crude Mahua oil (M100), Mahua Biodiesel (MB100) and Diesel (D) are shown in Fig 5.7 (a)-(h).

5.5.1.1 Engine performance

Variation of BSFC for M20, R20, N20 for entire load range was 0.475-0.294, 0.483-0.297 and 0.476-0.289 kg/kWh respectively. The variations among fuels were negligible at full load and maximum 3 % at lower loads only. At full load, the BSFC of M20, R20 and N20 were 10.5, 11.6 and 8.6 % higher than that of Diesel (D).

Variation of BSFC for MB20, M100, and MB100 for entire load range was 0.434-0.281, 0.645-0.360 and 0.608-0.313 kg/kWh respectively. At full load, the BSFC of MB20, M100 and MB100 were 5.6, 35.3 and 17.7 % higher than that of Diesel (D).
BSFC of MB20 was lowest among all test fuels.

Variation of BSEC showed similar trends. For M20, R20, N20, MB20, M100, and MB100 for entire load range, BSEC were 20.3-12.4, 20.1-12.5, 20.3-12.4, 20.4-11.7, 24.3-13.4 and 20.2-12.2 MJ/kWh respectively. At full load, the BSEC of MB20, M100 and MB100 were 1.5, 16.3 and 5.6 % higher than that of Diesel (D). BSEC of MB20 was lowest among all test fuels.

Variation of BTE for M20, R20, and N20 for entire load range was 17.7-29.02, 17.90-28.94 and 17.20-29.13 % respectively. The variations among fuels were negligible at full load and maximum 4 % at lower loads. At full load, the BTE of M20, R20 and N20 were 7.1, 7.4 and 6.8% lower than that of diesel.

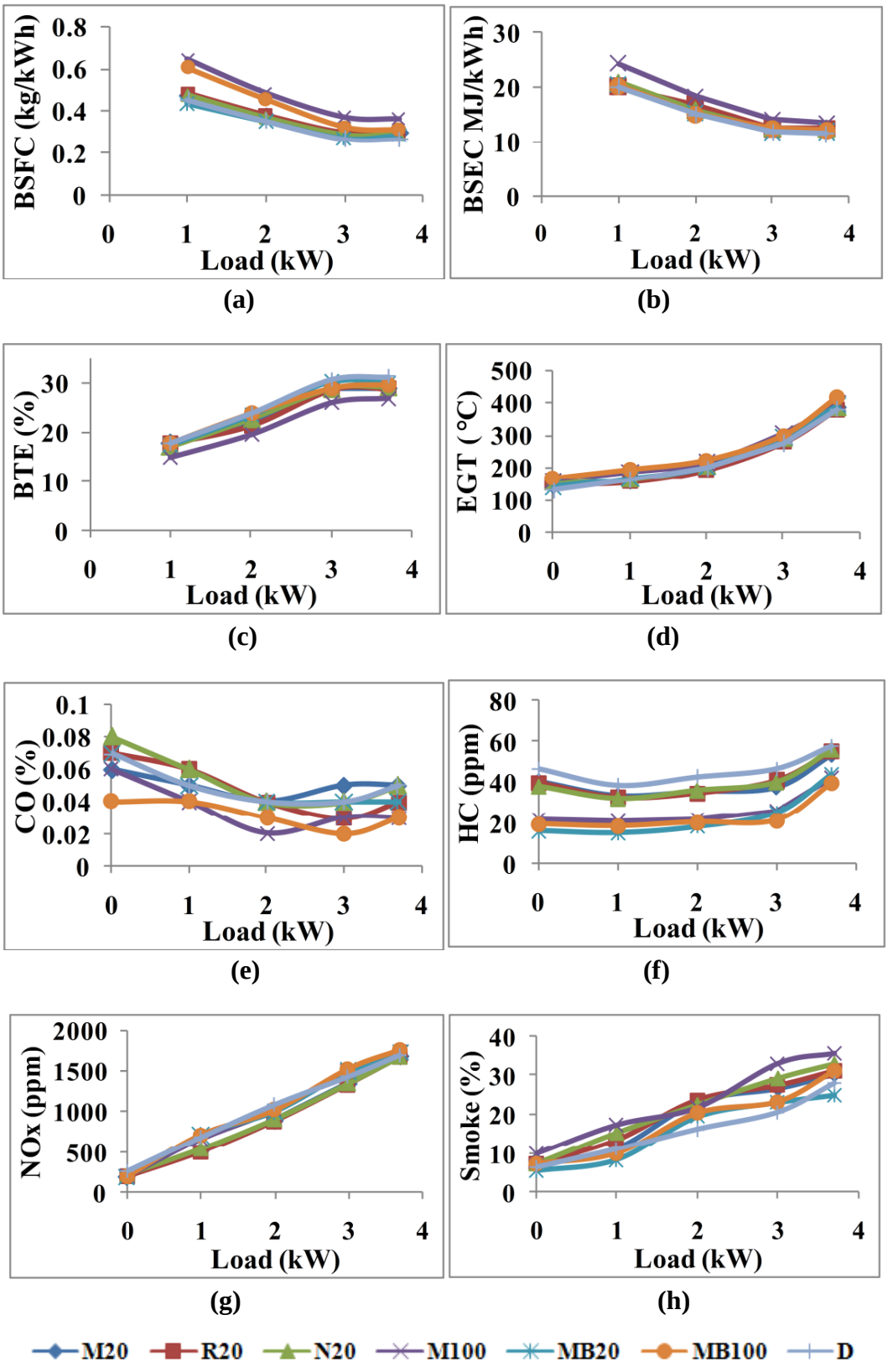

Fig. 5.7 (a)-(h) Engine performance and emission characteristics for various fuels at rated engine settings

Variations of BTE for MB20, M100, and MB100 for entire load range were 17.60-30.12, 14.80-26.88 and 17.80-29.61 % respectively. At full load, the BTE of MB20, M100 and MB100 were 3.6, 13.9 and 5.21% lower than that of Diesel (D). BTE of MB20 was lowest among test fuels.

BTE was low at part loads for all fuels. At higher loads, BTE was high as relatively less portion of the power is lost for countering the friction. BTE was found to be lower for SVO blends due to lower LCV compared to that of Diesel.

Maximum EGT for M20, R20, N20, MB20, M100, and MB100 was 386, 381 and 387, 390,395 and 418 ^{o}C respectively. EGT for MB100 was the highest. EGT was found to have linear relationship with load.

5.5.1.2 Engine emissions

Variation of CO for M20, R20, N20 fuels for entire load range was 0.06-0.05, 0.07-0.04, and 0.08-0.05 respectively. At full load, CO was comparable with that of Diesel (D). Variation of CO for MB20, M100, and MB100 for entire load range was 0.07-0.04, 0.06-0.03 and 0.04-0.03 % respectively. At full load, CO emission for MB20, M100 and MB100 were 20, 40 and 40 % lower than that of Diesel (D). CO for MB20 was lowest among test fuels. CO decreased with increasing load due to better combustion at higher loads. But, CO increased near full load due to comparatively richer fuel–air mixture and lack of oxygen.

Variation of HC for M20, R20, N20 MB20, M100 and MB100 for entire load range was 41-54, 40-55, 38-56, 16-44, 22-42 and 19-40 ppm respectively. At full load, the HC of M20, R20, N20, MB20, M100 and MB100were 6.90, 5.2, 3.4, 24.1, 27.6 and 31.1% lower than that of Diesel (D). Variation of HC for MB20, M100, and MB100 for entire load range was 16-28, 22-32 and19-30 ppm respectively. At full load, the HC of MB20, M100 and MB100 were 46.1, 38.5 and 42.3 % lower than that of Diesel (D). HC of MB20 was lowest among test fuels. Oxygen in fuel improves the combustion, hence lower HC was observed for SVOs/Biodiesel and their blends.

Maximum CO_2 for M20, R20, N20, MB20, M100 and MB100 was at full load and the values were respectively 9.9, 9.7, 9.8, 10.8, 10.5 and 10.3 %. Among all fuels, maximum CO_2 was with MB20, and was 14.9 % higher than Diesel.

At full load, NOx for M20, R20, and N20 at full load was lower than that of diesel by 0.76, 1.6 and 1.4 %. But, it was higher by 1.2, 2.6 and 3.6 % respectively for MB20, M100 and MB100. This may be due to higher calorific value of Mahua Biodiesel and blends and higher O_2 content in M100 and MB100.

Variation of Smoke opacity for M20, R20, N20, MB20, M100 and MB100 for entire load range was 7-30.5, 7.2-31.2, 7.2-32.9, 5.3-25.1, 9.7-35.8 and 7.4-31.3 % respectively. Smoke opacity of M20 was 10.2 % higher, but for MB20, it was 11.3 % lower than that of diesel.

In case of MB20, lower viscosity, and higher LCV than M20, along with fuel bound oxygen might have resulted in better combustion, and lower smoke.

5.6 Single generation and trigeneration

5.6.1 Tests with various fuels at rated engine settings in trigeneration for space heating

Tests in trigeneration were conducted at rated engine settings for engine loadings at 0, 1, 2, 3 and 3.7 kW (full load). The mode of operation in trigeneration included power generation, fuel preheating and hot exhaust fired space heating.

The variation of engine performance (BSFC, BSEC, BTE, EGT) and engine emissions (CO, HC, NOx and Smoke) for 20 % blends of Mahua, Ricebran and Neem (M20, R20, N20) with diesel, 20% blend of Mahua biodiesel (MB20) with diesel, and diesel (D) are shown in Fig 5.8 (a)-(h).

5.6.1.1 Engine performance

In trigeneration, the variation of BSFC, BSEC and BTE among M20, R20 and N20 fuels was negligible at full load.

At full load, the BSFC of M20, R20 and N20, and MB20 were 12.1, 13.2, 9.7 and 6.3% higher than that of diesel. BSEC values were 7.9, 8.1, 7.4 and 3.9% higher than that of diesel respectively.

At full load, the BTE of M20, R20 and N20, and MB20 were 7.4, 7.5, 6.9 and 3.7% lower than that of diesel.

For MB20, BSFC was lowest and BTE was highest among all test fuels. BTE was found to be lower for SVO blends, probably due to lower LCV compared to that of Diesel.

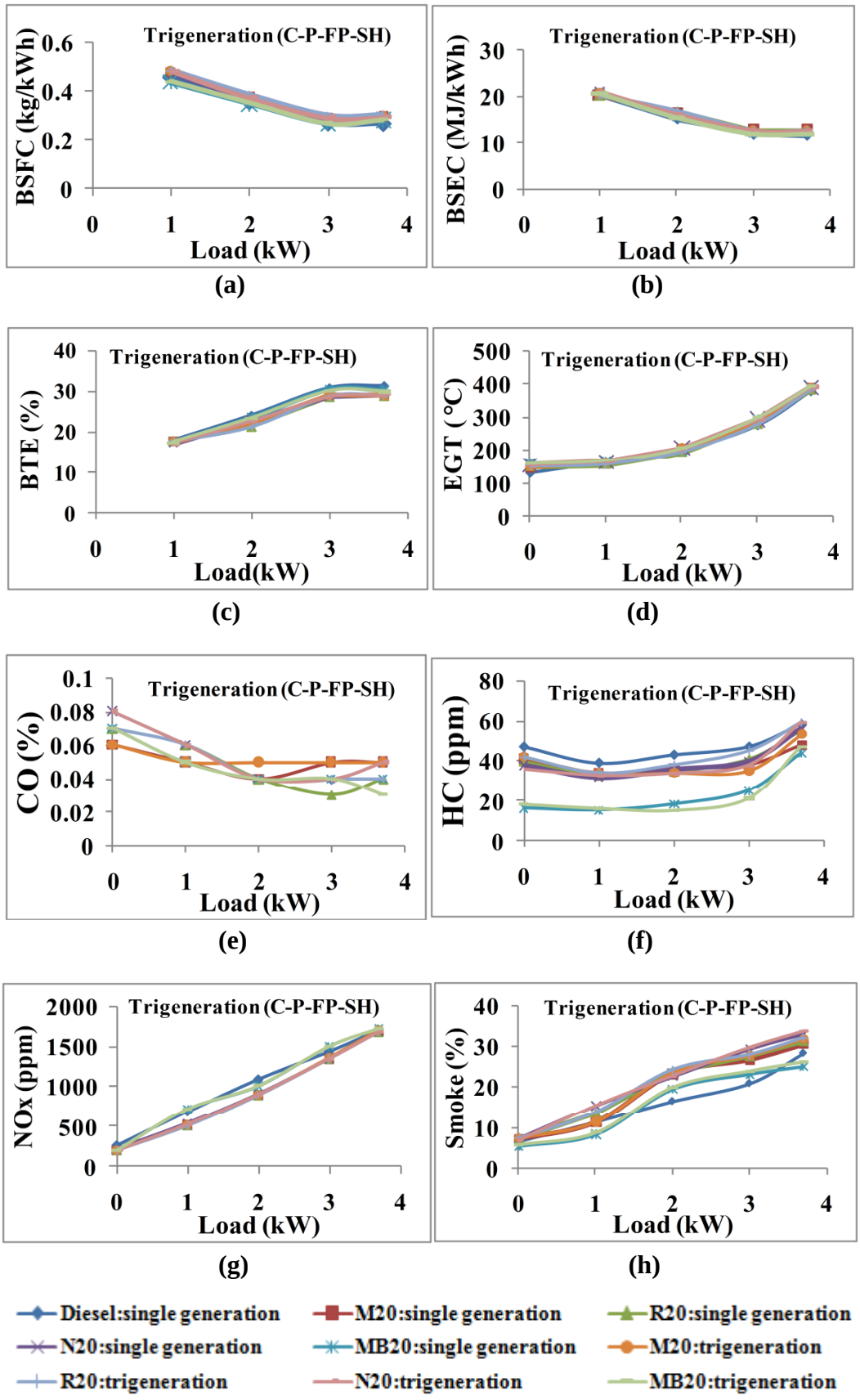

Fig. 5.8 (a)-(g) Engine performance and emission characteristics in trigeneration-power, fuel preheating and space heating, (C-P-FP-SH) for various fuels (rated engine settings)

EGT was found to have linear relationship with load. In trigeneration, maximum EGT for M20, R20, N20, MB20 were 389, 383, 393 and 396 ^{o}C respectively. EGT for MB100 was the highest.

5.6.1.2 Engine emissions

Variation of CO and HC for all test fuels was negligible in trigeneration, and also in comparison to single generation.

At full load, CO emission for MB20 was 40 % lower than that of Diesel (D), and was lowest among all test fuels.

In trigeneration, on average for all fuels, HC emissions increased by 8-12% than that in single generation, but still were lower than that of Diesel. Also, HC emissions for MB20 were 34.5 % lower than that of Diesel (D), and lowest among all test fuels.
Oxygen in fuel improves the combustion, hence lower HC was observed for SVOs/Biodiesel and their blends.

There was negligible change in NOx emissions for all test fuels in trigeneration. But, the NOx emissions were generally lower in trigeneration than in single generation. It was highest for MB 20 and higher than that of Diesel by 1.6 % only.

Similarly, for Smoke opacity, the variations in trigeneration mode as compared to single generation with alternate fuels tested was negligible. In general Smoke value increased with trigeneration at full load and the increase was in the range of 2-3 % only. For MB20, smoke was lower than Diesel in both single and trigeneration. Other fuels emitted marginally higher smoke than Diesel (6-12 %).

It could be concluded that during the trigeneration operation of alternate fuels, the performance and emission of the engine is not affected much. However, the biodiesel fuel, MB20 showed better performance and emission characteristics than other alternate fuels. It can be inferred that the addition and integration of the components of trigeneration for fuel preheating and space heating did not affect much the overall performance and emission characteristics of the diesel engine.

5.6.2 Tests with various fuels at rated engine settings in trigeneration for space cooling

Tests in trigeneration were conducted at rated engine settings for engine loadings at 0, 1, 2, 3and 3.7 kW (full load).

The mode of operation in trigeneration included power generation, fuel preheating and space cooling using exhaust gases.

The variation of engine performance (BSFC, BSEC, BTE and EGT) and engine emissions (CO, HC, NOx and Smoke) for 20 % blends of Mahua, Ricebran and Neem (M20, R20, N20) with diesel, 20% blend of Mahua biodiesel (MB20) with diesel, and Diesel (D) are shown in Fig 5.9 (a)-(h).

5.6.2.1 Engine performance

In trigeneration, the variation of BSFC, BSEC and BTE among M20, R20 and N20 fuels was negligible at full load.

At full load, the BSFC of M20, R20 and N20, and MB20 were 12.4, 13.5, 11.6 and 7.9 % higher than that of diesel. The BSEC variations were marginal. BSEC values were 8.7, 9.6, 8.5 and 5.6% higher than that of diesel respectively.

At full load, the BTE of M20, R20 and N20, and MB20 were 8.2, 8.7, 7.8 and 5.3% lower than that of Diesel (D).

For MB20, BSFC and BSEC were lowest and BTE was highest among all test fuels. BTE was found to be lower for SVO blends due to lower LCV compared to that of Diesel.

In trigeneration, maximum EGT for test fuels were 6-15^{o}C lower than that of Diesel. EGT for MB100 was the highest.

5.6.2.2 Engine emissions

Variation of CO and HC for all test fuels was negligible in trigeneration with space cooling, and also in comparison to single generation.

At full load, CO emission for MB20 was equal to that of diesel (D), and was lowest among all test fuels. For other fuels, CO was slightly higher than that of Diesel.

In trigeneration, on average for all fuels, HC emissions increased marginally than that in single generation, but still were lower than that of Diesel. Also, HC emissions for MB20 were 32.8 % lower than that of diesel (D), and lowest among all test fuels.

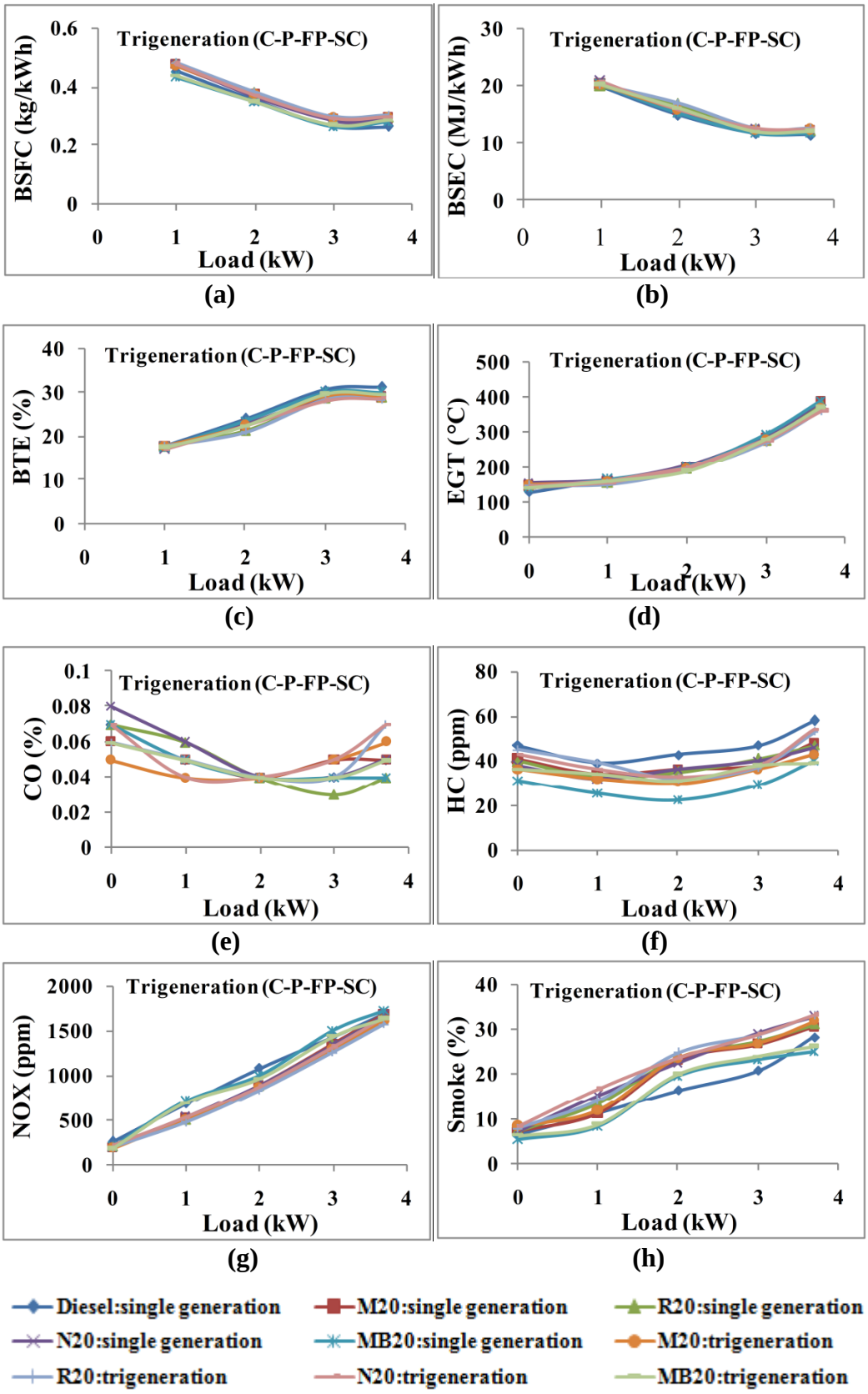

Fig. 5.9 (a)-(h) Engine performance and emission characteristics in trigeneration-power, fuel preheating and space cooling, (C-P-FP-SC) for various fuels (rated engine settings)

Lower HC in SVOs/Biodiesel blends may be due to oxygen content in these fuels, which improves the combustion.

There was negligible change in NOx emissions for all test fuels in trigeneration. But, the NOx emissions were generally lower in trigeneration than in single generation.

Similarly, for Smoke opacity, the variations in trigeneration mode as compared to single generation with alternate fuels tested were negligible. In general Smoke value increased with trigeneration at full load but the increase was marginal only. For MB20, smoke was lower than Diesel in both single and trigeneration.

It could be concluded that during the trigeneration operation of alternate fuels, the performance and emission of the engine is not affected much. However, the biodiesel fuel, MB20 showed better performance and emission characteristics than other alternate fuels. It can be inferred that the addition and integration of the components of trigeneration for fuel preheating and space cooling (vapour absorption units) did not affect much the overall performance and emission characteristics of the diesel engine.

5.6.3 Tests with M20 at optimised engine settings in cogeneration and trigeneration for space heating and cooling

Tests in cogeneration and trigeneration with 20 % blend of Mahua oil (M 20) at optimised engine settings were conducted in both cogeneration and trigeneration modes, for engine loadings at 0, 1, 2, 3 and 3.7 kW (full load).

The mode of operation in cogeneration included

(i) Power generation and hot exhaust fired, as well as hot water fired space heating,

(ii) Power generation and hot exhaust fired space cooling,

The mode of operation in trigeneration included

(i) Power generation, fuel preheating and hot exhaust fired, as well as hot water fired space heating,

(ii) Power generation, fuel preheating and hot exhaust fired space cooling,

The variation of engine performance (BSFC,BSEC, BTE, EGT) and engine emissions (CO, HC, NOx and Smoke) during different modes of operation are depicted in Fig 5.10 (a)-(g). M20 fuel at optimised settings was used at different modes of operation, and the results are displayed with nomenclature as shown below:

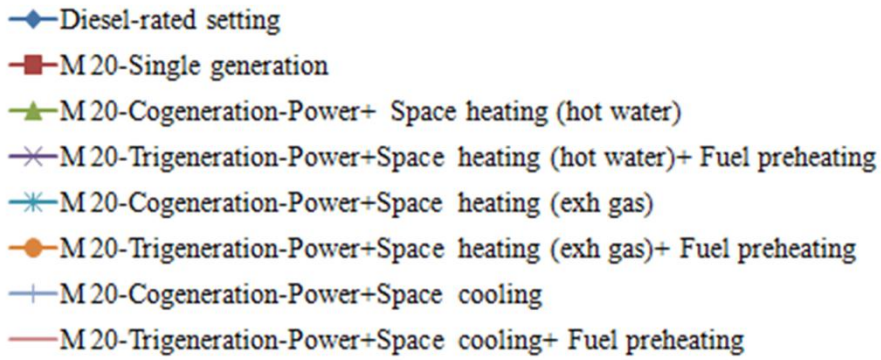

The results are compared for all modes of operation for M20 at optimised settings, as well as that from operation of engine with diesel at rated engine settings.

5.6.3.1 Engine performance

Variation of BSFC and BTE in all modes of operation was negligible at full load. In trigeneration modes, the BSFC was slightly lower than that in cogeneration modes. It may be because of the reason that preheated fuels (in trigeneration) might have lowered the viscosity of fuel leading to improved combustion.

At full load, the BSFC of M20 in cogeneration and trigeneration were only 2-3 % higher than that in single generation, but 5-7.9% higher than that of Diesel (D).
At full load, the BTE of M20 in cogeneration and trigeneration were only 1-2.5 % higher than that in single generation, but 3.2-5.2% higher than that of Diesel (D).

BSFC was lowest and BTE was highest in trigeneration with exhaust fired space heating followed by trigeneration with hot water fired space heating options.
The back pressure in piping and components must have been lower in space heating arrangement than in space cooling arrangement, which might be the cause of slightly lower BTE and slightly higher BSFC in space heating modes.

EGT variations were small in all modes of operation at full load. Maximum EGT was during exhaust fired space heating trigeneration option. Fuel preheating might have improved

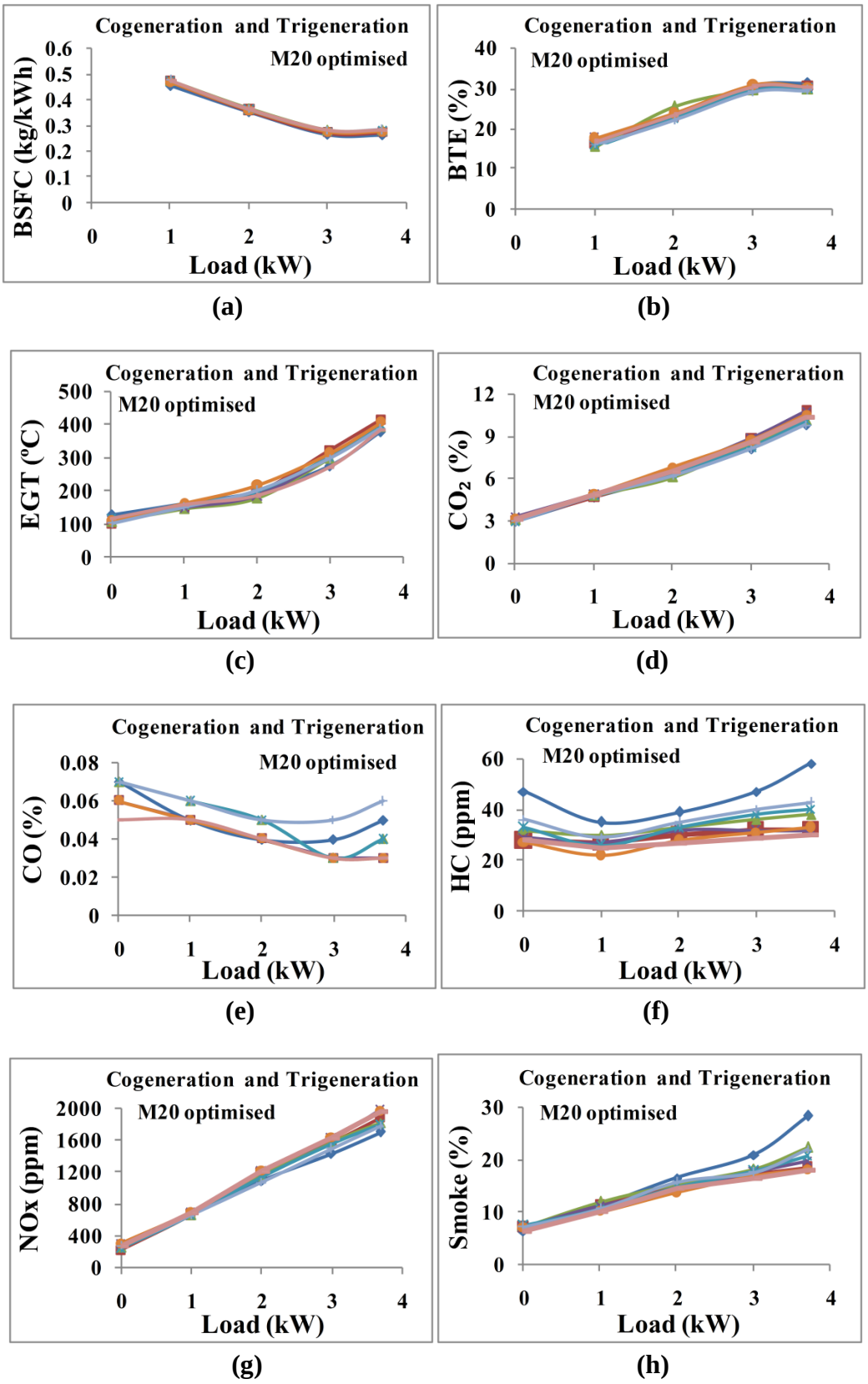

Fig. 5.10 (a)-(h) Engine performance and emission characteristics in trigeneration -power, fuel preheating and space cooling, (C-P-FP-SC) at entire engine loading for various fuels (rated engine settings)

the combustion and increased the EGT. Maximum drop in EGT was of 32 ^{o}C in space cooling trigeneration.

5.6.3.2 Engine emissions

CO emissions were higher in cogeneration than in trigeneration. Again fuel preheating might be the cause with reduced viscosityof fuel and improved combustion and lower values of CO. In all modes of operation, CO values were either equal or slightly higher than that in single generation, yet were lower than that in base case diesel. Lowest values of CO were found in trigeneration modes in both space heating and space cooling options.

Similar were the results with HC emissions. Highest HC emissions were in space cooling cogeneration, still 25.9% lower than base case diesel. Lowest values were during hot water fired space heating trigeneration, about 44.8 % lower than that in diesel case.

Variation in CO_2 emissions were very small, yet were slightly lower in case of single generation with base case diesel (rated settings) and M20 (optimised settings).

NOx emissions were higher than base case diesel in all modes of operation with M20. But as compared to M20 in single generation, these were higher in trigeneration and lower in cogeneration. Improved combustion with fuel preheating in trigeneration might have resulted in increased NOx emissions. NOx were higher by 13-15% than that of diesel and 3-4 % higher than that of M20 in single generation. An application of even 5-10% EGR was sufficient to bring down the NOx to the levels of base case diesel, with penalty of only1-2 % on BTE, BSFC and smoke.

Smoke emissions in all modes of operations increased from single generation operation, but still were much lower than that in diesel case, even with 5-10% EGR. Lsmoke emissions occurred during exhaust fired space heating cogeneration.

It could be concluded that during the trigeneration operation of alternate fuels, the performance and emission of the engine is not affected much. However, the biodiesel fuel, MB20 showed better performance and emission characteristics than other alternate fuels.

Addition or integration of the components of trigeneration for fuel preheating and space heating/cooling did not affect much the overall performance and emission characteristics of the diesel engine.

Optimisation of engine for M20 fuel and operating on this setting has resulted in reduced BSFCand increased BTE during trigeneration modes of operation for both space heating and space cooling. Fuel bound oxygen, engine optimisation and fuel preheating all have produced synergy effects in improving the performance and reducing the emissions.

5.6.4 Cogeneration experiments with finned pipes

Initially, three types of pipes were used- unfinned pipe, longitudinal finned pipe and annular finned pipe in direct exhaust fired system for space heating. The results were compared to select the type of pipe for further experiments.

The test parameters recorded were the ambient and cabin temperatures, ambient and cabin Relative Humidity, and the total time taken to reach the comfort range in the cabin. The temperatures and flow parameters of exhaust gas and hot water during space heating were also recorded.

The engine was started and when it reached full load condition, then the bypass valve was opened to allow exhaust gas in the pipes passing through the cabin, with maximum heating in the cabin.

Fig. 5.11 (a) and (b) shows the variation in cabin temperature with time during exhaust fired space heating arrangement using the three types of pipes- unfinned (bare) pipe, longitudinal pipe and annular finned pipe.

As can be seen, with unfinned (bare) pipe under similar conditions, the temperature of the cabin increased from 5^{o} C to 28^{o} C in 80 minutes, whereas for longitudinal pipe, it was 65 minutes, and least for annular pipe i. e., 55 minutes only. The RH value decreased from about 90 % to 40 % in 85 minutes for unfinned pipe, whereas for longitudinal and annular pipe, it was only 60 minutes and 55 minutes respectively. The exhaust temperature drops during the heat transfer in unfinned, longitudinal finned and annular finned pipes were 32, 40 and 44 ^{o}C respectively.

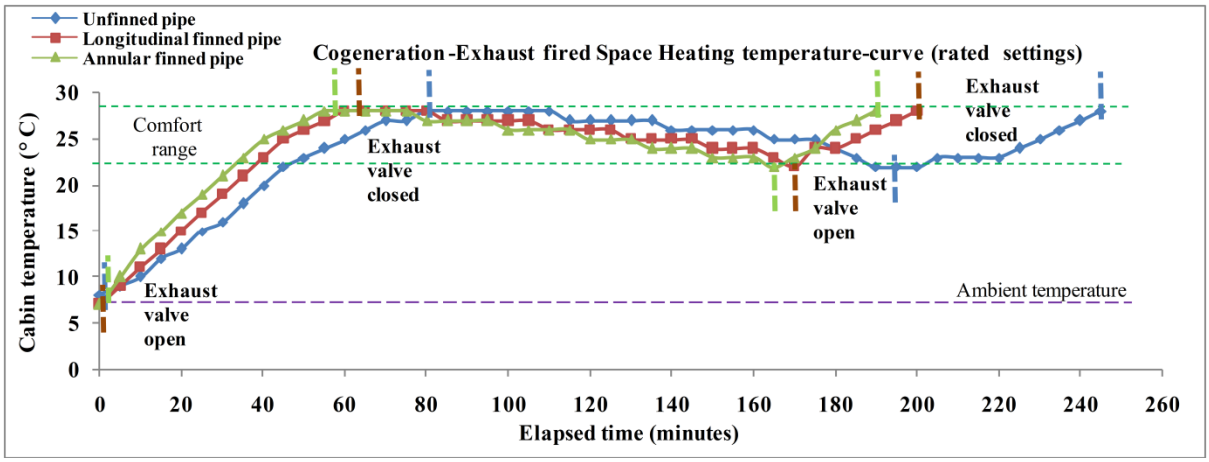

(a)

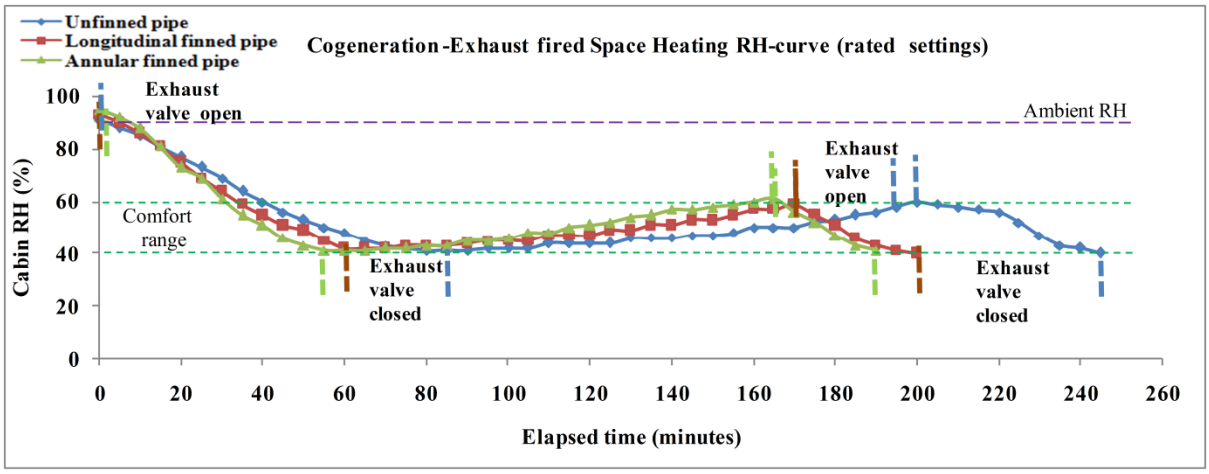

(b)

Fig. 5.11 Variation of (a) cabin temperature and (b) cabin RH with elapsed time for various pipes

For longitudinal and annular finned pipes, the fin effectiveness values were calculated to be in a range of 1.16-1.18 and 1.33-1.37, and fin efficiency values were calculated as 0.302-0.34 and 0.351-0.392 respectively. This range depicts the values for various modes of operation

The valve leading the exhaust to the cabin was kept closed, and steadily the temperature of the cabin dropped and RH value increased.

Again, as the temperature dropped, and RH increased beyond the comfort range, the exhaust bypass valve leading the exhaust to cabin was opened, and the cycle was repeated.

5.6.5 Direct Exhaust fired Space heating using various fuels at rated engine settings

Cogeneration operation, i e., simultaneous power and direct exhaust fired space heating was tested with various fuels, M20, R20, N20 and MB20, all at engine rated settings of 200 bar and 23^{o} btdc. Annular finned pipe was used in all cases.

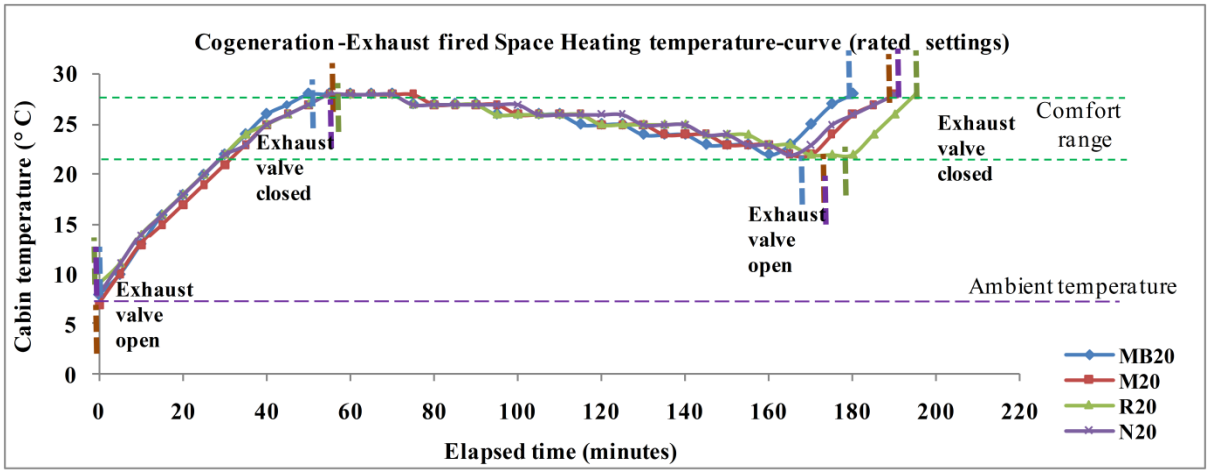

(a)

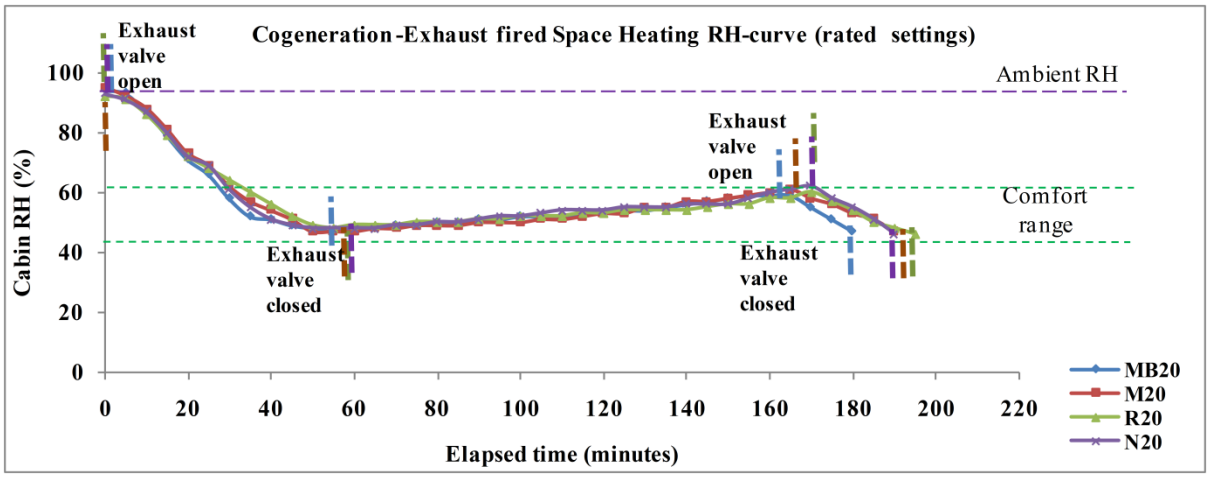

(b)

Fig. 5.12 Variation of (a) cabin temperature and (b) cabin RH with elapsed time for various fuels in space heating

The variation of cabin temperature and cabin RH with elapsed time are shown in Fig. 5.12 (a) and (b). As can be seen, the time taken to reach the comfort conditions with M20, R20, N20 and MB20 were respectively 55-60 minutes from the ambient conditions of 5-7^{o} C and 88-91 % RH. Yet, with MB20 fuel, it was earliest, may be due to higher heat content in MB20. For operation for longer hours, energy savings may occur with MB20.

5.6.6 Direct Exhaust fired Space heating in trigeneration using M20 at optimised engine settings

A case of trigeneration (simultaneous power, fuel preheating and space heating) was tested with M20 fuel at optimised engine settings of 230 bar and 25 ^{o}btdc.

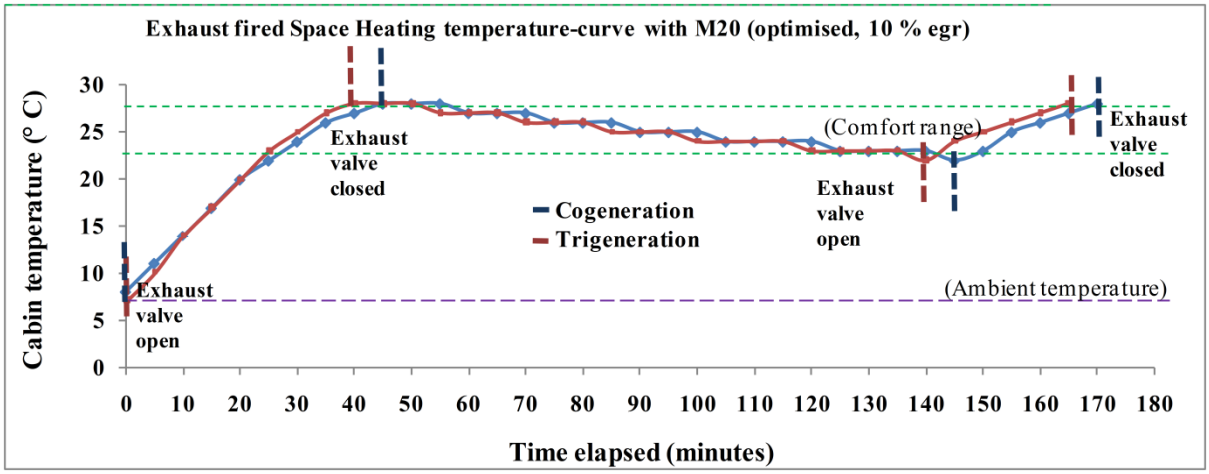

(a)

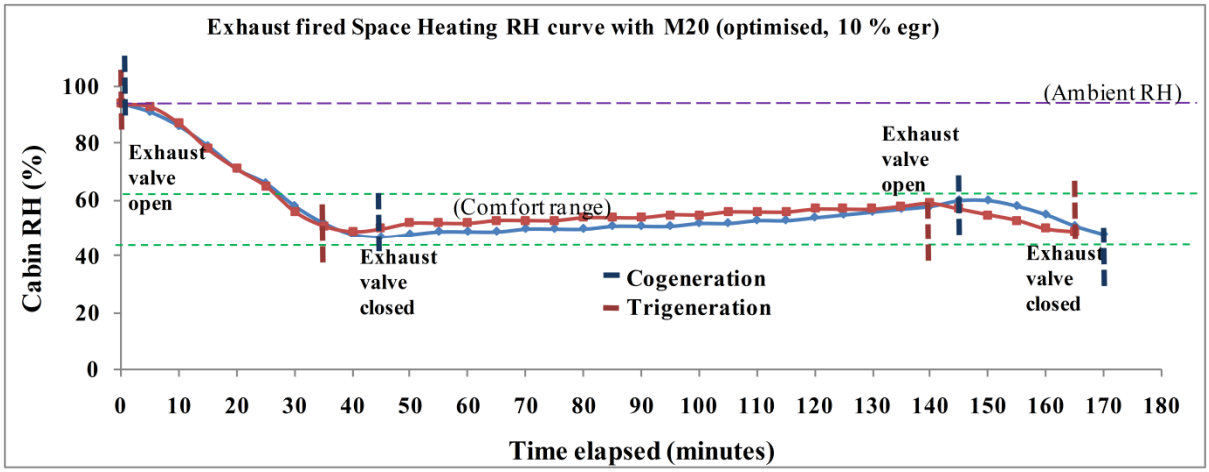

(b)

Fig. 5.13 Variation of (a) cabin temperature and (b) cabin RH with elapsed time for space heating in trigeneration

Both hot water fired space heating and direct exhaust fired space heating options were considered. Annular finned pipe was used in both cases. The variation of cabin temperature and cabin RH with elapsed time are shown in Fig. 5.13 (a) and (b). As can be seen, the time taken to reach the comfort conditions was 50 minutes and 70 minutes respectively for exhaust fired and hot water fired space heating respectively.

Although the heat content may be more in hot water, yet the operating temperature of hot water space heating was less (maintained at 75/55 mode), as compared to exhaust gases near 400 ^{o} C. The ambient conditions were 5-7 ^{o}C and 88-91 % RH.

5.6.7 Space cooling in cogeneration using various fuels at rated engine settings

A case of cogeneration operation (simultaneous power and space cooling) was tested with various fuels, M20, R20, N20 and MB20, all at engine rated settings of 200 bar and 23^{o} btdc.

The variation of cabin temperature and cabin RH with elapsed time are shown in Fig. 5.14 (a) and (b). As can be seen, the comfort conditions could be reached and maintained throughout the test duration of 9 hours in the day.

The nomenclature in the graphs shown, are as given below:

M20cscR = M20 fuel for cogeneration space cooling at rated settings
R20cscR = R20 fuel for cogeneration space cooling at rated settings
N20cscR = N20 fuel for cogeneration space cooling at rated settings
MB20cscR = MB20 fuel for cogeneration space cooling at rated settings

The tests were conducted in the months of March and April, when the temperatures do not normally cross 40^{o} C in the daytime. For the micro-trigeneration space cooling set up as installed, the maximum cooling of up to 8^{o} C could only be obtained, and comfort conditions could be obtained only for moderately hot temperatures.

During the tests with space cooling options, the ambient conditions were 35-38^{o} C and relative humidity was in the range of 22-28 %. With MB20 fuel, the temperature drop was maximum, may be due to higher heat content in MB20 which was used in generators of VAR units for space cooling. For operation for longer hours, energy savings may occur with MB20.

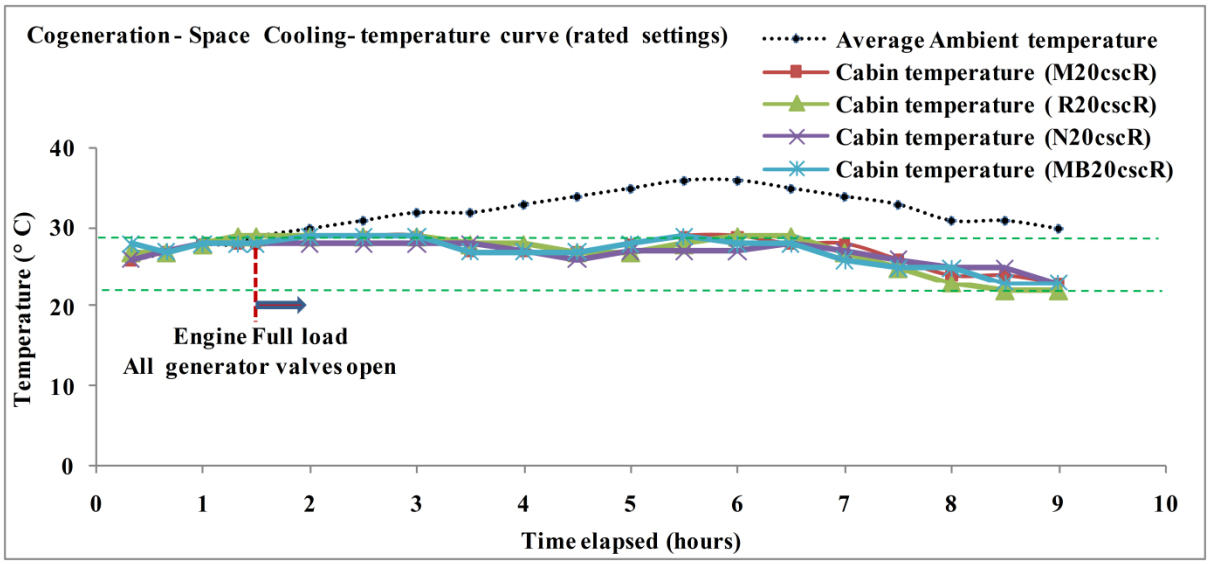

(a)

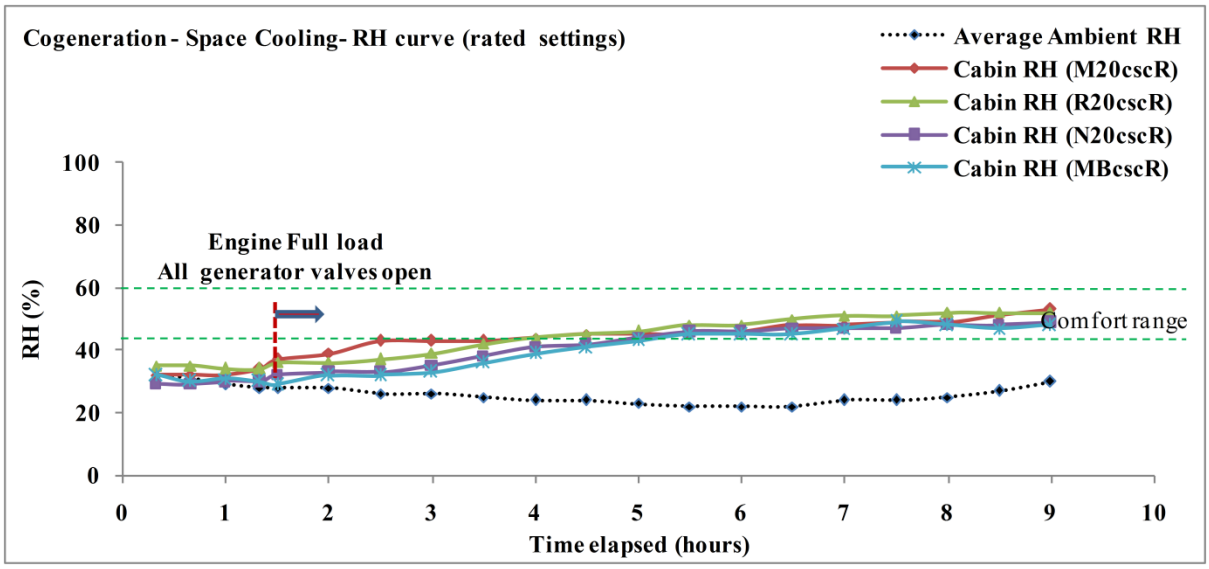

(b)

Fig. 5.14 Variation of (a) cabin temperature and (b) cabin RH with elapsed time for various fuels in space cooling

5.6.8 Space cooling in cogeneration and trigeneration using M20 at optimised engine settings

M20 fuel at optimised engine settings (230 bar, 23^{o} btdc) was used in both cogeneration (power and space cooling), and trigeneration (power, space cooling and fuel preheating).

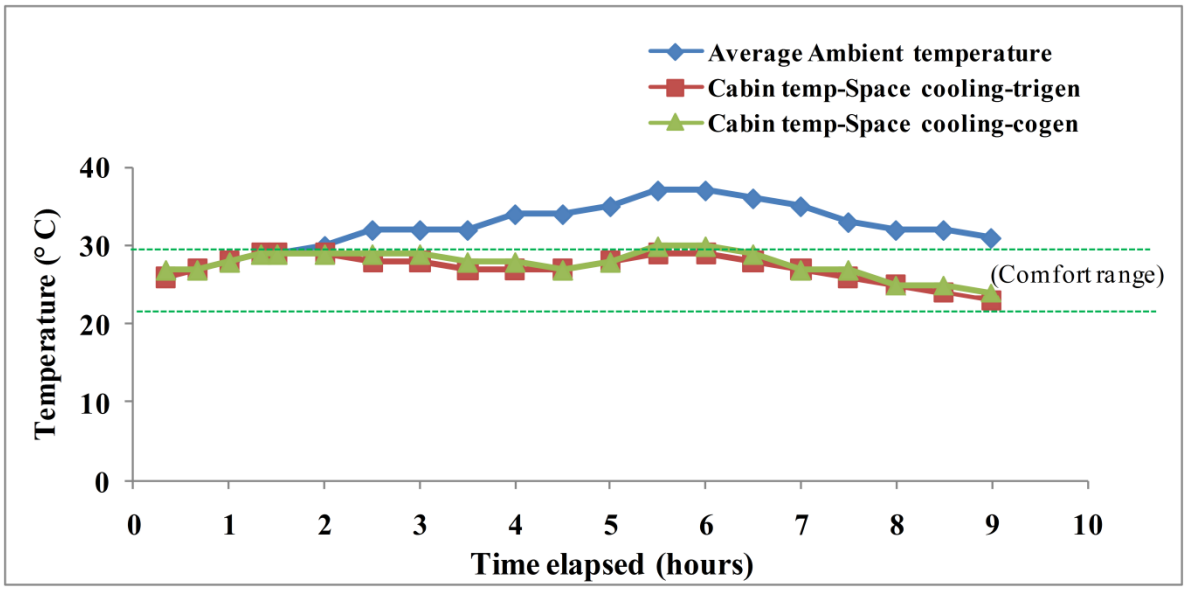

(a)

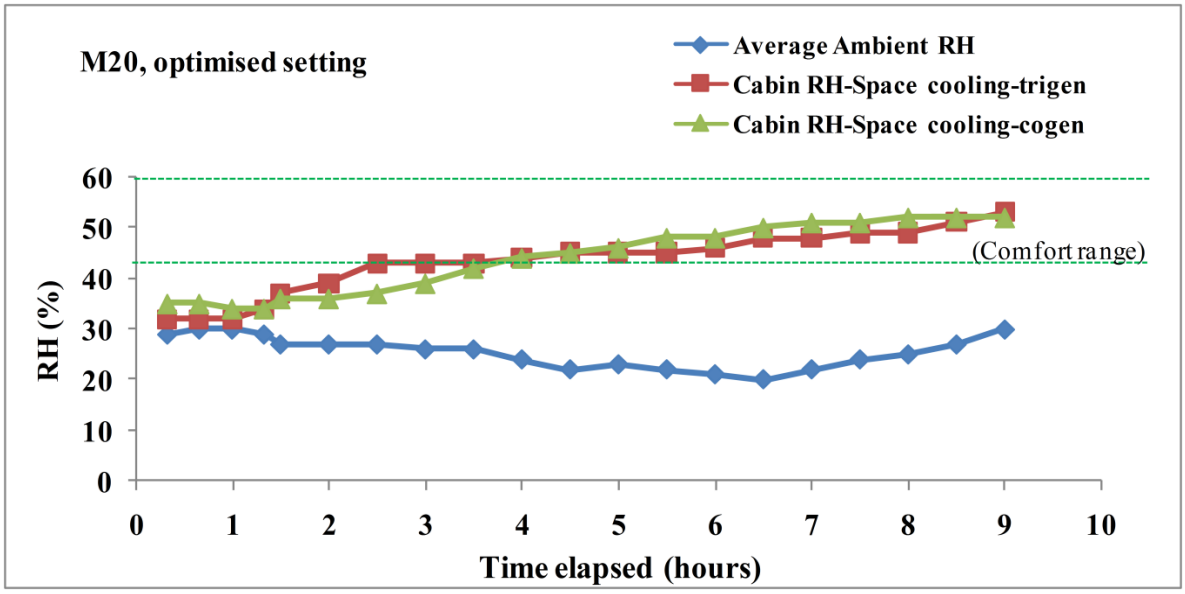

(b)

Fig. 5.15 Variation of (a) cabin temperature and (b) cabin RH with elapsed time for M20 in space cooling (optimised settings)

The variation of cabin temperature and cabin RH with elapsed time are shown in Fig. 5.15 (a) and (b). The comfort conditions were maintained throughout the test duration of 9 hours in the day.

As can be seen from the graphs in Fig. 5.14, the temperature drop with M20, N20 and R20 at rated settings was equal at about 7 ^{o}C. The RH increased from a minimum of 21- 24 % to 46-49 % for these fuels. But, for MB20 fuel at rated settings, maximum temperature drop

of 8 ^{o}C could be obtained, and RH increased up to 52%. At optimized settings too (Fig. 5.15), with M20 as fuel in cogeneration, the maximum temperature drop of 7.5 ^{o}C could be reached, and RH also increased up to 51 %. Results with M20 both at rated and optimized (cogeneration) conditions were nearly the same, but in trigeneration at optimized settings with M20, the temperature drop was maximum at 8 ^{o}C , and RH increased from a minimum of 23 % to 53%.

The ambient conditions were 34-39 ^{o}C and 20-25 % RH. With trigeneration operation, the temperature drop was maximum, may be due to fuel preheating with higher EGT and so the higher heat content used in generators of VAR units for space cooling. For operation for longer hours, energy savings may occur in trigeneration space cooling.

Fig. 5.16 and Fig. 5.17 depict the weather data for Jaipur during the year- the maximum and minimum values of temperatures and relative humidity (RH) respectively, during day and night. The range of all experiments for space heating as well as space cooling in the micro-trigeneration set-up has been shown.

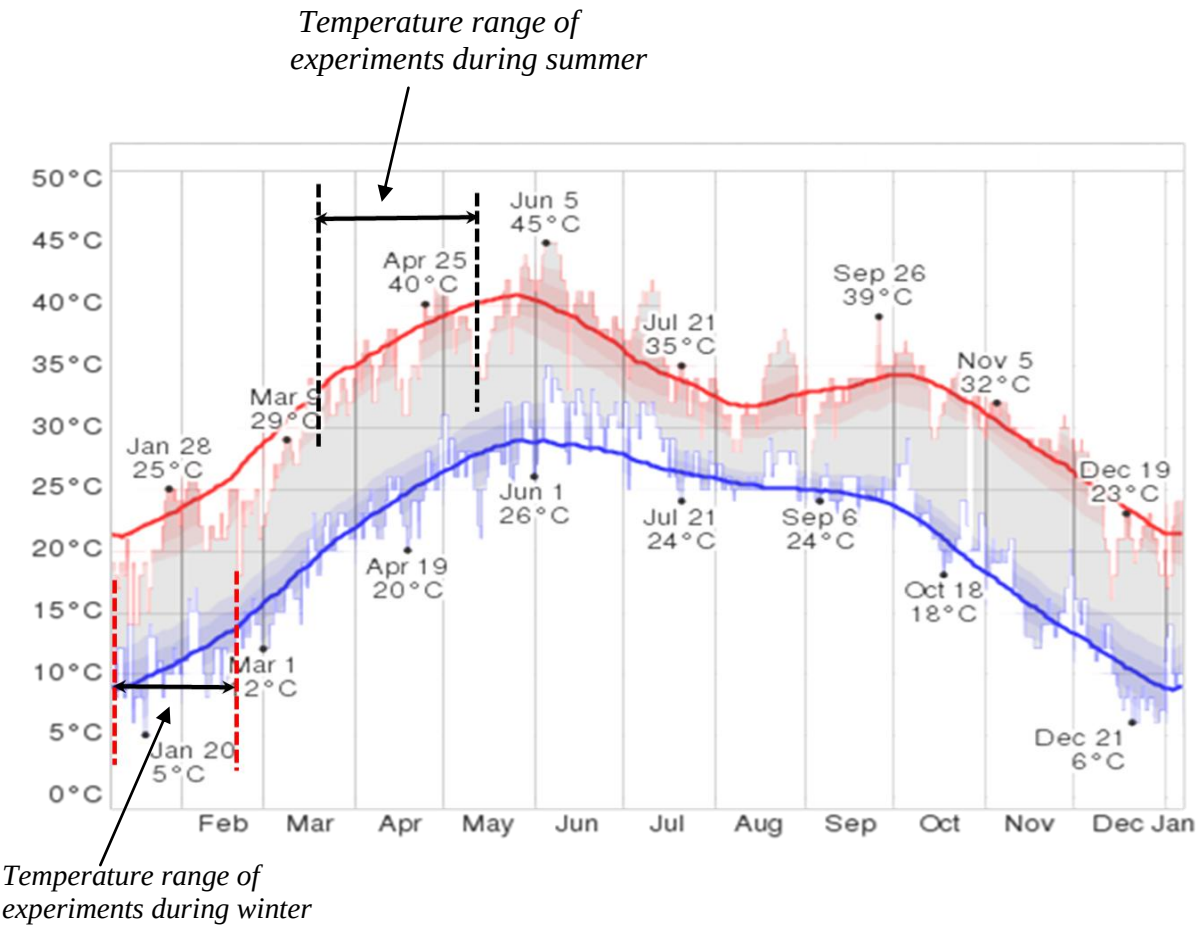

Fig. 5.16 Weather data (temperature), Jaipur (2014) and ambient range during all experiments [105]

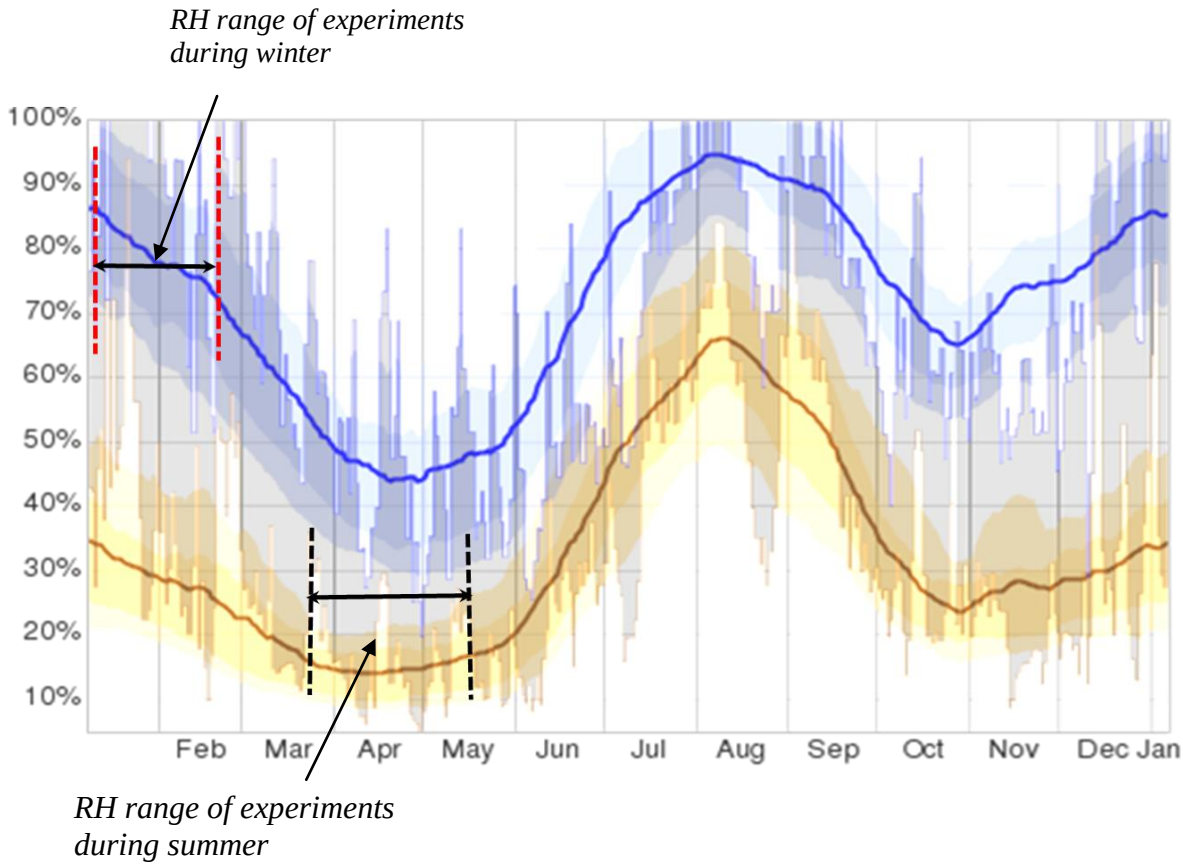

Fig. 5.17 Weather data (Relative Humidity), Jaipur (2014) and ambient range during all experiments [105]

The experiments were conducted both for cooling as well as heating in different times of the year. The space cooling experiments were conducted during March, April and May in 2014, while the space heating experiments were conducted in January and February of 2014.

The heating and cooling processes throughout the range of experimentations are depicted on the psychrometric chart as shown in Fig.5.18. As can be seen, for space heating during winter, the dry bulb temperature range was 5-11^{o} C, whereas the ambient RH range was 87-91 %.

For space cooling during summer, the dry bulb temperature range was 32-38^{o} C, while the ambient range for RH was 15-25 %.

Comfort conditions obtained in the test cabin are also depicted on this chart which are 22-28^{o} C and 40-60 % RH.

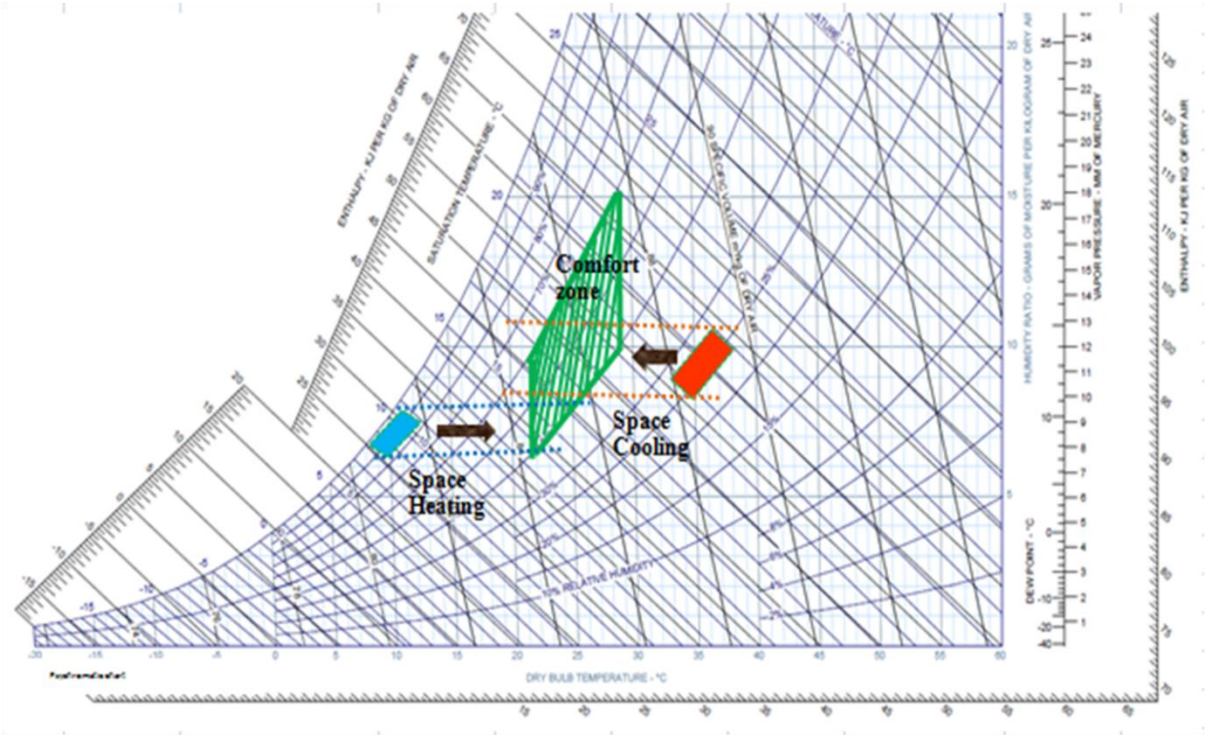

Fig. 5.18 Space heating and Space cooling range depicted on psychometric chart

5.7 VAR units in space cooling

5.7.1 Operation methodology of VAR units

For the four units assembled for the space cooling unit, four separate valves were provided to direct the flow of exhaust gases towards the generators of these four units. With increase in engine loading, the valves were opened in a sequence only. It was seen in another experiment that when all four valves were opened simultaneously in the beginning itself, no cooling effect could be generated even after 4-6 hours of running. The reason could be that heat required to start the VAR unit i. e., for the ammonia vapours to evaporate in a cycle is larger, and once the unit is operational, comparatively, a smaller quantity of heat is required for the VAR to remain operational.

The generator temperature required for full operation as per the manufacturer's catalogue is up to 120^{o} C. For a small engine like this and with total of four VAR units, mode and timings of operation for the valves to allow the exhaust gases to the generators was decided by running it for a number of times, and by hit and trial.

Various settings and sequence of valve operation were tried depending on average generator and evaporator temperatures until a final optimum sequence was determined for maximum cooling effect to be generated, which is as follows.

It was found that generator valve (for hot exhaust gas intake in the heat exchanger) of only one VAR unit was to be opened till the engine load was 3 kW, and then this VAR unit is fully functional and reaches steady state. The average evaporator temperature goes to below 10^{o} C, and the generator temperature is also steady. Then generator valve of the second unit was opened, and the engine load was increased to full load, 3.7 kW. After about half an hour of operation at full load, and about total two hours of operation, the second unit also reached the steady state with generator temperature and evaporator average temperatures reached steady state. Then, generator valve of the first unit was closed for 15-20 minutes, and simultaneously, the third generator valve was also opened for intake of exhaust gases in the heat exchanger at generator. When the generator temperature in the third VAR generator reached about 80^{o} C, and temperature drop was seen, the generator of the first unit was again opened. Both first and third units reached steady state in next half an hour. Now, three units were fully functional. Then about total of 2-1/2 to 3 hours of running, the generator valve of the fourth VAR unit was also opened for exhaust gas intake. At this time all four units were running and the exhaust heat was fully utilised. About after next half an hour, the fourth unit was also functional, although it could not reach the lowest evaporator temperature, (or highest generator temperature), as in case of other three units.

With the installation of the forced draught fans near the condensers of the four units, the maximum generator temperature for full operation of the VAR unit was seen to be lowered, and the fourth unit could also be made fully operational. After three hours of operation, all four units were working and the temperature drop of up to 4-5^{o} C in the cabin was registered.

With proper insulation of the exhaust intake piping, and the inside of the cabin, the temperature losses were minimised, and the maximum temperature drop in the cabin of up to 8^{o} C could be achieved with M20 at optimised engine settings after nearly total four hours of operation, when the ambient temperature was 38^{o} C. RH value also increased from 25 % for ambient to 45 % in the cabin, which was mainly the result of sensible cooling. The final steady state was achieved and cooling effect was generated continuously and maintained for next few hours of running.

5.7.2 Performance of vapor absorption refrigerator

Various performance parameters of the vapour absorption units (modified as space cooling unit) were recorded and evaluated in both cogeneration and trigeneration modes using different alternate fuels in the entire load range of the engine.

The important parameters are:

- Generator temperature of VAR unit, t_{gen};
- Evaporator temperature, t_{evap}.
- Heat input into the generator of VAR unit, Q_{gen};
- Cooling effect generated, Q_{cool};
- Coefficient of performance of the VAR unit, COP;

The generator temperature correspond to the heat energy input into the generator of VAR unit, Q_{gen} and the evaporator temperature correspond to the cooling effect generated, Q_{cool}. The refrigeration effect produced by the VAR units of the space cooling system was calculated by noting the temperature drop and the time taken to reach the steady state.

UA value of the cabin was calculated to determine the refrigerant effect. It was also estimated from the values of heat loss from the cabin and the heat absorbed by the components inside the cabin, etc. It was calculated from the following equation,

$$Q_{RE}=UA(T_{cabin}-T_{amb})$$

The heat supplied in the generator of VAR was calculated by the following formula:

$$Q_{gen}=\epsilon\, C_{min}\,(T_{hi}-T_{ci}),$$

Here, ϵ is the heat exchanger effectiveness at generator, C_{min} is the minimum heat capacity and T_{hi} and T_{ci} are the hot and cold fluid temperatures respectively at the generator heat exchanger. The effectiveness of heat exchangers calculated were in the range of 0.557-0.591 for VA system, in various modes of operation.

Then, COP was calculated using the following relation

$$COP = \frac{\text{Refrigeration effect } (Q_{RE})}{\text{Heat supplied to generator of VAR unit } (Q_{gen})}$$

For M20 operation at optimised settings and in trigeneration mode, the average generator temperature was 85-95^{o} C, and the average heat input was 1227.84 W. The average evaporator temperature was 9-11^{o} C, and the average refrigerant effect (cooling effect) was 273.81 W. The COP was calculated as 0.223.

5.8 Analysis of micro-trigeneration operation

5.8.1 Heat recovered in trigeneration

Waste heat in an I. C. engine can be recovered from various sources-engine exhaust, engine coolant, lube oil cooling water, etc. In the present work, heat from the engine exhaust gases, and engine jacket cooling water was recovered and utilised for the trigeneration operation. Quantity of waste heat available for use was calculated from the data collected from these sources.

Four options were available for use- Power, Space heating/cooling, water heating and fuel preheating. Fig 5.19 shows the case when maximum heat was recovered and utilised in the micro-trigeneration system, using M20 as fuel at optimised engine settings.

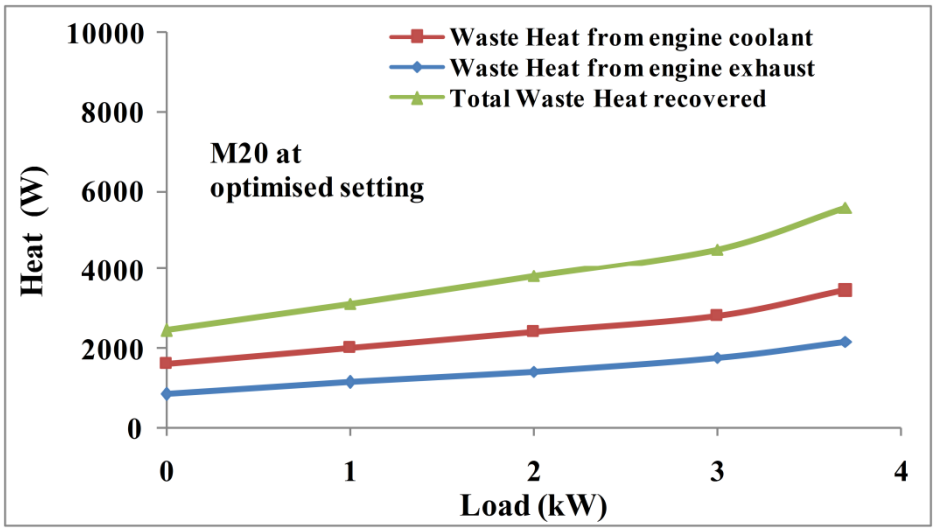

Fig 5.19 Variation of heat obtained from engine and engine coolant with load in trigeneration system

The heat recovered from engine exhaust from no load to full load was 824.3 W to 2136.2 W. The heat recovered from engine cooling jacket system varied from 1602.2 W at no load to 3434.1 W at full load. And the total heat recovered was 2426.5 W at no load to 5570.2 W at full load. The heat content in coolant was higher than that in exhaust gases in the entire load spectrum.

5.8.2 Comparison of trigeneration parameters in various modes of operation at full load

Trigeneration systems are generally operated at or near full load, especially if VAR units are incorporated. Various trigeneration parameters evaluated and compared are:

(a) Useful energy output
(b) Overall thermal efficiency
(c) Specific fuel consumption (SFC)
(d) Total CO_2 emissions

In the present work, there were options of generation of up to four outputs, and the evaluation of the above parameters was made for all possible combinations, which are:

1. Single generation (SG)
2. Combined power and fuel preheating (C-P-FP)
3. Combined power and space cooling (C-P-SC)
4. Combined power and space heating (C-P-SH)
5. Combined power, space cooling and fuel preheating (C-P-SC-FP)
6. Combined power, space heating and fuel preheating (C-P-SH-FP)
7. Combined power, space heating, fuel preheating and hot water production (C-P-SH-FP-HWP)
8. Combined power, space cooling, fuel preheating and hot water production (C-P-SC-FP-HWP)

Comparisons were made at full load condition for all the parameters and are given in Fig. 5.20 (a) to (d). M20 as fuel at optimized engine setting was used.

Useful output for single generation was the power output only, which was 3.7 kW. In combined power and fuel preheating mode, it increased slightly to 3.75 kW. In combined power and space cooling mode, it was 4.15 kW, which increased to 4.21 kW when combined with fuel preheating. In combined power and space heating mode, it was 7.2 kW, which increased to 7.26 kW when combined with fuel preheating. In quad generation- combined power, fuel preheating, space heating and hot water production mode, it was 8.76 kW, while maximum useful output was generated in quad generation- combined power, fuel preheating, space cooling and hot water production mode, when it was 9.27 kW.

Total thermal efficiency for single generation was 30.7 %. In combined power and fuel preheating mode, it increased slightly to 31.2 %. In combined power & space cooling mode, it was 34.5 %, which increased to 35.1 % when combined with fuel preheating. The very low efficiency in space cooling may be due to very low COP of the VAR units.

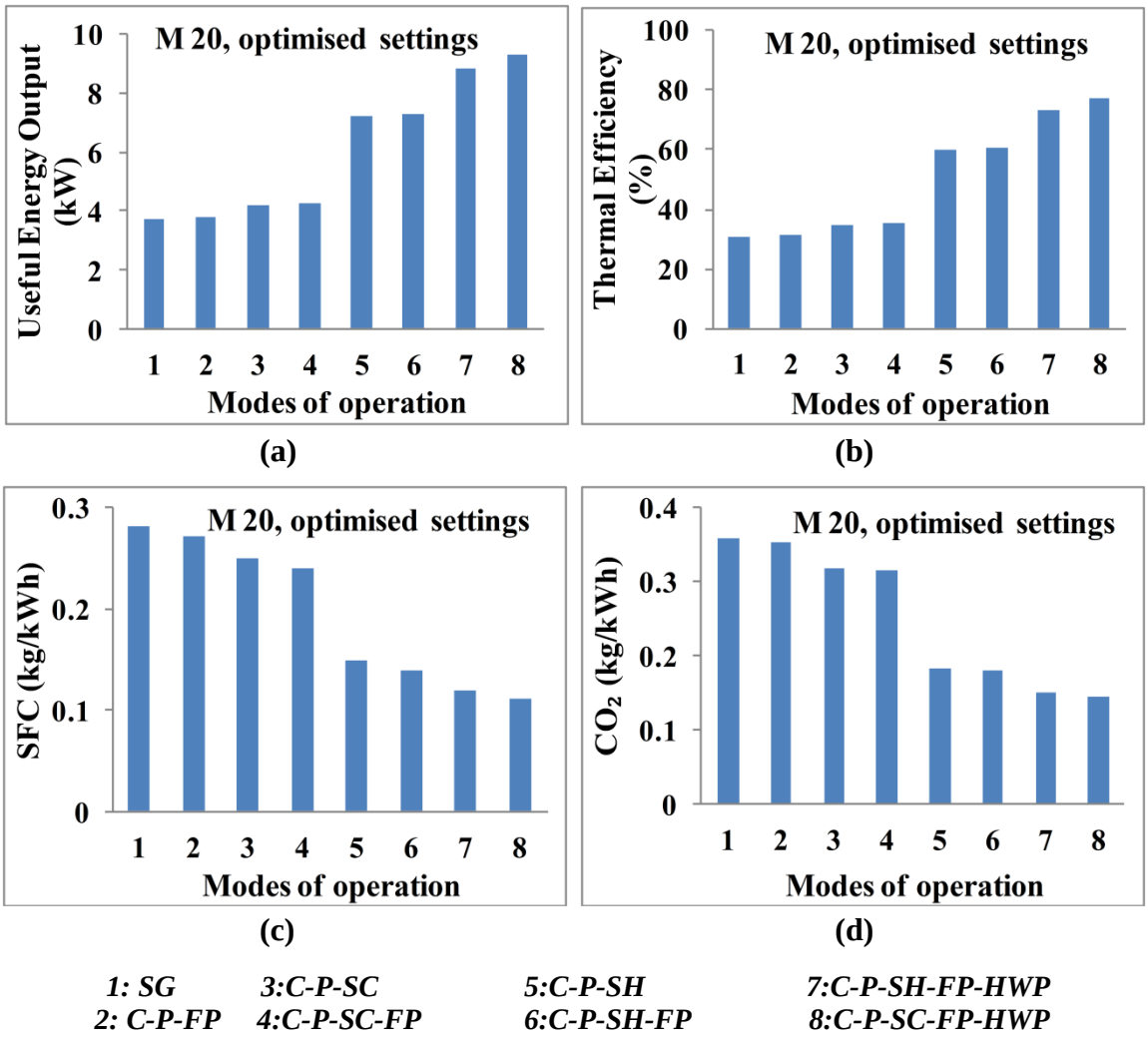

Fig. 5.20 Comparison of trigeneration parameters (a) Useful Energy Output (b)Thermal Efficiency (c) SFC and (d) CO_2 per kWh, in various modes of operation at full load

In combined power and space heating mode, it was 59.9 %, which increased to 60.4 % when combined with fuel preheating.

In quad generation-combined power, fuel preheating, space heating and hot water production mode, it was 78.4 %, while maximum thermal efficiency was generated in quad generation with combined power, fuel preheating, space cooling and hot water production mode, when it was 77.2 %. Similarly, the specific fuel consumption from single generation to quad generation decreased drastically, and varied from 0.28 kg/ kWh in single generation to the lowest value of 0.11 kg/ kWh in quad generation with combined power, fuel preheating, space cooling and hot water production mode.

Emissions of CO_2 also decreased from 0.357 kg per kWh to the lowest value of 0.142 kg/kWh respectively in case of single generation and quad generation with combined power, fuel preheating, space cooling and hot water production mode.

5.8.3 Trigeneration parameters for maximum generation (C-P-SC-FP-HWP) in entire load range (case of quad generation)

As was discussed in previous section, the maximum generation was fourfold with maximum values of useful output & total thermal efficiency, and lowest values of specific fuel consumption and CO_2 emissions. So, all the parameters were evaluated and discussed for this case (quad generation) in the entire load range of the engine and compared with that of single generation, and are shown in Fig. 5.21 (a)-(d).

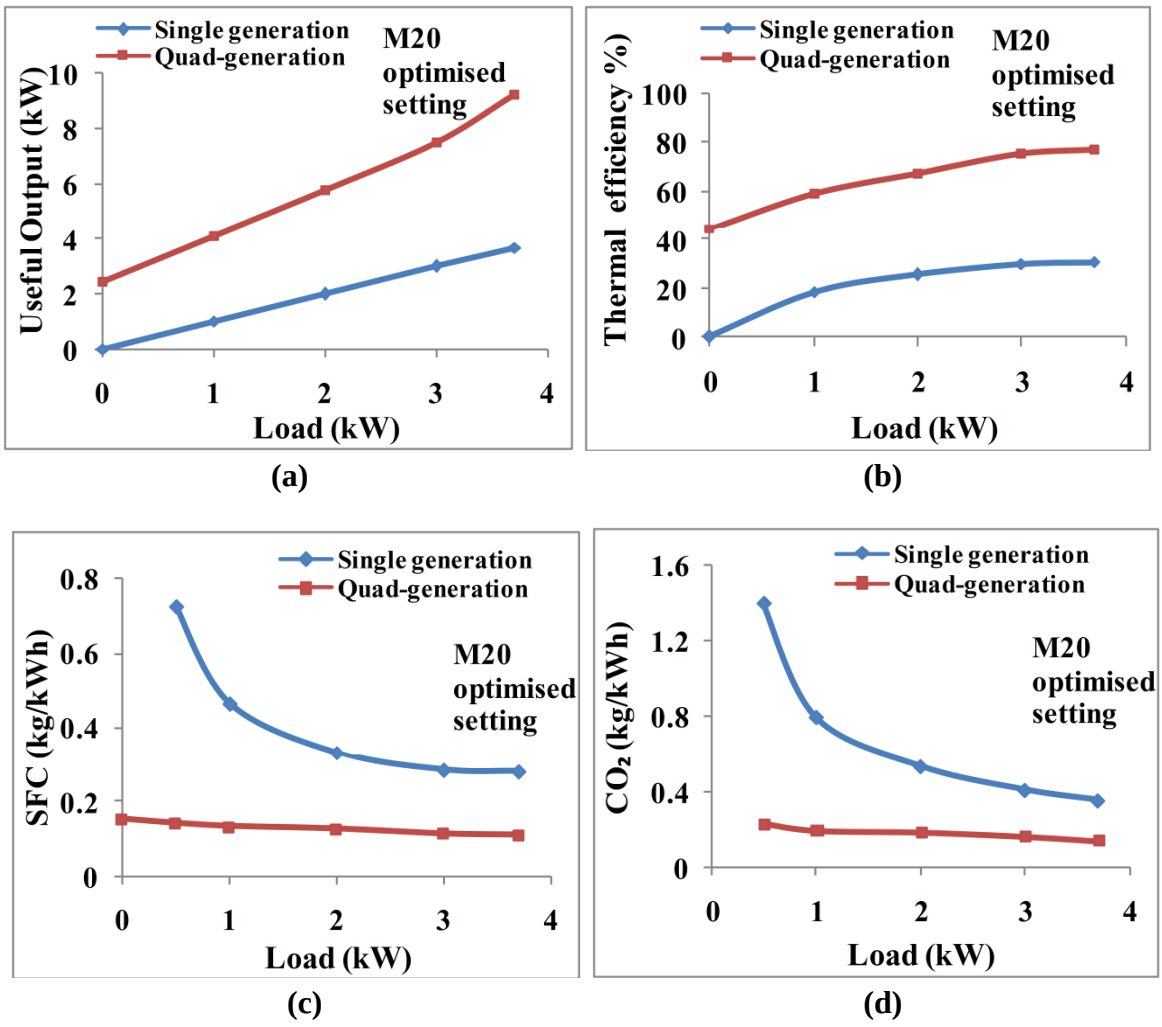

Fig. 5.21 Variation of (a) Useful energy output (b) Total thermal efficiency (c) SFC, and (d) CO_2 emissions with load for single generation and quad-generation with M20 as fuel

It was found that from no load to full load, useful output varied from 2.426 to 9.27 kW, the overall thermal efficiency increased from 44.21% to 77.12 %, SFC decreased from 0.152 to 0.11 kg/kWh and total CO_2 emissions decreased from 0.229 to 0.142 kg/kWh.

The useful output increased by 150.54 %, the total thermal efficiency increased by 169.24 %. The specific fuel consumption decreased by 60.1 % and the total CO_2 emissions decreased by 61.27 %. in quad generation, as compared to single generation.

5.9 Simulation results of the operation of microtrigeneration unit with M100 fuel

A simplified simulation model was developed for micro-trigeneration system working on vegetable oils. A thermodynamic software DIESEL-RK interfaced with an external code (*ExtContr.BAT* file), and also an excel based file, was used for the calculation of the useful energy output, specific fuel consumption and total thermal efficiency of micro-trigeneration system working on alternate fuel blends of different origin.

The database for fuel properties were modified according to the fuel used. Properties such as temperature, pressure, etc at each stroke or crank angle were used to calculate the parameters for different SVO used. Using the energy and mass balance, and interfacing with DOS based file, the proposed trigeneration was simulated in Diesel RK software.

Fundamental operating conditions were defined for the simulation model: the heat source temperature and power, the useful cold temperature and ambient temperature. The waste heat recovery system and engine working processes were simulated.

The performance of micro-trigeneration with pure Mahua oil (M100) as fuel was evaluated. The obtained results were validated with experimental results, and a good agreement has been achieved without recalibration of the model for different operating modes.

The derived graphs showing the comparison of simulation and experimental results are presented in Fig. 5.22 (a)-(c). The useful output values in the entire load range were within 4.3% for the useful output, 3.99% for thermal efficiency, and 3.01 % for specific fuel consumption.

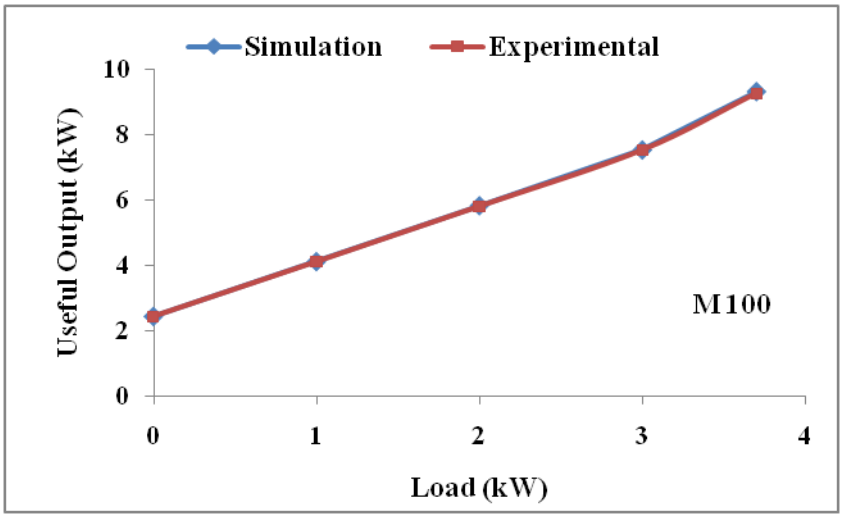

(a)

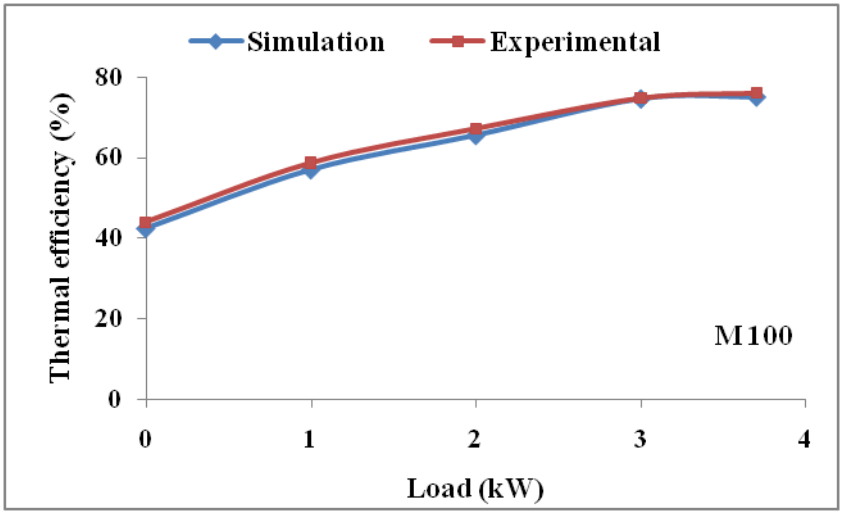

(b)

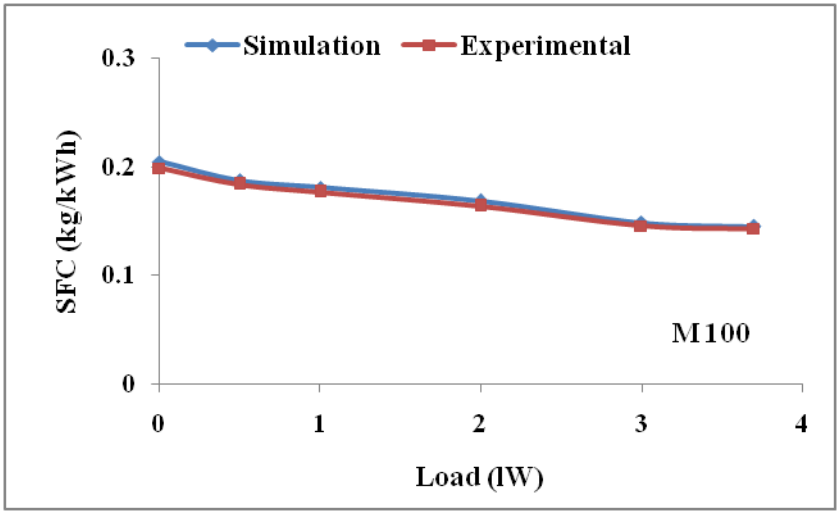

(c)

Fig. 5.22 Variation of (a) Useful energy output (b) Total thermal efficiency (c) SFC with load for simulation and experiments with M100 as fuel

Simulation results predicted for M100 reveal that useful energy output varied from 2.112 kW at no load to 8.34 kW at full load; the total thermal efficiency varied from 43.15% at no load to 75.68 % at full load and the specific fuel consumption varied from 0.217 kg/kWh at no load to 0.123 kg/kWh at full load.

Comparative values between simulation and experiments, in the entire load range were within 3.5 % for the useful output, 2.5 % for thermal efficiency and 3.9 % for specific fuel consumption.

5.10 Exergy analysis

A brief exergetic analysis was conducted to predict the losses in the energy flows in the micro-trigeneration system.

The ratio of exergy of fuel to its lower calorific value for homologous series of hydrocarbons was given by Brzustowski and Brena [106].They concluded that it is equal to 1.065, i. e,

$Eex_{fuel}/LHV= 1.065$

While using alternate biofuels, many times the chemical composition is not known, or cannot be predicted with certainty, because the composition of such fuels may vary in different applications. This equation can be used for heavy hydrocarbons of undetermined composition. This equation was used to obtain the fuel exergy of M20 fuel.

Energy and exergy formulations were used to find the recovered exergy and the total exergetic efficiency of the trigeneration system using M20 fuel. The results are as follows:

1. Chemical energy of fuel = 42.30 kJ/kg
2. Chemical exergy of fuel = 45.30 kJ/kg
3. Energy content in fuel = 11.12 kW
4. Exergy content in fuel = 11.89 kW
5. Energy efficiency of engine = 30.79%
6. Exergy efficiency of engine = 28.91 %
7. Total maximum output from trigeneration = 9.27 kW
8. Overall efficiency of trigeneration system = 77.12 %
9. Exergy efficiency of trigeneration system = 36.24 %

5.11 Economic analysis

A simplified economic analysis was conducted to estimate the economic feasibility of the micro-trigeneration system.

The yearlong operation of the micro-trigeneration unit was considered which includes both summer and winter seasons. But, extreme summer days are excluded in space cooling. To cover up the days of non operation and maintenance, it is assumed that the micro-trigeneration system will operate fully for 10 months of the year, with 8 hours of operation per day.

Economic analysis is conducted only for M20 fuel as an example, although the fuel cost calculations are tabulated for all fuels used in the experiments.

It is also assumed that full utilisation of all the options (power, space cooling/heating, fuel preheating and hot water production) will be done and the engine will run mostly at full load condition, and the maximum useful output from the system has been considered.

The material and energy inputs and outputs during transesterification process, along with the prices used for calculation of direct fuel costs have been tabulated.

Table 5.3 gives the average costs (Jan-2014) of diesel and raw vegetable oils used in this study. Table 5.4 shows the total cost of mahua biodiesel preparation on small scale.

Table 5.3 Costs of different CI engine fuels used in the study

	Diesel	Ricebran oil	Neem oil	Mahua oil	Mahua biodiesel
Cost (Rs/litre)	60.42	74.25	71.35	66.50	89.69
Density (kg/litre)	0.832	0.926	0.936	0.912	0.883
Cost (Rs/kg)	72.62	80.18	77.05	72.92	101.57
Calorific value (MJ/kg)	43.5	38.2	37.9	37.6	39.4
Cost (Rs/MJ)	1.67	2.10	2.03	1.94	2.58

Table 5.4 Cost calculations for mahua biodiesel preparation

	*Price (Rs)
Inputs:	
Mahua oil (for 92% BD yield)	72.28
Methanol (for 2-step process)	18.45
Reagents	1.53
Electricity	0.35
Labour	2.10
Other costs (transportation, storage, losses etc)	1.25
Sub total	98.96
Revenue from sale of glycerol	9.27
Net cost of biodiesel (litre)	89.69

*For 1 litre of mahua biodiesel production

Table 5.5 and Table 5.6 shows the various approximate investment costs in trigeneration and separate energy production respectively

Table 5.5 Investment costs in trigeneration-

Item	Cost (Rs)
Diesel engine-generator set	60000
VAR units	50000
Heat exchangers	25000
Fabrication, installation, erection etc	25000
Plumbing and pipings, insulation etc	25000
Miscellaneous items	15000
Total	200000

Table 5.6 Investment costs in separate production-

Item	Cost (Rs)
VC air conditioning unit (0.5 ton)	25000
Electrical radiator for space heating (2 kW)	3000
Electrical hot water heater (geyser, 3 kW)	7000
Plumbing and pipings, insulation etc	10000
Miscellaneous items	5000
Total	50000

Calculations for payback period:

Net investment costs for micro-trigeneration system = 150000.00

With 8 hrs of operation of micro-trigeneration unit, (total yearly hours =2400)

Total fuel cost in trigeneration operation per year = 181307.00

Lube oil cost = 5327.00

Maintenance and spare parts inventory costs = 2220.00

Total electrical energy costs of cooling in months of summer, costs of heating in months of winter and hot water production throughout the year in separate production, (taking electrical energy charges as Rs 10/unit) = 222480.00

Avoided costs = 41173.00

Net annual savings =33626.00

Payback period =150000/33626= 4.46 years

So, the present system, if run on M 20 blend at optimised settings, at 8 hours of operation and for 10 months in a year in trigeneration (maximum generation) mode, it will payback the investments on micro-trigeneration unit in nearly 4 years and 6 months, and thereafter savings will be generated.

5.12 Guidelines for alternative fuel operated micro-trigeneration system

- Blends of 20% biodiesel or vegetable oils as fuel must be used for better performance.
- Fuel preheating with the help of engine exhaust gases up to a temperature of 90^{o} C must be incorporated to improve the performance of trigeneration system.
- The diesel engine must be optimised for the best performance by varying the IOP, IT or other parameters to get the maximum efficiency from the engine. Increased NOx values can be reduced by applying 5-15 % EGR.
- To utilise the full potential of the micro-trigeneration unit, it must be operated in quad generation or trigeneration, rather than single or cogeneration. Proper thermal load following or electric load following must be decided beforehand.
- Space heating using emitter pipes are cost effective as compared to hydronic system, with good energy performance, and can be used with both direct exhaust fired and hot water fired space heating.
- Direct exhaust fired as well as hot water fired space heating using annular finned pipes is feasible and can cut down the energy costs in space heating.
- For VAR units of the space cooling unit to be fully functional to give maximum cooling effect, it must always be operated at full load.
- To obtain maximum temperature drop in the cabin, it requires proper layered insulation to minimise the heat losses.
- The space cooling unit consists of Electrolux VAR systems with very low COP, so to obtain comfort conditions, it may be used only when ambient temperature is below 40^{o} C
- Forced draught fans must be placed near the condensers of the four VA units to enable full operation of all four units.
- The valves at the generator for intake of exhaust gases must be operated in the sequence described in the previous section, otherwise full cooling effect may not be generated.

CHAPTER 6

CONCLUSIONS

6.1 Conclusions

Diesel engine operated micro-trigeneration system for power, fuel preheating, space cooling /heating, and water heating, using alternative fuels was developed and investigated. From the results of the study, the following conclusions can be drawn:-

1. It was feasible to realize a micro-trigeneration system using a small agricultural engine using alternative fuels. Integration of the components of trigeneration did not affect much the performance and emission characteristics of the diesel engine.

2. Variations in BSFC and BTE among M20, R20 and N20 fuels were negligible at full load, with maximum variations of 3-4 % at lower loads. With M20, BTE was highest. Emissions of CO, HC, NOx and smoke using M20 were lower than that with diesel.

3. Fuel preheating up to 90^{o} C was found to be optimum considering BTE, BSEC and emissions. Using preheated M100 and M20 fuels in single generation, BSEC decreased by 7.5% and 3.5 % respectively, and BTE increased by 8.1% and 3.5% respectively from their corresponding unheated values.

4. A synergic effect was seen for the optimised combination of 230 bar IOP and 25 ^{o} btdc IT. With M20 at full load, BSFC reduced by 5.44 % and BTE increased by 6.13 % as compared to corresponding values at rated settings. Emissions of CO, HC and smoke decreased by 40%, 25.6% and 39.4%, but NOx increased by 12.1%. EGR rates of 5-15% were effective in controlling the increased NOx emissions in all modes of operation, with a better trade-off between HC, CO, NOx and smoke emissions and little penalty on BSFC and BTE.

5. At rated engine settings and full load, in trigeneration with space heating/cooling, among all test fuels, BTE values were 3.7 %- 8.7 % lower, and BSEC values were 7.9 %-11.6 % higher than that with diesel in single generation. CO and HC increased, yet were lower than that with diesel. NOx was slightly lower, but smoke increased by 6-12 % using SVOs. MB20 emitted slightly higher NOx but less smoke in trigeneration.

6. At optimised engine settings with M20 at full load, variations in BSFC and BTE were negligible. In cogeneration and trigeneration, BSFC values were nearly 2 % and 3 % higher, and BTE values were nearly 1% and 2.5 % lower respectively than those in single generation. CO, HC and smoke in cogeneration as well as trigeneration was much lower than base case diesel in single generation, but NOx was higher by 13-15% than that of diesel in single generation, which could be reduced drastically by applying EGR up to 15% with penalty of only 1-2 % on BTE, BSFC and smoke.

7. In cogeneration with direct exhaust fired system for space heating using M20 at rated settings, comfort conditions were attained from ambient conditions (5-7^{o} C, 88-91 % RH) in 80, 65 and 55 minutes respectively with unfinned, longitudinal finned and annular finned pipes respectively. In trigeneration with space heating using annular finned pipe at optimised settings, comfort conditions were attained in 50 and 70 minutes respectively for exhaust fired and hot water fired space heating respectively.

8. In space cooling, steady state was attained after nearly four hours of operation. At optimised engine settings, the maximum temperature drop in the cabin was 8^{o} C in trigeneration, and 7^{o} C in cogeneration.

9. Forced draught fans near the condensers of the four VA units lowered the maximum generator temperature and enabled full operation of all four units.

10. Average COP of VAR systems using M20 at optimised settings was 0.223.

11. At full load, the heat recovered from engine exhaust was 2136.21W, from engine cooling system was 3434.03 W and the total heat recovered was 5570.24 W.

12. Useful output in single generation (only power) was 3.7 kW. In quad generation, i. e., power, fuel preheating, space cooling and hot water production, it increased tremendously to a maximum of 9.27 kW, the overall thermal efficiency increased to 77.12 %, SFC dropped to 0.11 kg/kWh and total CO_2 emissions were 0.142 kg/kWh.

13. The increase in useful output and total thermal efficiency were 150.54 % and 169.24 % respectively. The decrease in specific fuel consumption and total CO_2 were by 60.1 % and 61.27 % respectively in quad generation, than in single generation.

14. The effectiveness of heat exchangers in maximum generation mode were calculated as 0.591 for VA system, 0.623 in fuel preheating and 0.678 for water heating. For longitudinal and annular finned pipes, the fin effectiveness values were calculated to be 1.18 and 1.37, and fin efficiency values were calculated as 0.34 and 0.39 respectively.

15. Simulation results predicted for M100 revealed that the useful output values in the entire load range were within 3.5 % for the useful output, 2.5 % for thermal efficiency and 3.9 % for specific fuel consumption.

16. Economic analysis conducted for M20 fuel at optimised settings in trigeneration (maximum generation) mode, at 8 hours of operation for 10 months in a year will pay back the investments on micro-trigeneration unit in nearly 4 years and 6 months, and thereafter savings will be generated.

6.2 Future work

Some investigation objectives listed below, though not exhaustive, may be considered as future scope of work:

- An actual representative micro-trigeneration system for a residential family using a bigger diesel engine, say up to 15 kWe power, along with triple-effect ammonia-water system, can be used for further investigations, as an extension of the present work.

- Engine stability, noise and vibrations characteristics with alternative fuels in micro-trigeneration system can be studied. Durability tests and tribological investigation for long term operation of alternative fuel operated micro-trigeneration system may also be investigated.

- Both thermal energy storage and electrical energy storage devices may be integrated with the micro-trigeneration system to meet the variable energy demands, and also to improve the overall efficiency in a house or building.

- Different types of prime movers, like micro-turbines, sterling engine, fuel cells etc, could be utilized as power generating unit in the micro-trigeneration system. Further, the micro-trigeneration system may also be designed for integration with a renewable source of energy like solar or wind energy, and the investigations may be carried out.

APPENDIX-A

UNCERTAINTY ANALYSIS

Uncertainties in the experimental measurements may occur due to various reasons like experimental methods adopted, instruments used and calibration, working conditions, environment etc. So, uncertainty analysis is necessary to ascertain the accuracy of the measurements.

In this investigation, the uncertainty associated with the measured parameters is evaluated according to the equipment manuals and the standard procedure suggested in the Guide to the expression of uncertainty in measurement (GUM)—JCGM 2008.

Uncertainties in measurements were calculated using standard analytical techniques and statistical analysis. Principle of propagation of uncertainty was used to calculate the combined uncertainty of parameters. Root-sum-square method was adopted, which is as given below.

Let a number of input measured parameters be X_1, X_2….. X_N, and their measured values be x_1, x_2… x_N.

Let Y be the resulting parameter determined from the input quantities, and f be the functional relationship between Y and X_1, X_2….. X_N,

If y is the estimation of measure, the combined standard uncertainty u(y) is due to propagation of uncertainty in individual parameters associated to a measured value and Y.

u (y) is given by the following relation,

$$u\,(y) = \sqrt{\sum_{i=1}^{N} (\partial f/\partial x_i)^2 . u(x_i)^2}$$

Uncertainty of main parameters in Trigeneration system at engine full load condition was determined based on the uncertainties in the measured parameters, and using the above equation. All uncertainties of measurements were evaluated for a confidence level of 95 %.

Uncertainties in specific properties like density, specific heat etc were neglected.

The maximum uncertainties in the measured and calculated results are given in Table 2.

Table A 2 The accuracies of the measurements and the uncertainties in the calculated results

Parameter	Unit	Measuring range	Accuracy	Percentage uncertainty*
AVL 4000 Light gas analyser				
CO	% volume	0-10% volume	< 0.6% vol: ±0.03 % vol > 0.6% vol: ±5 % of indicated value	± 0.4%
HC	ppm volume	0-20000 ppm volume	< 200 ppm vol: ±10 ppm vol > 200 ppm vol: ±5% of indicated value `	± 0.3%
NOx	ppm volume	0-5000 ppm volume	< 500 ppm vol: ±50 ppm vol ± 0.3% > 500 ppm vol: ±10% of indicated value	
AVL 437 Smoke meter				
Smoke	% opacity	0-100%	±1%	± 1.0%
K-type thermocouple				
Temperature	^{o}C	0-600 ^{o}C	±1^{o}C	± 0.2%
Burette				
Volumetric fuel flow	mL	0-100 ml	±1ml	± 1%
Digital Stopwatch				
Time	s	--	±0.2s	± 0.5%
RH_{air}	%	0-100 %	± 1 %	± 0.5 %
BTE	%	--	--	±1.2%
BSFC	kg/kWh	--	--	± 1.2%
COPvar	--	--	--	± 0.6 %
PER_{trigen}	--	--	--	± 4.8 %

*(*All values at 0.95 significance)*

REFERENCES

1. Onovwionaa H.I., Ugursal V. I. "Residential cogeneration systems: review of the current technology". Renewable and Sustainable Energy Reviews 10 (2006) 389–431

2. Wu D.W., Wang R.Z.,"Combined cooling, heating and power: A review" Progress in Energy and Combustion Science 32 (2006) 459–495

3. Mingxi Liu, Yang Shi, Fang Fang "Combined cooling, heating and power systems: A survey"., Renewable and Sustainable Energy Reviews 35(2014)1–22

4. A. Abusoglu, Kanoglu M."Exergetic and thermoeconomic analyses of diesel engine powered cogeneration: Part 1 – Formulations" Applied Thermal Engineering 29 (2009) 234–241

5. Temir G. , Bilge D. Emanet O, "An Application of Trigeneration and Its Economic Analysis.. Energy Sources", 26:9 (2004) 857-867

6. Wang Y., Huang Y., Chiremba E., Roskilly Anthony P., Hewitt N., Y. Ding, Wu D., Yu H., Chen X., Li Y., Huang J., Wang R., J. Wu, Xia Z., C Tan. "An investigation of a household size trigeneration running with hydrogen". Applied Energy 88 (2011) 2176–2182

7. Lin L., Wang Y., Al-Shemmeri T., Ruxton T., Turner S., Zeng S., Huang J., Y He, X Huang. "An experimental investigation of a household size trigeneration". Applied Thermal Engineering 27 (2007) 576–585

8. Remer D. S., Tamar L. Di Franco, Johnson R. A."Technical and Economic feasibility of a prototype 4 kW cogeneration package". Energy Vol. 14-5, (1989) 277-290, 0360-54

9.Kanoglu M., Dincer I. "Performance assessment of cogeneration plants". Energy Conversion and Management 50 (2009) 76–81

10. Micro-Trigeneration:-The Best Way for Decentralized Power, Cooling and Heating, Easowa R., Muley P., 978-1- IEEE (2010) 4244-6078-6

11. Jayasekara S., Siriwardana J., Halgamuge S. “Enhanced Thermal Performance of Absorption Chillers Fired by Multiple Dynamic Heat Sources”. International Journal of Precision Engineering and Manufacturing Vol. 13, No. 7(2012) 1231-1238

12. Jradi M., Riffat S. “Tri-generation systems: Energy policies, prime movers, cooling technologies, configurations and operation strategies”. , Renewable and Sustainable Energy Reviews 32 (2014) 396–415

13. Khatri K. K., Sharma D., Soni S.L. Tanwar D. “Experimental investigation of CI engine operated Micro-Trigeneration system”. Applied Thermal Engineering 30 (2010) 1505-1509

14. Mohammadi M., Maghanki, B Ghobadian, G Najafi, R Janzadeh Galogah. “Micro combined heat and power (MCHP) technologies and applications”. Renewable and Sustainable Energy Reviews 28 (2013) 510–524

15. Micro-CHP Systems for Residential Applications Final Report June 2006 Prepared by United Technologies Research Center 411 Silver Lane East Hartford, CT 06108, Prepared for U.S. Department of Energy.

16. Rosato A., Sibilio S. “Energy performance of a micro-cogeneration device during transient and steady-state operation: Experiments and simulations”. Applied Thermal Engineering 52 (2013) 478-491

17. Abusoglu A., Kanoglu M. “First and second law analysis of diesel engine powered cogeneration systems”. Energy Conversion and Management 49 (2008) 2026–2031

18. Abedin M.J., Masjuki H.H., Kalam M.A., Sanjid A., Ashrafur Rahman S.M., Masum B.M. “Energy balance of internal combustion engines using alternative fuels”, Renewable and Sustainable Energy Reviews 26(2013)20–33.

19. Technology and Literature Review, Dr. Tomas N., Fraunhofer ISE PolySMART (POLYgeneration with advanced Small and Medium scale thermally driven Air-conditioning and Refrigeration Technology) Integrated Project partly funded by the European Union

20. J. Godefroy, R. Boukhanouf, S. Riffat, "Design, testing and mathematical modelling of a small-scale CHP and cooling system (small CHP-ejector trigeneration)", Applied Thermal Engineering 27 (2007) 68–77

21. Aleixo A. Manzela, Hanriot S. M., Cabezas-Gomez L., Sodre J. R. "Using engine exhaust gas as energy source for an absorption refrigeration system". Applied Energy 87 (2010) 1141–1148

22. Talom H. L., Beyene A. "Heat recovery from automotive engine". Applied Thermal Engineering 29 (2009) 439–444.

23. Meunier F.. "Sorption contribution to climate change control". Clean Techn Environ Policy 6 (2004) 187–195 DOI 10.1007/s10098-003-0226-7

24. Kilkis B. "Exergy metrication of radiant panel heating and cooling with heat pumps", Energy Conversion and Management 63 (2012) 218–224

25. Zalba B., Marin J.M,. Cabeza L.F, Mehling H., "Review on thermal energy storage with phase change: materials, heat transfer analysis and applications", Appl. Therm. Eng. 23 (2003) 251-283.

26. Nakata T., Silva D., Odionov M., "Application of energy system models for designing a low-carbon society", Prog. Energy Combust. Sci. 37 (2011) 462-502.

27. Manfren M., Caputo P., Costa G., "Paradigm shift in urban energy systems through distributed generation: methods and models", Appl. Energy 88 (2011) 1032-1048.

28. Shati A. K. A., Blakey S. G., Beck S. B. M. "The effect of surface roughness and emissivity on radiator output". Energy and Buildings 43 (2011) 400–406

29. Maurizio L, Cinelli C. “Micro-trigeneration plant: development of a small-size Ammonia-water absorption system”. 61st ATI National Congress –International Session “Solar Heating and Cooling”

30. Kong X. Q., Wang R. Z., Wu J. Y., Huang X. H., Huangfu Y., D. W. Wu, Y. X. Xu. “Experimental investigation of a micro-combined cooling, heating and power system driven by a gas engine”. International Journal of Refrigeration 28 (2005) 977–987

31. Minciuc E., Le Corre O., Athanasovici V., Tazerout M., I. Bitir. “Thermodynamic analysis of tri-generation with absorption chilling machine”. Applied Thermal Engineering 23 (2003) 1391–1405

32. Abdullah Yildiz, Ali Gungor “Energy and exergy analyses of space heating in buildings” Applied Energy 86 (2009) 1939–1948

33. Khan K.H., Rasul M.G., Khan M.M.K. “Energy conservation in buildings: cogeneration and cogeneration coupled with thermal-energy storage”, Applied Energy 77 (2004) 15–34

34. Anand S. Gupta A. Tyagi S. K. “Critical analysis of a biogas powered absorption system for climate change mitigation”, Clean Techn Environ Policy (2014) 16:569–578 DOI 10.1007/s10098-013-0662-y

35. Santoyoa J. H., Cifuentes A S “Trigeneration: an alternative for energy savings”, Applied Energy 76 (2003) 219–227

36. Suleyman Y. K. “Experimental investigation of a comfort heating system for a passenger vehicle with an air-cooled engine”, Applied Thermal Engineering 25 (2005) 2790–2799

37. Onovwiona H. I., Ugursal V. I., Fung A. S. “Modeling of internal combustion engine based cogeneration systems for residential applications”, Applied Thermal Engineering 27 (2007) 848–861

38. Ziher D., Poredos A. “Cooling power costs from a trigeneration system in a hospital”. Forsch Ingenieurwes (2006) 70: 105–113,DOI 10.1007/s10010-005-0019-8

39. Coronado C. R., Villela A. C., Silveira J.L. “Ecological efficiency in CHP: Biodiesel case”, Applied Thermal Engineering 30 (2010) 458–463

40. Naphon P. “Second law analysis on the heat transfer of the horizontal concentric tube heat exchanger”, International Communications in Heat and Mass Transfer 33 (2006) 1029–1041

41. Ge Y.T., Tassou S.A., Chaer I., Suguartha N. “Performance evaluation of a tri-generation system with simulation and experiment”, Applied Energy 86 (2009) 2317–2326

42. Hamdan M.A., Khalil R. H. “Simulation of compression engine powered by Biofuels” , Energy Conversion and Management 51 (2010) 1714–1718

43. Lang S., Joe Huang Y. “Energy Conservation Standard For Space Heating In Chinese Urban Residential Buildings”, Energy Vol. 18, No. 8, pp. 871-892, 1993

44. Maivel M., Kurnitski J. “Low temperature radiator heating distribution and emission efficiency in residential buildings”, Energy and Buildings 69 (2014) 224–236

45. Sidibe S.S., Blin J., G. Vaitilingom, Y. Azoumah “Use of crude filtered vegetable oil as a fuel in diesel engines state of the art: Literature review”, Renewable and Sustainable Energy Reviews 14 (2010) 2748–2759

46. Fontaras G., Kousoulidou M., Karavalakis G., E. Bakeas, Z. Samaras “Impact of straight vegetable oil-diesel blends application on vehicle regulated and non-regulated emissions over legislated and real world driving cycles”, Biomass and Bioenergy 35 (2011) 3188-3198

47. Subramaniam D., Murugesan A., Avinash A., Kumaravel A. “Bio-diesel production and its engine characteristics—An expatiate view”, Renewable and Sustainable Energy Reviews 22 (2013) 361–370

48. Lin L., Cunshan Z., Vittayapadung S., S. Xiangqian, Dong M. “Opportunities and challenges for biodiesel fuel”, Applied Energy 88 (2011) 1020–1031

49. Giakoumis E. G. “A statistical investigation of biodiesel physical and chemical properties, and their correlation with the degree of unsaturation”, Renewable Energy 50 (2013) 858-878

50. Luis F. Verduzco R “Density and viscosity of biodiesel as a function of temperature: Empirical models”, Renewable and Sustainable Energy Reviews 19 (2013) 652–665

51. Agarwal D., Kumar L., Agarwal A K. “Performance evaluation of a vegetable oil fuelled compression ignition engine”, Renewable Energy 33 (2008) 1147–1156

52. Saravanan N., Nagarajan G., Puhan S. “Experimental investigation on a DI diesel engine fuelled with Madhuca Indica ester and diesel blend”., Biomass and Bioenergy 34 (2010) 838-843

53. Tanwar D, Ajayta, Sharma D, Mathur Y. P. “Production And Characterization Of Neem Oil Methyl Ester”, International Journal of Engineering Research & Technology (IJERT) Vol. 2 Issue 5, May - 2013 ISSN: 2278-0181

54. Sundaram P. K., Singh J., Bhattacharya T. K., Patel S. K., “Fuel Properties of Rice Bran Oil Methyl Ester-Ethanol Blends “ Environment & Ecology 33 (1A) : 362—366, January—March 2015ISSN 0970-0420

55. Chauhan B. S., Kumar N., Jun Y. D., Lee K B “Performance and emission study of preheated Jatropha oil on medium capacity diesel engine”, Energy 35 (2010) 2484-2492

56. Hazar H., Aydin H. “Performance and emission evaluation of a CI engine fueled with preheated raw rapeseed oil (RRO)–diesel blends”, Applied Energy 87 (2010) 786–790

57. Pugazhvadivua M.`, Jeyachandran K., “Investigations on the performance and exhaust emissions of a diesel engine using preheated waste frying oil as fuel”Renewable Energy 30 (2005) 2189–2202

58. Karabektas M., Ergen G., Hosoz M. “The effects of preheated cottonseed oil methyl ester on the performance and exhaust emissions of a diesel engine , Applied Thermal Engineering 28 (2008) 2136–2143

59. Raheman H.,. Ghadge S.V “Performance of diesel engine with biodiesel at varying compression ratio and ignition timing”, Fuel 87 (2008) 2659–2666

60. Saravanan S., Nagarajan G., Lakshmi Narayana Rao, S. Sampath, “Theoretical and experimental investigation on effect of injection timing on NOx emission of biodiesel blend” Energy 66 (2014) 216-221

61. Sayin C., Gumus M, Mustafa Canakci, “Effect of fuel injection pressure on the injection, combustion and performance characteristics of a DI diesel engine fuelled with canola oil methyl esters-diesel fuel blends”. Biomass and Bioenergy 46 (2012) 435-446

62. Çelikten, Koca I A., Ali Arslan M “Comparison of performance and emissions of diesel fuel, rapeseed and soybean oil methyl esters injected at different pressures”, Renewable Energy 35 (2010) 814–820

63. Narayana Reddy J., Ramesh A. “Parametric studies for improving the performance of a Jatropha oil-fuelled compression ignition engine”., Renewable Energy 31 (2006) 1994–2016

64. Mohan B., Yang W., Raman V, Vedharaj S, S Kiang Chou, “Optimization of biodiesel fueled engine to meet emission standards through varying nozzle opening pressure and static injection timing”. Applied Energy 130 (2014) 450–457

65. Pradeep V., Sharma R.P. “Use of HOT EGR for NOx control in a compression ignition engine fuelled with bio-diesel from Jatropha oil”, Renewable Energy 32 (2007) 1136–1154

66. Mani M. , Nagarajan, G. Sampath, S. “An experimental investigation on a DI diesel engine using waste plastic oil with exhaust gas recirculation”. Fuel 89 (2010) 1826–1832

67. Saleh H.E. “Experimental study on diesel engine nitrogen oxide reduction running with jojoba methyl ester by exhaust gas recirculation”., Fuel 88 (2009) 1357–1364

68. Agarwal D, Sinha S, Agarwal A. K. “Experimental investigation of control of NOx emissions in biodiesel-fueled compression ignition engine”., Renewable Energy 31 (2006) 2356–2369

69. Vicente B, M. Jose Lujan, Pla B, Linares W. G. “Effects of low pressure exhaust gas recirculation on regulated and unregulated gaseous emissions during NEDC in a light-duty diesel engine”, Energy 36 (2011) 5655-5665

70. Kent Hoekman S Robbins C. “Review of the effects of biodiesel on NOx emissions”, , Fuel Processing Technology 96 (2012) 237–249

71. Saleh H.E. “Effect of exhaust gas recirculation on diesel engine nitrogen oxide reduction operating with jojoba methyl ester”, Renewable Energy 34 (2009) 2178–2186

72. Agarwal D, Agarwal A. K. “Performance and emissions characteristics of Jatropha oil (preheated and blends) in a direct injection compression ignition engine”, Applied Thermal Engineering 27 (2007) 2314–2323

73. Khatri K K, Sharma D, Soni S. L., Kumar S, Tanwar D “Investigation of Optimum Fuel Injection Timing of Direct Injection CI Engine Operated on Preheated Karanj-Diesel Blend”, Jordan Journal of Mechanical and Industrial Engineering (JJMIE) *Volume 4, Number 5, November 2010 ISSN 1995-6665 Pages 6*29 - 640

74. Jindal S., Nandwana B.P., Rathore N.S., Vashistha V. “Experimental investigation of the effect of compression ratio and injection pressure in a direct injection diesel engine running on Jatropha methyl ester”, Applied Thermal Engineering 30 (2010) 442–448

75. Labecki L., Ganippa L.C. “Effects of injection parameters and EGR on combustion and emission characteristics of rapeseed oil and its blends in diesel engines”, Fuel 98 (2012) 15–28

76. Ramadhas A.S., Jayaraj S., Muraleedharan C. “Use of vegetable oils as I.C. engine fuels—A review”, Renewable Energy 29 (2004) 727–742

77. Murugesan A., Umarani C., Subramanian R., Nedunchezhian N. “Bio-diesel as an alternative fuel for diesel engines—A review’, Renewable and Sustainable Energy Reviews 13 (2009) 653–662

78. Silitonga A.S, Masjuki H.H., Mahlia T.M.I., Ong H.C., W.T.Chong, M.H.Boosroh, “Overview properties of biodiesel diesel blends from edible and non-edible feedstock” Renewable and Sustainable Energy Reviews 22 (2013) 346–360

79. Sukumar P, N. Vedaraman, Boppana V.B. Ram, G. Sankarnarayanan, K. Jeychandran “Mahua oil (Madhuca Indica seed oil) methyl ester as biodiesel-preparation and emission characterstics”., Biomass and Bioenergy 28 (2005) 87–93

80. No S.Y. “Inedible vegetable oils and their derivatives for alternative diesel fuels in CI engines: A review” Renewable and Sustainable Energy Reviews 15 (2011) 131–149

81. Ashwani K, Satyawati S “Potential non-edible oil resources as biodiesel feedstock: An Indian perspective”, Renewable and Sustainable Energy Reviews 15 (2011) 1791–1800

82. Yilmaz N., Morton B. “Effects of preheating vegetable oils on performance and emission characteristics of two diesel engines”, Biomass and Bioenergy 35 (2011) 2028-2033

83. Misra R.D., Murthy M.S. “Straight vegetable oils usage in a compression ignition engine—A review”, Renewable and Sustainable Energy Reviews 14 (2010) 3005–3013

84. Saravanan S., Nagarajan G., Sampath S. “Combined effect of injection timing, EGR and injection pressure in NOx control of a stationary diesel engine fuelled with crude rice bran oil methyl ester”, Fuel 104 (2013) 409–416

85. Aninidita K, Karmakar S, Mukherjee S “Properties of various plants and animals feedstocks for biodiesel production”, Bioresource Technology 101 (2010) 7201–7210

86. Ju, Y. H. Vali S R “Rice bran oil as a potential resource for biodiesel: A review” Journal of Scientific and Industrial Research 64 (2005) 866-882

87. Dhar A, Kevin R, Agarwal A K “Production of biodiesel from high-FFA neem oil and its performance, emission and combustion characterization in a single cylinder DICI engine” Fuel Processing Technology 97 (2012) 118–129

88. Prasad B R, Reddy V C.and Vijayakumar Reddy K. “Experimental Study On Emission And Performance Analysis Of Non Edible Rice Bran Oil As An Alternative Fuel For Direct Injection Diesel Engine”, ARPN Journal of Engineering and Applied Sciences ISSN 1819-6608 7 (2012)1495-1500

89. Srivastava A, Prasad R. Triglycerides-based diesel fuels. Renew Sust Energ Rev 2000;4:111–33.

90. R. Raghu, G. Ramadoss, “Optimization of injection timing and injection pressure of a DI diesel engine fueled with preheated rice bran oil” International Journal of Energy and Environment, Volume 2 (2011) 661-670

91. Khatri K.K., Studies on Straight Vegetable oil-diesel blend operated trigeneration system-A thesis submitted to MNIT, Jaipur for Doctor of Philosophy , July, 2010

92. ‘Product Overview Absorption Technology’ http://www2.dometic.com/ last retrieved on 15/06/2015

93. Bansal P. K. and Martin A., “Comparative study of vapour compression, thermoelectric and absorption refrigerators”, International Journal of Energy Research Vol. 24, pp. 93-107, 2000.

94. Operating manual and Agri Engine Catalogue of Kirloskar Oil Engines, “Specifications of Kirloskar Single Cylinder Engine AV1”

95. Specifications of Domestic type Rahul make water flow meters, Available at http: //www.rahulmeters.com/domestic.html Last accessed on May 30, 2010.

96. Offficial website AVL 4000 light, AVL 437 www.avlditest.com, last retrieved on 10/06/2015

97. S. Naga Sarada, M.Shailaja, A.V. Sita Rama Raju, K. Kalyani Radha, "Optimization of injection pressure for a compression ignition engine with cotton seed oil as an alternate fuel" International Journal of Engineering, Science and Technology, 2-6 (2010) 142-149

98 M. Pandian, S.P. Sivapirakasam, M. Udayakumar, "Investigation on the effect of injection system parameters on performance and emission characteristics of a twin cylinder compression ignition direct injection engine fuelled with pongamia biodiesel–diesel blend using response surface methodology" Applied Energy 88 (2011) 2663–2676

99. Saravanan S, Nagarajan G, Sampath S " Combined effect of injection timing, EGR and injection pressure in NOx control of a stationary diesel engine fuelled with crude rice bran oil methyl ester". Fuel 104(2013)409–416

100. Kannan GR, Anand R Effect of injection pressure and injection timing on DI diesel engine fuelled with biodiesel from waste cooking oil. Biomass Bioenergy 46(2012)343–352

101. Bari S, Lim TH, Yu CW "Effects of preheating of crude palm oil (CPO) on injection system, performance and emission of a diesel engine". Renew Energy 27 (2002) 339–351

102. Esteban B, Riba JR, Baquero G, Rius A, Puig R "Temperature dependence of density and viscosity of vegetable oils". Biomass Bioenergy 42 (2012)164–177

103 M. Pugazhvadivua, K. Jeyachandran, "Investigations on the performance and exhaust emissions of a diesel engine using preheated waste frying oil as fuel", Renewable Energy 30 (2005) 2189–2202

104. Karabektas M, Ergen G, Hosoz M "The effects of preheated cottonseed oil methyl ester on the performance and exhaust emissions of a diesel engine". Appl Therm Eng 28(2008)2136–2143

105. “Weather report, Jaipur” from www.weatherspark.com, last retrieved, 01/01/2015

106. Brzustowski TA, Brena A. “Second law analyses of energy processes”. Trans. Can. Soc. Mech. Engr.;10-12(1986)1–8.

PUBLICATIONS

International Journals:

1. D. Sonar, S.L. Soni, D. Sharma, Micro-Trigeneration for Energy Sustainability : Technologies, Tools and Trends, Applied Thermal Engineering, (2014) 71(2) 790-796 *(Elsevier).*
2. D. Sonar, S.L. Soni, D. Sharma, Performance and emission characteristics of a diesel engine with varying injection pressure and fuelled with raw mahua oil (preheated and blends) and mahua oil methyl ester, Clean Technologies and Environmental Policy, (2015) 17: 1499-1511 *(Springer).*

International Conferences:

1. D. Sonar, S.L.Soni, Dilip Sharma, Micro-trigeneration for Sustainable Development, 3rd International Conference on Microtrigeneration and related Technologies, Microgen III, 15-17 April, 2013, Naples , Italy.
2. D. Sonar, S.L.Soni, Dilip Sharma, Performance and Emission studies on unaltered mahua-oil blends with varying injection pressure in a diesel engine, 4th International Conference on Advances in Energy Research (ICAER-13), 10-12 December 2013, Indian Institute of Technology (IIT), Bombay
3. D. Sonar, S.L.Soni, Dilip Sharma, Emission Reduction with Alternate Fuels in I. C. Engines, International Conference on Alternate Fuels for I. C. Engines (ICAFICE 2013) , 6-8 February, 2013, Malaviya National Institute of Technology (MNIT), Jaipur.
4. D. Sonar, S.L.Soni, Dilip Sharma, Sustainable Development through Trigeneration Technologies and practices, International Conference on Creating a Sustainable Business (ICSBMC-12), 7-9 December, 2012, Jaipuria Institute of Management, Jaipur.

National Conferences:

1. D. Sonar, S.L.Soni, Dilip Sharma, CO_2 Abatement Potential of Trigeneration Systems, National Conference on 'Eclectic Mechanical Engineering' , 12 April, 2013 Global Technical Campus, Jaipur.
2. D. Sonar, S.L.Soni, Dilip Sharma, Waste Heat Recovery Systems: A review, National Conference on 'Energy Efficient System Design and Manufacturing'(EESDM-2012), 30-31 March 2012, Vivekananda Institute of Technology, Jaipur.
3. D. Sonar, S.L.Soni, Dilip Sharma, New Alternate Fuels for I. C. Engines, National Conference on 'Eclectic Mechanical Engineering', 29-30 March, 2012, Global Institute of Technology, Jaipur.
4. D. Sonar, S.L.Soni, Dilip Sharma, Emerging Trends in Thermal Storage Systems, National Conference on 'Emerging Trends in Renewable Energy Technology (ETRET-2012), 20-21 April, 2012, UDML (JECRC) College of Engineering, Jaipur.
5. D. Sonar, S.L.Soni, Dilip Sharma, Alternate Transportation Fuels and Fuel Saving Technologies, National Conference on 'Emerging Trends in Renewable Energy Technology (ETRET-2012), 20-21 April, 2012, UDML (JECRC) College of Engineering, Jaipur.

PROFILE OF THE AUTHOR

The author of this work, Deepesh Sonar was born on 27th September, 1968 to Mr. Jagdish Chandra Sonar and Smt Suraj Sonar. He passed his Bachelor of Engineering in Mechanical Engineering in 1989, and Master of Engineering with specialization in Tribology and Maintenance Engineering in 1994 from Shri G. S. Institute of Technology and Science, Indore, M.P. After post graduation, he joined as a Lecturer in Mechanical Engineering at Government Polytechnic College, Ujjain in 1994 and working there since then.

He has worked in industry for two years in the field of operation and maintenance. He is a member of various professional bodies, and has published a few papers in International Journals and Conferences. He is also reviewer of two International Journals, Applied Thermal Engineering (Elsevier) and Clean Technologies and Environmental Policy (Springer). He is pursuing his Doctoral studies at Malaviya National Institute of Technology, Jaipur since July 2011.